



Prediction of large-scale spatial and temporal variability of droughts over Indian region

File Number : PDF/2023/001763

Submitted By : Mr. Thotli Lokeswara Reddy
[SERB Qualified Unique Identification Document: SQUID-1992-TR-0986]
Submission Date : 09-Aug-2023

PROPOSAL DETAILS

(PDF/2023/001763)

Principal Investigator	Mentor & Host Institution
Mr. Thotli Lokeswara Reddy lokus5658@gmail.com (Physics) Contact No : +918886767128 Date of Birth : 16-Apr-1992 Name of Father/Spouse : Thotli Koti Reddy	Krishnareddigari Krishnareddy krishna.kreddy@gmail.com Professor(Physics) Yogi Vemana University Vemana puram, yogi vemana university rd, ganganapalle, andhra pradesh, Kadapa, Andhra pradesh-516005 Contact No. : +919966220933 Registrar Email : registryvu@gmail.com No. of PHD Scholars : 9 No. Post-Doctoral Fellow : 0

Details of Post Doctorate**Ph.D. (Earth and Atmospheric Science) [Not yet Awarded. Thesis Submitted On : 06-Jan-2023]***Climatological studies on droughts and meteorological parameters over a Semi-arid station in Southern Peninsular India***Research Supervisor/Guide & Institution :**

Prof. Katalo Rama Gopal

Sri Krishnadevaraya University, Anantapur, Andhra Pradesh

Brief details of Thesis work :

The climate scientists have observed a distinct climate anomaly over the Indian Ocean in the last two decades. These anomalous events of the Indian Ocean, known as Indian Ocean Dipole (IOD) events, are related to the climatic variability of sea surface anomalies in the eastern and western tropical Indian Ocean. Interannual variability of Indian summer monsoon rainfall is strongly influenced by the El Niño/Southern Oscillation (ENSO) phenomenon, anomalies in the eastern tropical Indian Ocean north-south SST gradient, and the development of a positive Indian Ocean Dipole (pIOD). The pIOD is a coupled ocean-atmosphere mode of variability that is marked by lower Sea Surface Temperature (SST) than normal in the Eastern Equatorial Indian Ocean (EEIO) and warmer than normal in the Western Tropical Indian Ocean (WEIO) coupled with a reversal of zonal wind direction. The SST gradient between the eastern equatorial Indian Ocean and the Bay of Bengal is important for the seasonal climatic transition and changes in year-to-year variability.

The measurement location was geographically (14.62 °N, 77.65 °E and 331 m above sea level) located at Sri Krishnadevaraya University (SKU) campus, a very dry, tropical rural, semi-arid, continental and rain shadow region of Rayalaseema, Andhra Pradesh (AP), India. After Jaisalmer (Rajasthan), Anantapur receives the second least amount of rainfall, the driest part of the AP state. The measurement location has been identified as one of the nodal centers in India by Indian Space Research Organization (ISRO), Bangalore. Due to the heterogeneous characteristics of the study area, including rainfall, soils, and cropping patterns, it makes sense to measure agricultural drought vulnerability in this area. During the monsoon, a low rainfall period has been observed in this district; nearly 85% of people experience drought, high temperatures, low rainfall and heat waves. In this district, annual rainfall is moderate, with less than 500 mm, compared to the average rainfall of AP (900 mm), in which the southwest monsoon rainfall contributes more over the study region.

The long-term variability of meteorological parameters over the semi-arid region for the period 2001-2020. The present study focused on the temporal variation of rainfall and temperature trends to analyse the drought characteristics over the past 20 years (2001-2020) using ground-based Automatic Weather Station (AWS) data at a semi-arid station Anantapur in southern peninsular India. The seasonal maximum mean temperature (Tmean) was observed in summer (32.20 ± 1.36 °C), followed by the monsoon (29.08 ± 1.02 °C), post-monsoon (26.45 ± 2.44 °C), and winter (25.45 ± 1.01 °C) during the study period. The Mann-Kendall trend test result showed a decreasing trend in seasonal mean temperature during the drying period [winter (-0.069 °C/year) and summer (-0.081 °C/year)] and an increasing trend in the wetting period [monsoon (0.012 °C/year) and post-monsoon (0.034 °C/year)]. On the other hand, the seasonal rainfall decreases in the post-monsoon (-2.276 mm/year) while increasing in winter (0.5 mm/year), summer (2.137 mm/year), and monsoon (6.901 mm/year) seasons. The annual trends of minimum, maximum, and mean monthly temperatures decrease at the rate of -0.121, -0.123 and -0.022 °C/year, respectively, while the rainfall increases at the rate of 8.979 mm/year. Furthermore, the temporal evolution of meteorological drought characteristics was estimated with the help of the Standardized Precipitation Index (SPI) and Standardized Precipitation Evapotranspiration Index (SPEI) on multiple time scales ranging from 1-month to 24-month on a monthly basis during the study period. The 24-month SPI values showed that 1 'severely dry' and 29 'moderately dry' long-term drought events. From 24-month SPEI, a total of 15 'severely dry' and 20 'moderately dry' long-term droughts were observed during the study period. The severely dry years were observed in 2002 and 2003, while the wettest periods were observed in 2007 and 2010. Both indices were identified as more severe dry periods from 2002-2006 & 2013-2017 than rest periods. The SPI values were compared with El Niño Southern Oscillation (ENSO) and Normalized Difference Vegetation Index (NDVI) and found that the SPI vs ENSO index negatively correlates with the coefficient of -0.58 significantly, while the SPI vs NDVI correlation is insignificant.

The impact of extreme IOD events on the southern Indian Rainfall, its long-term variability and drought characteristics over southern peninsular India. The present study focused on the characteristics of IOD and its influence on southern Indian rainfall. Also, the temporal variation of rainfall and Sea Surface Temperature (SST), Outgoing Longwave Radiation (OLR), and zonal winds over the Western Equatorial Indian Ocean (WEIO) and Eastern Equatorial Indian Ocean (EEIO). Furthermore, the Standardized Precipitation Index (SPI) were calculated to study the drought characteristics over the study region. The data used in this study were obtained from different satellites and model data from 1980 to 2021 (42 years). During the study period, three excess rainfall events were observed in the years 1994, 1997, and 2019 due to strong pIOD events, while two deficit rainfall was observed in 1992 and 1996 because of the nIOD events. The long-term trends of rainfall (IOD) show an increasing trend with a value of 0.002 mm/day year (0.009 per year). The correlation between IOD and rainfall suggests that the frequency of strong positive IOD events is projected to increase in rainfall over Indian subcontinents and African countries. The observed rainfall trends over WEIO (EEIO) region show decreases (increases), which suggest that the rainfall is increasing over the Indian peninsular and African regions and decreasing over Australian and Indonesian regions.

Technical Details :**Research Area :** Earth & Atmospheric Sciences (Earth & Atmospheric Sciences)**Project Summary :**

Many research initiatives have explored the consequences of anticipated alterations in climate patterns on hydrological systems spanning various regions of the country. These investigations have notably concentrated on unraveling the potential implications of climate change for the characteristics of imminent droughts under different climatic scenarios. In contrast, there has been a noticeable escalation in the frequency of severe climatic events within the area over the past few decades. Consequently, a pressing necessity exists for an all-encompassing framework that comprehensively evaluates drought conditions in any given study area. This framework should include a meticulous and temporally explicit analysis of drought characteristics. Meanwhile, the bulk of these investigations has predominantly directed their attention **toward evaluating trends in various hydrometeorological factors like precipitation, evapotranspiration, temperature, and similar variables, along with studying drought phenomena**. In recent decades, a multitude of researchers have dedicated their efforts to investigating drought patterns in different regions of India and unraveling their intricate interplay with other variables, including factors like rainfall and temperature (Pandey et al., 2021; Saharwardi et al., 2021), trends, dominant and significant periodic components, propagation of meteorological to hydrological drought at river basin scale (Bhardwaj et al., 2020) to the best of our knowledge, but **none of them have used Standardized Precipitation Index (SPI) and Standardized Precipitation Evapotranspiration Index (SPEI) approach as a primary drought indicator under changing climate over spatiotemporally over Indian region**. A wide range of locations across India have been susceptible to experiencing drought events of varying degrees of severity. However, a comprehensive exploration of the spatiotemporal forecasting and characterization of droughts in the Indian region has yet to be extensively examined.

This is the first study focused on spatiotemporal variability of droughts, prediction, and onset, as well as long-term trends and their periodicity over the Indian region. To the best of the proposer's knowledge, the present proposed work is the first of its kind to be carried out over the Indian region.

Objectives :

- To analyze the enduring spatiotemporal fluctuations of drought across the Indian region, employing the Standardized Precipitation Index (SPI) and Standardized Precipitation Evapotranspiration Index (SPEI) as drought metrics across various timescales (1-, 3-, 6-, 9-, 12-, and 24-month).**

- To predict the spatiotemporal droughts characteristics using AR5 data from the Canadian Earth System Model (CanESM5.0.3).**

- To study the prolonged periods of meteorological and hydrological drought events, their eventual culmination, and the initiation of drought conditions.**

- To analyze the spatiotemporal distribution of drought in terms of occurrence, severity, and periodicity to highlight phase transition/modulation during the drought episodes.**

- To assess the trends of climatic factors across spatiotemporal dimensions within the Indian region, employing the Mann-Kendall trend test and Sen's Slope estimator.**

Keywords :

Prediction of Droughts, Mann-Kendall trend test, Climate change, Canadian Earth System Model, SPI, SPEI

Expected Output and Outcome of the proposal :

The outcomes of the proposed work seek to predict drought characteristics utilizing both in-situ and remote sensing data. Meteorological and remote sensing data will be used as independent variables to derive prediction models and may identify the spatiotemporal drought characteristics over the Indian region. The Standardized Precipitation Index (SPI) and Standardized Precipitation Evapotranspiration Index (SPEI) may provide a clear sketch of the spatiotemporal distribution characteristics of drought and the main driving factors in India. The above outcomes lead to identifying the drought events for a particular period and provide regional early drought warning and prediction over the Indian region. The significance of the research will be acknowledged through its publication in 4 international journals and presentation at 4 technical seminars/conferences.

Reference Details :

S.No	Reference Details
1	Prof. P Abdul Azeem, Department of Physics, National Institute of Technology, Warangal - 506004, Telangana, INDIA. [+9190108924] drazeem2002@nitw.ac.in
2	Prof. K Rama Gopal, Department of Physics, Sri Krishnadevaraya University, Anantapur - 515 003, Andhra Pradesh, INDIA. [+9190178609] krgverma@yahoo.com

Proposed Research Topic For SERB-NPDF

Title of the Proposal: Prediction of large-scale spatial and temporal variability of droughts over Indian region.

Background

Drought, a gradual manifestation of extreme climatic conditions, is widespread across the globe. The augmentation of damp and moisture-laden areas resulting from the influence of planetary warming gives rise to significant harm to both the environment and people's means of sustenance (IPCC-2021, Eyring et al., 2021). Forecasting the occurrence, intensity, and precise geographical distribution of weather and climate conditions remains a formidable task within numerical weather prediction. Due to its intricate interplay with climatic and socioeconomic variables, drought displays multifaceted spatiotemporal characteristics. This issue holds significant prominence across various regions globally, leading to a decline in agricultural, industrial, and potable water supply quality and quantity. This issue holds considerable significance worldwide, affecting diverse regions and decreasing the quality and quantity of agricultural, industrial, and drinkable water resources. Both surface and subsurface water reservoirs experience the brunt of their influence (Faiz et al., 2020; Gond et al., 2023). Several drought indicators have been extensively adopted for drought assessment; however, doubts have arisen concerning their precision in representing real drought conditions (Gupta et al., 2022). Drought and flood events inflict substantial damage on agricultural livelihoods (Shruti et al., 2022; Soumik et al., 2022; Shivani et al., 2023; Subash et al., 2023; Yasmeen, 2023). Notably, India has recently witnessed an escalation in both flood and drought incidents (Preethi et al., 2019). The Indian summer monsoon, contributing to 80% of the nation's total annual precipitation, exhibits phase shifts resulting in frequent episodes of severe to moderate droughts and floods attributed to climate change. With a substantial one-third of its landmass classified as semi-arid and arid tropical regions, India remains highly susceptible to recurrent droughts and desertification. A recent study by Christian et al. (2021) has designated 'India' as a flash drought hotspot on a global scale. In the evolving climate scenario, localized climate shifts are poised to induce more severe ramifications on society, encompassing human casualties, depletion of natural resources, indirect repercussions on groundwater reserves, and substantial economic losses.

Origin of the research problem

Many research initiatives have explored the consequences of anticipated alterations in climate patterns on hydrological systems spanning various regions of the country. These investigations have notably concentrated on unraveling the potential implications of climate change for the characteristics of imminent droughts under different climatic scenarios. In contrast, there has been a noticeable escalation in the frequency of severe climatic events within the area over the past few decades. Consequently, a pressing necessity exists for an all-encompassing framework that comprehensively evaluates drought conditions in any given study area. This framework should include a meticulous and temporally explicit analysis of drought characteristics. Meanwhile, the bulk of these investigations has predominantly directed their attention toward evaluating trends in various hydrometeorological factors like precipitation, evapotranspiration, temperature, and similar variables, along with studying drought phenomena. In recent decades, a multitude of researchers have dedicated their efforts to investigating drought patterns in different regions of India and unraveling their intricate interplay with other variables, including factors like rainfall and temperature (Pandey et al., 2021; Saharwardi et al., 2021), trends, dominant and significant periodic components, propagation of meteorological to hydrological drought at river basin scale (Bhardwaj et al., 2020) to the best of our knowledge, but none of them have used Standardized Precipitation Index (SPI) and Standardized Precipitation Evapotranspiration Index (SPEI) approach as a primary drought indicator under changing climate over spatiotemporally over

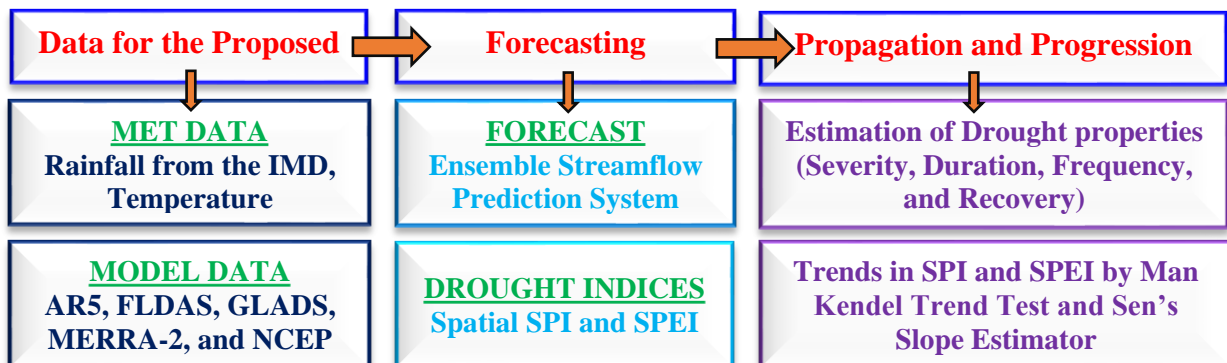
Indian region. A wide range of locations across India have been susceptible to experiencing drought events of varying degrees of severity. However, a comprehensive exploration of the spatiotemporal forecasting and characterization of droughts in the Indian region has yet to be extensively examined. This is the first study focused on spatiotemporal variability of droughts, prediction, and onset, as well as long-term trends and their periodicity over the Indian region. To the best of the proposer's knowledge, the present proposed work is the first of its kind to be carried out over the Indian region.

Specific Scientific Objectives of the Study

This proposed research focuses on the following issues framed as objectives derived from the literature and background research stated above:

- (1) To analyze the enduring spatiotemporal fluctuations of drought across the Indian region, employing the Standardized Precipitation Index (SPI) and Standardized Precipitation Evapotranspiration Index (SPEI) as drought metrics across various timescales (1-, 3-, 6-, 9-, 12-, and 24-month).
- (2) To predict the spatiotemporal droughts characteristics using AR5 data from the Canadian Earth System Model (CanESM5.0.3).
- (3) To study the prolonged periods of meteorological and hydrological drought events, their eventual culmination, and the initiation of drought conditions.
- (4) To analyze the spatiotemporal distribution of drought in terms of occurrence, severity, and periodicity to highlight phase transition/modulation during the drought episodes.
- (5) To assess the trends of climatic factors across spatiotemporal dimensions within the Indian region, employing the Mann-Kendall trend test and Sen's Slope estimator.

Research design and Methodology



Implementation Schedule: The proposed schedule will be used to assess and evaluate the proposed research project.

Project Implementation Schedule	Quarters				Year 1		Year 2	
	Q1	Q2	Q3	Q4	Q1	Q2	Q3	Q4
- Literature review								
- Collection of in-situ and remote sensing Data								
- Model simulations								
- Analyzing the Data								
- Interpretation of Results								
- Communication to International Journals								
- Presentation in local / international conferences								
- Annual Report Writing								
- Final Report								

Expected outcomes

The outcomes of the proposed work seek to predict drought characteristics utilizing both in-situ and remote sensing data. Meteorological and remote sensing data will be used as independent variables to derive prediction models and may identify the spatiotemporal drought characteristics over the Indian region. The Standardized Precipitation Index (SPI) and Standardized Precipitation Evapotranspiration Index (SPEI) may provide a clear sketch of the spatiotemporal distribution characteristics of drought and the main driving factors in India. The above outcomes lead to identifying the drought events for a particular period and provide regional early drought warning and prediction over the Indian region. The significance of the research will be acknowledged through its publication in 4 international journals and presentation at 4 technical seminars/conferences.

References

- Bhardwaj, K., Shah, D., Aadhar, S., Mishra, V., 2020. Propagation of meteorological to hydrological droughts in India. *Journal of Geophysical Research: Atmospheres*, 125.
- Christian, J.I., Basara, J.B., Hunt, E.D., Otkin, J.A., Furtado, J.C., Mishra, V., Xiao, X., Randall, R.M., 2021. Global distribution, trends, and drivers of flash drought occurrence. *Nat. Commun*, 12 (1), 1–11.
- Faiz, M.A., Liu, D., Fu, Q., Naz, F., Hristova, N., Li, T., et al., 2020. Assessment of dryness conditions according to transitional ecosystem patterns in an extremely cold region of China. *Journal of Cleaner Production*, 255, 120348.
- Gond, S., Gupta, N., Patel, J., Dikshit, P.K.S., 2023. Spatiotemporal evaluation of drought characteristics based on standard drought indices at various timescales over Uttar Pradesh, India. *Environmental Monitoring and Assessment*, 439.
- Gupta, A.K., Nair, S.S., Ghosh, O., Singh, A., Dey, S., 2014. Bundelkhand Drought, vols. 1–134.
- Subash, N., Debasish, D., Ghasal, P.C., Punia, P., Vinay P.M., Brahmadut, Ved P.C., 2023. Relevance of climatological information on spatial and temporal variability of Indian Summer monsoon rainfall (ISMR) in recent El Niño years and its impact on four important kharif crops over India. *Climate Services*, 30 (2023) 100370.
- Pandey, V., Srivastava, P.K., Singh, S.K., Petropoulos, G.P., Mall, R.K., 2021. Drought identification and trend analysis using long-term chirps satellite precipitation product in bundelkhand, India. *Sustainability*, 13 (3), 1–20.
- Preethi, B., Ramya, R., Patwardhan, S.K., Mujumdar, M., Kripalani, R.H., 2019. Variability of Indian summer monsoon droughts in CMIP5 climate models. *Climate Dynamics*, 53 (3), 1937–1962.
- Saharwardi, M.S., Mahadeo, A.S., Kumar, P., 2021. Understanding drought dynamics and variability over Bundelkhand region. *J. Earth Syst. Sci.* 130 (3).
- Shivani, G., Nitesh, G., Dikshit, P.K.S., Jitendra, P., 2023. Assessment of drought variability using SPEI under observed and projected climate scenarios over Uttar Pradesh, India. *Physics and Chemistry of the Earth*, 131 (2023) 103440.
- Shruti, V., Bhatla, R., Shahi, N.K., Mall, R.K., 2022. Regional modulating behavior of Indian summer monsoon rainfall in context of spatio-temporal variation of drought and flood events. *Atmospheric Research*, 274 (2022) 106201.
- Soumik G., Sinha, P., Bhatla, R., Mall, R.K., Abhijit, S., 2022. Assessment of Lead-Lag and Spatial Changes in simulating different epochs of the Indian summer monsoon using RegCM4. *Atmospheric Research*, 265 (2022) 105892.
- Yasmeen Telwala, 2023. Unlocking the potential of agroforestry as a nature-based solution for localizing sustainable development goals: A case study from a drought-prone region in rural India. *Nature-Based Solutions*, 3 (2023) 100045.

PROFORMA FOR BIO-DATA

- 1. Name and full correspondence address:** Mr. Thotli Lokeshwara Reddy, Senior Research Fellow, ISRO-GBP (NOBLE) Project, Department of Physics, Sri Krishnadevaraya University, Anantapur, Andhra Pradesh – 515 003.
- 2. Email(s) and contact number(s):** loku5658@gmail.com, lokeshwarareddy.rs@skuniversity.ac.in, and 8886767128.
- 3. Institution:** Sri Krishnadevaraya University, Anantapur, Andhra Pradesh – 515 003
- 4. Date of Birth:** 16-04-1992
- 5. Gender (M/F/T):** M
- 6. Category Gen/SC/ST/OBC:** EWS
- 7. Whether differently abled (Yes/No):** No

8. Academic Qualification (Undergraduate Onwards)

	Degree	Year	Subject	University/Institution	% of marks
1.	B.Sc.	April 2012	Mathematics Physics Computer Science	S.K University, Anantapur Andhra Pradesh,India	77.94
2.	M.Sc.	June 2014	Physics	S.K University, Anantapur Andhra Pradesh,India	77.50
3.	M.Phil.	March 2020	Atmospheric Physics	S.K University, Anantapur Andhra Pradesh,India	NA
4.	Ph.D.	Submitted on 06-01-2023	Atmospheric Physics	S.K University, Anantapur Andhra Pradesh,India	NA

- 9. Ph.D. thesis title, Guide's Name, Institute/Organization/University, Year of Award:** Climatological studies on droughts and meteorological parameters over a Semi-arid station in Southern Peninsular India, Prof. K. Rama Gopal, Department of Physics, Sri Krishnadevaraya University, Anantapur, Andhra Pradesh, India – 515003, Submitted on 06-01-2023.

- 10. Work experience (in chronological order).**

S. No.	Positions held	Name of the Institute	From	To	Pay Scale

- 11. Professional Recognition/ Award/ Prize/ Certificate, Fellowship received by the applicant.**

S. No.	Name of Fellowship	Awarding Agency	Year
01.	Junior Research Fellow	Indian Space Research Organization	08-06-2015 to 07-06-2017
02.	Senior Research Fellow	Indian Space Research Organization	08-06-2017 to till date

- 12. Publications (List of papers published in SCI Journals, in year wise descending order).**

S. No.	Author(s)	Title	Name of Journal	Volume	Page	Year
1	Suryanarayana Vadde, Raja Obul Reddy Kalluri, Balakrishnaiah Gugamsetty, Rama Gopal Kotalo, Usha Kajjer Virupakshappa, Bhavyasree Akkiraju, Lokeswara Reddy Thotli , Siva Sankara Reddy Lingala, Jeevan Kumar Rapole	Classifying aerosol type using in situ and satellite observations over a semi-arid station, Anantapur, from southern peninsular India	Advances in Space Research	72	1109–1122	2023
2	Bhavyasree Akkiraju, Raja Obul Reddy Kalluri, Balakrishnaiah Gugamsetty, Rama Gopal Kotalo, Lokeswara Reddy Thotli , Usha Kajjer Virupakshappa, Siva Sankara Reddy Lingala & Narasimhulu Kuncham	Measurements of aerosol optical depth and equivalent black carbon aerosols over a semi-arid station in Southern India	Environment, Development and Sustainability	25	7903–7925	2023
3	Lokeswara Reddy Thotli , Balakrishnaiah Gugamsetty, Raja Obul Reddy Kalluri, Rama Gopal Kotalo*, Bhavyasree Akkiraju, Siva Sankara Reddy Lingala	Long-term (2001–2020) trend analysis of temperature and rainfall and drought characteristics by in-situ measurements at a tropical semi-arid station (Anantapur) over a peninsular India	International Journal of Climatology	42(16)	8928–8949	2022
4	Raja Obul Reddy Kalluri, Lokeswara Reddy Thotli , Balakrishnaiah Gugamsetty, Rama Gopal Kotalo, Bhavyasree Akkiraju, Usha Kajjer Virupakshappa, Siva Sankara Reddy Lingala	An assessment of the impact of Indian summer monsoon droughts on atmospheric aerosols and associated radiative forcing at a semi-arid station in peninsular India	Science of The Total Environment	813	152683	2022
5	Surya Nagi Reddy Palle, Chakradhar Rao Tandule, Raja Obul Reddy Kalluri, Balakrishnaiah Gugamsetty, Rama Gopal Kotalo, Lokeswara Reddy Thotli , Bhavyasree Akkiraju, Siva Sankara Reddy Lingala	The Impact of Lockdown on eBC Mass Concentration over a Semi-arid Region in Southern India: Ground Observation and Model Simulations.	Aerosol and Air Quality Research	21(11)	1-18, 210101	2021
6	Elijahthamma Busa, Balakrishnaiah Gugamsetty, Raja Obul	Diurnal, seasonal and vertical distribution of carbon monoxide	Atmósfera	35(1)	165-178	2022

	Reddy Kalluri, Rama Gopal Kotalo, Chakradhar Rao Tandule, Lokeswara Reddy Thotli , and Manjunatha Chakala, Surya nagi reddy Palle	levels and their potential sources over a semi-arid region, India				
7	Raja Obul Reddy Kalluri, Balakrishnaiah Gugamsetty, Chakradhar Rao Tandule, Rama Gopal Kotalo, Lokeswara Reddy Thotli , Ramakrishna Reddy Rajuru, Surya Nagi Reddy Palle	Impact of aerosols on surface ozone during COVID-19 pandemic in southern India: A multi-instrumental approach from ground and satellite observations, and model simulations	Journal of Atmospheric Solar-Terrestrial Physics	212	105491	
8	Lokeswara Reddy T , G Balakrishnaiah, Raja Obul Reddy K, Siva Kumar Reddy N, Chakradhar Rao T, Rama Gopal K, Bhavyasree A	Perturbations of atmospheric surface layer characteristics during the annual solar eclipse on 26 December 2019 over a semi-arid region Anantapur in southern India	Journal of Atmospheric Solar-Terrestrial Physics	211	105467	2020
9	Raja Obul Reddy Kalluri, Balakrishnaiah Gugamsetty, Rama Gopal Kotalo, Lokeswara Reddy Thotli , Chakradhar Rao Tandule, Bhavyasree Akkiraju	Long-term (2008–2017) analysis of atmospheric composite aerosol and black carbon radiative forcing over a semi-arid region in southern India: Model results and ground measurement	Atmospheric Environment	240	117840	2020
10	Chakradhar Rao Tandule, Raja Obul Reddy Kalluri, Balakrishnaiah Gugamsetty, Rama Gopal Kotalo, Lokeswara Reddy Thotli , Ramakrishna Reddy Rajuru, Shalini Vaddin	Long term observations of the spatial and vertical distributions of tropospheric aerosol over the Arabian Sea based on satellite observations.	International Journal of Climatology	1–14	40(10)	2020
11	Shalini Vaddin, Narasimhulu Kuncham, Raja Obul Reddy Kalluri, Balakrishnaiah Gugamsetty, Lokeswara Reddy Thotli , Chakradhar Rao Tandule, Elijabetthamma Busa, Manjunatha Chakala, Ramakrishna Reddy Rajuru	Chemical characterization and source identification of particulate matter at Bellary, Karnataka over Southern Indian region	Journal of Atmospheric Solar-Terrestrial Physics	200	105192	2020

12	C. Manjunatha, S. Pavankumari, G. Balakrishnaiah, B. Elijahbetthamma, K. Rama Gopal, T. Chakradhar Rao, T. Lokeshwara Reddy	Estimation of diffuse fraction of global solar radiation over a semi-arid region, Anantapur, A.P.	Journal of Emerging Technologies and Innovative Research	6 (4)	251-263	2019
13	C. Manjunastha, T. Chakradhar Rao, G. Balakrishnaiah, K. Rama Gopal, T. Lokeshwara Reddy , B. Elijahbetthamma, R. Ramakrishna Reddy	Analysis of exceedance in the daily PM ₁₀ mass concentrations over five mega south Indian cities.	International Journal of Research in Advent Technology	7 (4)	699-710	2019
14	S. Nazeer Hussain, T. Chakradhar Rao, G. Balakrishnaiah, K. Rama Gopal, K. Raja Obul Reddy, N. Siva Kumar Reddy, T. Lokeshwara Reddy , S. Pavan Kumari, P. Ramanjaneya Reddy, R. R. Reddy	Investigation of Black Carbon Aerosols and their Characteristics over Tropical Urban and Semi-Arid Rural Environment in Peninsular India.	Journal of Atmospheric Solar-Terrestrial Physics	167	48-57	2017
15	S. Nazeer Hussain, K. Rama Gopal, G. Balakrishnaiah, K. Raja Obul Reddy, K. Uma devi, N. Siva Kumar Reddy, S. Pavan kumari, T. Chakradhar Rao, T. Lokeshwara Reddy , P. Ramanjaneya Reddy, M. Vasudeva Reddy and R. R. Reddy	Measurements of black carbon aerosols and their associated absorption characteristics at Anantapur, Andhra Pradesh, India.	Journal of Neutral Atmosphere	1	03-20	2017
16	K. Raja Obul Reddy, G. Balakrishnaiah, K. Rama Gopal, N. Siva Kumar Reddy, T. Chakradhar Rao, T. Lokeshwara Reddy , S. Nazeer Hussain, M. Vasudeva Reddy, R. R. Reddy, and S. Suresh Babu	Seasonal variation of near surface black carbon and satellite derived vertical distribution of aerosols over a semi - arid station in India.	Atmospheric Research	184	77-87	2017
17	K. Rama Gopal, G. Balakrishnaiah, S. Md. Arafath, K. Raja Obul Reddy, N. Siva Kumar Reddy, S. Pavan Kumari, K. Raghavendra Kumar, T. Chakradhar Rao, T. Lokeshwara Reddy , R. R. Reddy, S. Nazeer Hussain, M. Vasudeva Reddy, S. Suresh Babu and P. Mallikarjuna Reddy	Measurements of scattering and absorption properties of surface aerosols at semi-arid site, Anantapur.	Atmospheric Research	183	84–93	2017
18	K. Raja Obul Reddy, G. Balakrishnaiah, K. Rama Gopal, N. Siva Kumar Reddy, T. Chakradhar Rao, T. Lokeshwara Reddy , S. Nazeer Hussain, M. Vasudeva Reddy, R. R. Reddy, S. K. R. Boreddy and S. Suresh Babu	Long term (2007-2013) observations of columnar aerosol optical properties and retrieved size distributions over Anantapur, India using multi wavelength solar radiometer	Atmospheric Environment	142	238-250	2016

19	K. Rama Gopal, K. Raja Obul Reddy, G. Balakrishnaiah, S. MD. Arafath, N. Siva Kumar Reddy, T. Chakradhar Rao, T. Lokeswara Reddy , R. Ramakrishna Reddy	Regional trends of aerosol optical depth and their impact on cloud properties over southern India using MODIS data.	Journal of Atmospheric Solar-Terrestrial Physics	146	38-38	2016
20	K. Raja Obul Reddy, G. Balakrishnaiah, K. Rama Gopal, N. Siva Kumar Reddy, T. Chakradhar Rao, T. Lokeswara Reddy , R. R. Reddy and S. Suresh Babu	Direct radiative forcing properties of atmospheric aerosols over semi-arid region, Anantapur in India.	Science of the total Environment	566-567	1002-1013	2016
21	K. Rama Gopal, S. Pavan Kumari, G. Balakrishnaiah, K. Raja Obul Reddy, S. Md. Arafath, N. Siva Kumar Reddy, T. Chakradhar Rao, T. Lokeswara Reddy , and R. R. Reddy	Evaluation of clearness and diffuse index at a semi-arid station (Anantapur) using estimated global and diffuse solar radiation	International Journal of Advances in Earth Science & Engineering	5(1)	347-363	2016

13. Detail of patents.

S. No.	Patent Title	Name of Applicant(s)	Patent No.	Award Date	Agency/ Country	Status

14. Books/Reports/Chapters/General articles etc.

S. No.	Title	Author's Name	Publisher	Year of Publication
01.	Microphysical Characteristics of Tropical Precipitating Clouds	K. Hemalatha Punyashesudu T. Lokeswara Reddy	Lambert Academic Publishing	2022
02.	Studies on Atmospheric Boundary Layer Parameters with Doppler SODAR	Thotli Lokeswara Reddy Kotalo Rama Gopal Kapa Hemalatha	Scholar's Press	2023

15. Any other Information (maximum 500 words)

In addition to above information, Qualified Andhra Pradesh State Eligibility Test (APSET-2019) conducted by Andhra University on 20th October 2019. NASA Giovanni has recognized one of the my article figure for the Class of NASA Giovanni Hall of Fame Images 2017. Also, he attended and presented several research papers over 12 international and 48 national-level Conferences/workshops/Symposiums /Seminars/Webinars.

**BOARD OF SECONDARY EDUCATION
ANDHRA PRADESH**

FF 449165



PC/24/23086/349157/2

SECONDARY SCHOOL CERTIFICATE

CERTIFIED THAT THOTLI LOKESWARAREDDY

S/o THOTLI KOTIREDDY
belongs to **Z P HIGH SCHOOL, THUMMALA**

has appeared and PASSED SSC EXAMINATION held in MARCH 2007 in **FIRST**

Division with **TELUGU** as medium of instruction.

DATE OF BIRTH	16/04/1992	DAY	MONTH	YEAR
		ONE SIX	APRIL	ONE NINE NINE TWO

THE CANDIDATE SECURED THE FOLLOWING PERCENTAGE OF MARKS

SUBJECT	Marks Secured (in figures)	Marks Secured (in words)
FIRST LANGUAGE : (TELUGU)	76	SEVEN SIX
THIRD LANGUAGE : ENGLISH	53	FIVE THREE
MATHEMATICS :	77	SEVEN SEVEN
GENERAL SCIENCE :	85	EIGHT FIVE
SOCIAL STUDIES :	68	SIX EIGHT
TOTAL :	359	THREE FIVE NINE
SECOND LANGUAGE : (HINDI)	53	FIVE THREE
GRAND TOTAL :	412	FOUR ONE TWO

Life Skills Education : GRADE SECURED :

Marks of Identification : A black mole on the left chest
A black mole on the left thigh

**Head of Institution
with School Stamp**

Shanu
Head Master
Z. P. HIGH SCHOOL
THUMMALA
Anadagur (Mdl.) Anantapur (Dt.)

Date of issue : 10/05/2007

Leanne
SECRETARY
BOARD OF SECONDARY EDUCATION
A.P. HYDERABAD

1. Life skills Education : The Grade shall be incorporated by the respective Heads of the Institutions before delivery of the certificates to the candidates.
2. Any corrections in the certificate will not be entertained after one year from the date of issue.
3. Any unauthorised correction in the certificate will result in cancellation of certificate.
4. The Marks with asterisk indicates the old marks secured in previous appearances.

2007



Undertaking by the Fellow

I, Mr. Thotli Lokeshwara Reddy, Son/Daughter/Wife of Shri Thotli Koti Reddy, resident of 13-35, Malakavari Palli (V), Thummala (P), Amadagur (M), Anantapur (D), Andhra Pradesh – 515556 agree to undertake the following, If I am offered the SERBN-PDF.

1. I shall abide by the rules and regulations of SERB during the entire tenure of the fellowship.
2. I shall also abide by the rules, discipline of the institution where I will be implementing my fellowship
3. I shall devote full time to research work during the tenure of the fellowship
4. I shall prepare the progress report at the end of each year and communicate the same to SERB through the mentor
5. I shall send two copies of the consolidated progress report at the end of the fellowship period.
6. I further state that I shall have no claim whatsoever for regular/permanent absorption on expiry of the fellowship.

Date: 09 - 08 - 2023

T. Lokeshwara Reddy
Signature

SRI KRISHNADEVARAYA UNIVERSITY
ANANTAPUR - 515 003, ANDHRA PRADESH, INDIA

Prof. K. RAMA GOPAL
Principal Investigator
ISRO- Research Projects
Department of Physics



Mobile : +91 6301718609
Email : krgverma@yahoo.com

09-08-2023

TO WHOM SO EVER IT MAY CONCERN

This is to certify that **Mr. Thotli Lokeshwara Reddy**, Research Scholar, submitted his Ph.D. Thesis entitled "**Climatological studies on droughts and meteorological parameters over a Semi-arid station in Southern Peninsular India**" to Sri Krishnadevaraya University, Anantapur on 06th January 2023 under my supervision.

A handwritten signature in black ink, followed by the name in black text.
(K. RAMA GOPAL)
Dr. K. Rama Gopal
Professor
Department of Physics
S.K. University
Anantapur - 515 003, A.P.

SRI KRISHNADEVARAYA UNIVERSITY ANANTAPURAMU

DEPARTMENT OF PHYSICS

Place: Anantapuramu,
Date : 06-01-2023.

From

T. Lokeshwara Reddy

Research Scholar (Ph.D., Full-Time),
Department of Physics,
S.K. University,
Anantapuramu – 515 003.

To

The Dean,

Research & Development cell,
S.K. University,
Anantapuramu – 515 003.

THROUGH THE PROPER CHANNEL

Respected sir,

Sub: Department of Physics – Submission of Ph.D. Thesis – Reg.

OK

I am herewith submitting 4 copies of my Ph.D. Thesis entitled "Climatological studies on droughts and meteorological parameters over a semi-arid station in southern peninsular India" under the guidance of Dr. K. Rama Gopal, Assistant Professor, Department of Physics, S.K. University, Anantapuramu. Hence, I request you kindly do the needful in this regard.

Thanking you sir,

Forwarded & Recommended
Dr. K. Rama Gopal
Assistant Professor
Department of Physics,
S.K. University,
ANANTHAPURAMU - 515 003

Forwarded
Rama Gopal
6/1/2023
HEAD
Department of Physics
Sri Krishna Devaraya University
Anantapuramu - 515003

Yours faithfully,

T. Lokeshwara Reddy
T. Lokeshwara Reddy,
Research Scholar,
Dept. of Physics,
S. K. University
Anantapuramu.

8/6/2023
PRINCIPAL
S.K. University College of Sciences
ANANTHAPURAMU-515003



RMetS
Royal Meteorological Society

Volume 42 Number 16 30 December 2022

10970088, 2022, 16, Downloaded from https://onlinelibrary.wiley.com/doi/10.1002/joc.7741 by Thotl Lakeswara Reddy - National Medical Library The Director - Wiley Online Library on [29/12/2022]. See the Terms and Conditions (https://onlinelibrary.wiley.com/terms-and-conditions) on Wiley Online Library for rules of use; OA articles are governed by the applicable Creative Commons License

International Journal of Climatology

The Royal Meteorological Society Journal of Climate Science



Editors

Bill Collins and Enric Aguilar

WILEY

ISSN-0899-8418

wileyonlinelibrary.com/journal/joc

Enhancement of the relationship between spring extreme precipitation over Southwest China and preceding winter sea surface temperature anomalies over the South Indian Ocean after the late 1980s Y. Nan, J. Sun, M. Zhang, H. Hong, Y. Nie and J. Yuan	8539
A statistical downscaling prediction model for winter temperature over Xinjiang based on the CFSv2 and sea ice forcing J. Liu, L. Chen and Y. Liu	8552
Extreme rainless periods in Pannonian Basin B. Srdjevic, Z. Srdjevic and P. Benka	8568
Information entropy-based projection of temperature variability under the warming trend in China M. Sun, H. Zhang, X. Yao, M. Zhang and Q. Xing	8591
The emergence of prolonged deadly humid heatwaves X.-S. Wang, L. He, X.-H. Ma, Q. Bie, L. Luo, Y.-C. Xiong and J.-S. Ye	8607
Anthropogenic influence on extreme temperature changes over the mid-high latitudes of Asia W. Jiang, H. Chen and Z. Shi	8619
Spatiotemporal patterns and evolution of heavy rainfall trajectories in China C. Xu, Z. Chen and Z. Zhu	8632
Relationship between interhemispheric Rossby wave propagation and South Atlantic convergence zone during La Niña years H. A. Braga, T. Ambrizzi and N. M. J. Hall	8652
Assessment of dry and heavy rainfall days and their projected changes over Northeast Brazil in Coupled Model Intercomparison Project Phase 6 models F. J. de Medeiros and C. P. de Oliveira	8665
Future warming accelerates lake variations in the Tibetan Plateau Y. Liu and H. Chen	8687
Representation of moist convective processes in Coupled Model Intercomparison Project Phase 5 and Phase 6 models for the simulation of Indian summer monsoon intraseasonal variability S. Tirkey, P. Mukhopadhyay and R. P. M. Krishna	8701
How can the positive Indian Ocean Dipole events co-occur with La Niña? G. Song and R. Ren	8724
Climatology and variability of wind speeds along the southwest coast of India derived from Climate Forecast System Reanalysis winds C. P. Abdulla, V. M. Aboobacker, P. R. Shanas, V. Vijith, R. Sajeev and P. Vethamony	8738
Development of an ensemble Bayesian inference-based copula approach for bivariate risk evaluation of extreme precipitation under climate change L. Sun, J. Sun, Y. Li, C. Suo, J. Liu and P. Gao	8755
The observed connection between the Quasi-Biennial Oscillation and the persistence of the North Atlantic Oscillation in boreal winter Q. Cai, T. Ma, W. Chen, K. Wei, A. I. Pogoreltsev and A. V. Koval	8777
Decreases in the urban heat island effect during the Coronavirus Disease 2019 (COVID-19) lockdown in Wuhan, China: Observational evidence S. Shanlei, Z. Decheng, C. Haishan, L. Jinjian, R. Yongjian, L. Hong and L. Yibo	8792
Contribution of precipitation and temperature to multiscale drought variations over Asia: Dependence on the time scale J. Zhang, R. Wu, X. Jia and Y. Zhang	8804
Projected climate change impacts on groundwater recharge in the Urucuia aquifer system, Brazil B. H. F. Pereira, C. Dereczynski, G. C. da Silva Junior and E. A. G. Marques	8822
Using the daily change in the Southern Oscillation Index to develop analogues and the relationship to severe weather outbreaks J. S. Renken, C. L. Brown, G. Kennedy, J. Mainguy, N. Wergelas and A. R. Lupo	8839
The 2014 severe drought over northeast China and its comparison with droughts over the southern regions: A perspective from synergic effects of water vapour and cold air D. Yuan, J. Hao, E. Lu, W. Dai, R. Gao, C. Zhao, Q. Zhang and H. Zhao	8854
Interdecadal variation in atmospheric water vapour content over East Asia during winter and the relationship with autumn Arctic sea ice W. He, B. Sun, J. Ma and H. Wang	8868
Impacts of regional uplift of the Tibetan Plateau on local summer precipitation and downstream moisture budget: A simulation study K. Yang, J. Chen, C. Lu, J. Li, T. Liu, L. Deng and Y. Li	8882
Assessing extreme precipitation from a regional climate model in different spatial–temporal scales: A hydrological perspective in South America J. P. L. F. Brêda, R. C. D. de Paiva, S. C. Chou and W. Collischonn	8904
Long-term (2001–2020) trend analysis of temperature and rainfall and drought characteristics by in situ measurements at a tropical semi-arid station from southern peninsular India L. R. Thotli, B. Gugamsetty, R. O. R. Kalluri, C. R. Tandule, R. G. Kotalo, B. Akkiraju and S. S. R. Lingala	8928
Historical trends in climate indices relevant to surface air temperature and precipitation in Japan for recent 120 years T. Nakaegawa and K. Murazaki	8950
Changing temporal volatility of precipitation extremes due to global warming C. L. E. Franzke	8971
Cloud macrophysical characteristics in China mainland and east coast from 2006 to 2017 using satellite active remote sensing observations Y. Chi, C. Zhao, Y. Yang, Z. Ma and J. Yang	8984
Long-term variations of clouds and precipitation on the Tibetan Plateau and its subregions, and the associated mechanisms J. Tang, X. Guo, Y. Chang, G. Lu and P. Qi	9003

Long-term (2001–2020) trend analysis of temperature and rainfall and drought characteristics by in situ measurements at a tropical semi-arid station from southern peninsular India

Lokeswara Reddy Thotli  | Balakrishnaiah Gugamsetty |
Raja Obul Reddy Kalluri | Chakradhar Rao Tandule | Rama Gopal Kotalo  |
Bhavyasree Akkiraju | Siva Sankara Reddy Lingala

Aerosol & Atmospheric Research Laboratory, Department of Physics, Sri Krishnadevaraya University, Anantapur, India

Correspondence

Rama Gopal Kotalo, Aerosol & Atmospheric Research Laboratory, Department of Physics, Sri Krishnadevaraya University, Anantapur 515003, Andhra Pradesh, India.
Email: krgverma@yahoo.com

Funding information

Indian Space Research Organisation, Grant/Award Number: ISRO-GBP (NOBLE)

Abstract

With the effects of climate change prevailing worldwide, it is essential to understand the long-term rainfall and temperature trends at regional scales to plan for adaptation strategies. Investigating the temporal dynamics of meteorological variables in climate-induced changes, particularly in rain-fed agriculture countries such as India, is needful. The present study focused on the temporal variation of rainfall and temperature trends to analyse the drought characteristics over the past 20 years (2001–2020) using ground-based Automatic Weather Station (AWS) data at a semi-arid station Anantapur in southern peninsular India. The seasonal maximum mean temperature (T_{mean}) was observed in summer ($32.20 \pm 1.36^\circ\text{C}$), followed by the monsoon ($29.08 \pm 1.02^\circ\text{C}$), postmonsoon ($26.45 \pm 2.44^\circ\text{C}$), and winter ($25.45 \pm 1.01^\circ\text{C}$) during the study period. The Mann–Kendall trend test result showed the decreasing trend in seasonal mean temperature during the drying period (winter $[-0.069^\circ\text{C}\cdot\text{year}^{-1}]$ and summer $[-0.081^\circ\text{C}\cdot\text{year}^{-1}]$) and increasing trend in the wetting period (monsoon $[0.012^\circ\text{C}\cdot\text{year}^{-1}]$ and postmonsoon $[0.034^\circ\text{C}\cdot\text{year}^{-1}]$). On the other hand, the seasonal rainfall decreases in the postmonsoon ($-2.276 \text{ mm}\cdot\text{year}^{-1}$) while increasing in winter ($0.5 \text{ mm}\cdot\text{year}^{-1}$), summer ($2.137 \text{ mm}\cdot\text{year}^{-1}$), and monsoon ($6.901 \text{ mm}\cdot\text{year}^{-1}$) seasons. The annual trends of minimum, maximum, and mean monthly temperatures decrease at the rate of -0.121 , -0.123 , and $-0.022^\circ\text{C}\cdot\text{year}^{-1}$, respectively, while the rainfall increases at the rate of $8.979 \text{ mm}\cdot\text{year}^{-1}$. Furthermore, the temporal evolution of meteorological drought characteristics was estimated with the help of the standardized precipitation index (SPI) and standardized precipitation evapotranspiration index (SPEI) on multiple timescales ranging from 1 to 24 months on a monthly basis during the study period. The 24-month SPI values showed that 1 “severely dry” and the 29 “moderately dry” long-term

drought events were observed. From 24-month SPEI, a total of 15 “severely dry” and 20 “moderately dry” long-term droughts were observed during the study period. The severely dry years were observed in 2002 and 2003, while the wettest periods were 2007 and 2010. Both indices are identified as more severe dry periods from 2002 to 2006 and 2013 to 2017 than rest periods. Also, a significant decreasing tendency of droughts was observed in both indices. The SPI values are compared with El Niño–Southern Oscillation (ENSO) and normalized difference vegetation index (NDVI) and found that the SPI versus ENSO index negatively correlates with the coefficient of -0.58 significantly, while the SPI versus NDVI correlation is insignificant. The study region converted to wetter conditions during the last 20 years.

KEY WORDS

ENSO, NDVI, rainfall, semi-arid region, SPEI, SPI, temperature, trend analysis

1 | INTRODUCTION

Rainfall and temperature are the most significant climatic variables related to the changing climate, and its impacts of climate change on temperatures and rainfall differ from place to place (Animashaun *et al.*, 2020). Understanding variability, trend, and changes in precipitation in a changing climate are crucial in the agricultural sector and hydrological modelling (Mumo *et al.*, 2019). The spatiotemporal analysis of meteorological variables is critical for detecting climatic changes at various timescales (Shrestha *et al.*, 2019). Significant changes in the frequency, magnitude, and pattern of extreme rainfall-related hydrological events include floods and droughts (Agilan and Umamahesh, 2017). Researchers frequently use trend detection in rainfall and temperature time series to track the magnitude of climate change and its variability (Loo *et al.*, 2015; Animashaun *et al.*, 2020). The trends were estimated using the non-parametric Mann–Kendall test (Mann, 1945; Kendall, 1948) and the magnitude of trends from Sen’s slope estimator (Sen, 1968). Numerous researches have investigated the long-term trends in rainfall and temperature in the Indian subcontinent (Mooley and Parthasarathy, 1983; Parthasarathy and Pant, 1985; Kumar *et al.*, 2010). Jhajharia *et al.* (2021) mentioned several studies carried out over different parts of India to analyse trends in various climatic parameters. The spatial and temporal homogeneity of trends is an essential aspect in trend analysis of any hydrometeorological parameter in any region (Jhajharia *et al.*, 2014). According to the 6th Assessment Report (AR6) of the Intergovernmental Panel on Climate Change (IPCC), in the 21st century (2001–2020), the human-caused global surface

temperature increased from 1850–1900 to 2010–2019 is 0.8 to 1.3°C (Eyring *et al.*, 2021).

Drought has been one of the most complex hydroclimatic natural disasters in recent decades, which seriously affects society development (agricultural, ecology, hydrology, environment, socioeconomics, and other disciplines) and the survival of human beings (Mishra and Singh, 2010; Sheffield *et al.*, 2012; Yao *et al.*, 2020; Liu *et al.*, 2021; Tehseen *et al.*, 2021). Monitoring drought should be the highest priority to implement appropriate measures to control its negative impacts (Sharma *et al.*, 2021). It is one of the most complex recurring natural disasters caused by persistent water scarcity due to a lack of precipitation (Islam *et al.*, 2021). The drought characteristics were classified into four types: meteorological, agricultural, hydrological, and socioeconomic droughts (Pei *et al.*, 2020). The most prevalent type of drought is meteorological drought, caused by low rainfall and a prolonged dry season (Vicente-Serrano *et al.*, 2010). However, drought frequency and intensity have increasingly grown as the global climate has continued to warm (Mishra and Singh, 2010; Allen, 2011; Kang and Sridhar, 2017; Thilakarathne and Sridhar, 2017; Animesh *et al.*, 2021), which affects a larger number of people than any other climate-related hazard (Godfray *et al.*, 2010). It is a term that describes a slow-moving event that can last for months or years (Li and Huang, 2021). Droughts will be more severe in magnitude and duration in the coming decades as global temperatures increase (Sivakumar *et al.*, 2014; Nicholson, 2017; Haile *et al.*, 2020; Celso *et al.*, 2021). Furthermore, numerous studies have shown that future drought severity will be directly proportional to future increases in greenhouse gas emissions (Cook *et al.*, 2014; Wang and Chen, 2014; Wang *et al.*, 2018).

Because of global warming and its effects on regional climate, trend analysis of extreme events such as drought has received more attention in recent decades (Dong *et al.*, 2019; Polong *et al.*, 2019; Danandeh Mehr and Vaheddoost, 2020). The drought characteristics are estimated based on the standardized precipitation index (SPI; McKee *et al.*, 1993) and standardized precipitation evapotranspiration index (SPEI; Vicente-Serrano *et al.*, 2010). The SPI and SPEI are widely used to indicate the drought indices (Smakhtin and Hughes, 2007; Naresh Kumar *et al.*, 2009; Zamani *et al.*, 2017; Kisi *et al.*, 2019; Jeongeun *et al.*, 2020; Satish Kumar *et al.*, 2021; Sharma *et al.*, 2022). The Pettit test is a statistical and nonparametric rank test developed by Pettitt (1979) to assess the presence of sudden changes in the time series of meteorological data (Chakraborty *et al.*, 2017).

Human-induced climate change has affected many kinds of extreme weather events in many regions across the globe; water-scarce events observed in very high rainfall regions, including one of the wettest place in the world situated in the northeastern region of India (Sharma *et al.*, 2022). Drought is an extensive phenomenon in India, occurring roughly every 3 years in various areas (Mishra and Singh, 2011). Mishra *et al.* (2019) reported that the previous drought events in India have resulted in millions of deaths. Since 1965, droughts have been more frequent in India than in many other countries (Setti *et al.*, 2020; Satish Kumar *et al.*, 2021). Drought stress is widespread over the country due to the deficiency of southwest monsoonal rainfall (Kumar *et al.*, 2013). Each region will experience unique drought characteristics depending on the climate and human activity (Animesh *et al.*, 2021). Mallya *et al.* (2016) observed a spatial shift of droughts towards coastal peninsular India, central Maharashtra, and the Indo-Gangetic plains. Between 1991 and 2015, the increasing drought trend throughout India was observed in various agro-ecological areas (Alam *et al.*, 2017). The anomaly in monsoon rainfall and droughts over the region is linked to El Niño–Southern Oscillation (ENSO; Thomas and Prasannakumar, 2016, and reference therein). The independent La Niña and El Niño events influence droughts and floods (Murphy and Timbal, 2008; Schepen *et al.*, 2012; Liu *et al.*, 2018; Fang *et al.*, 2021). Dabanch *et al.* (2017) reported that ENSO could not associate with the variation of multiscale SPI, indicating that ENSO influenced only 1-month SPI. India's dry and wet extremes are linked to ENSO (Mooley and Parthasarathy, 1983; Ramao, 1983; Rasmusson and Carpenter, 1983), impacting the normalized difference vegetation index (NDVI). The spatiotemporal characteristics and variability of the impact of ENSO on drought were analysed (Zhou *et al.*, 2021).

The Anantapur district in Andhra Pradesh has deficit rainfall with high interannual variability and also the district has been declared a chronic drought-prone area. The drought in this district has occurred consistently for so many years that it has caused great stress to the local economy and especially the agriculture sector (Naresh Kumar *et al.*, 2009). Srinivasa Reddy *et al.* (2008) reported the negative consequences of the drought in 2002–2003 in terms of groundwater depletion, crop failure, suicides, migration, and indebtedness, among other things, over this study region of Anantapur. The vulnerable group of mandals comprises 57% of the agricultural land and 67% of the rainfed crop areas in Andhra Pradesh (Murthy *et al.*, 2015). Therefore, the ground-based collection of long-term (2001–2020) temperature and rainfall trends and their corresponding drought characteristics are essential over the rainfed region of this district.

In the present study, the meteorological parameters (such as temperature and rainfall) data were obtained from the Automatic Weather Station (AWS) for the study between 2001 and 2020. The main research objectives of the current study are as follows: (a) to observe the long-term seasonal and annual trends in temperature and rainfall time series using Mann–Kendall test and Sen's slope estimator, (b) to understand the temporal variation of drought characteristics using SPI and SPEI drought index at various timescales (1, 3, 6, 12, 24 months), the drought frequency and the long-term trends in the drought index, (c) to identify the correlations between the 1-month SPI with ENSO and NDVI index for the monsoon period from 2001 to 2020.

2 | DESCRIPTION OF THE STUDY AREA AND DATA USED

The meteorological data have been measured at the Sri Krishnadevaraya University (SKU) campus, a very dry, tropical rural, semi-arid, continental, and rain shadow region of Rayalaseema, Andhra Pradesh (AP), India. The measurement location was geographically (14.62°N, 77.65°E and 331 m above sea level) located at SKU campus (Gopal *et al.*, 2016; Raja Obul Reddy *et al.*, 2016; Kalluri *et al.*, 2020; Thotli *et al.*, 2020). After Jaisalmer (Rajasthan), Anantapur receives the second least amount of rainfall, the driest part of the AP state (Kalluri *et al.*, 2022). During the monsoon, a low-rainfall period has been observed in this district; nearly 85% of people experience drought, high temperatures, low rainfall, and heat waves. In the district, annual rainfall is moderate, with less than 500 mm, compared to the average rainfall of AP (900 mm), in which the southwest monsoon rainfall contributes more over the study region (Rama Gopal

TABLE 1 Technical details of the instruments used in the present study

Instrument/website	Parameter (sensor)	Range	Resolution
Automatic weather station (AWS) (make: Campbell Scientific, Canada)	Temperature (RTD probe) Rainfall (Tipping Bucket rain gauge)	–40 to +60°C Unlimited	±0.1°C 0.5 mm
National Oceanic and Atmospheric Administration (NOAA)	Niño3 index (https://ggweather.com/enso/oni.htm)		
Advanced Very High-Resolution Radiometer (AVHRR)	NDVI (https://giovanni.gsfc.nasa.gov/)		1° × 1°

et al., 2017). The measurement location has been identified as one of the nodal centres in India by India's Indian Space Research Organization (ISRO) (Kalluri *et al.*, 2017). Due to the heterogeneous characteristics of the study area, including rainfall, soils, and cropping patterns, it makes sense to measure agricultural drought vulnerability in this area (Murthy *et al.*, 2015). Accordingly, the prevailing climatological conditions, the year is divided into four seasons based on Indian meteorological Department (IMD) classifications, winter: December–January–February, summer: March–April–May, and monsoon: June–July–August–September, and the post-monsoon: October–November.

The near-surface weather variables, like daily air temperature (AT) and rainfall, are obtained from the AWS developed by Astra Microwave Products Ltd., India. The sensors are mounted at 4 m height above ground level over the measurement location. The location of the experimental site is approximately 50 m south of the Physics Department, SKU. The meteorological data used in this study were obtained from the AWS for every 1 hr from January 2001 to December 2020. A Resistance Temperature Detector (RTD) type sensor is used to measure air temperature. The change in resistance of the device with temperature is measured and converted to a linearly varying direct current (DC) voltage proportional to the temperature. The temperature sensors have an accuracy of ±0.2°C with a resolution of ±0.1°C and the range between –40 and +60°C. The Tipping Bucket raingauges uses a tipping bucket mechanism to produce a contact closure every time it receives a predetermined quantity of rainfall. The tipping bucket raingauge has rainfall accuracy of better than 1 mm with a resolution of 0.5 mm. Daily temperature and rainfall data are converted to monthly, seasonal, and annual scales used for further analysis. Table 1 provides the statistical data for monthly measurement location and seasonal and annual average prevailing weather conditions during the study period (2001–2020). ENSO activity is represented by the 3-month running mean of the Niño3 index, which is downloaded from the National Oceanic and Atmospheric Administration (NOAA) website (<http://www.esrl.noaa.gov/psd/data/climateindices>).

According to the methodology proposed by de Bodas Terassi *et al.* (2018), the classification of ENSO events is mentioned in Table 2. The NDVI measures vegetation parameters based on remote sensing data (Yao *et al.*, 2018, and reference therein). The NOAA Advanced Very High-Resolution Radiometer (AVHRR) onboard MODIS (Moderate Resolution Imaging Spectroradiometer) Terra (MOD13C2v006) derives NDVI data for monitoring vegetation health and growth. In addition to being widely recognized as an indicator of terrestrial vegetation productivity, the NDVI is also used for estimating net primary production, crop yields, crop growth conditions, land cover, early warning systems, rainfall, and drought monitoring. The monthly NDVI data can be retrieved from the website with a 0.05° × 0.05° resolution (<https://giovanni.gsfc.nasa.gov/>), and it is further averaged for the months of June, July, and August (JJA). The details of the data and their sources are indicated in Table 1.

3 | METHODOLOGY

3.1 | Coefficient of variation

The coefficient of variation (CV) is a statistical measure of the dispersion of data points in a series of data from the mean. It was computed to evaluate the variability within sample values used in the present study. Hence, the level of variability is a function of the indicator and therefore, the lower (higher) the CV value, the lower (higher) the variability (Asfaw *et al.*, 2018). According to Hare (2003), CV can be classified as the degree of variability of rainfall events in high, moderate, and low is CV > 30, 20 < CV < 30, and CV < 20, respectively.

3.2 | Simple linear regression

Data trend line in time series is made easier by linear regression, one of the most basic and useful methods. This method is used in the current study to estimate

SPI categories	Range of values	ENSO categories	Range of values
Extremely wet	$\geq +2.0$	El Niño strong	≥ 1.70
Very wet	1.5–1.99	El Niño moderate	0.90–1.69
Moderately wet	1.0–1.49	El Niño weak	0.50–0.89
Near normal	–0.99 to 0.99	Neutral	0.49 to –0.49
Moderately dry	–1.49 to –1.0	La Niña weak	–0.49 to –1.49
Severely dry	–1.99 to –1.5	La Niña moderate	–1.49 to –1.69
Extremely dry	≤ -2	La Niña strong	≤ -1.70

TABLE 2 Classification of drought severity for the SPI and SPEI (Svoboda *et al.*, 2012) and ENSO rating scale (de Bodas Terassi *et al.*, 2018)

any trend line in a time series of temperature and rainfall (Gocic and Trajkovic, 2013; Ogunrinde *et al.*, 2019).

3.3 | Mann–Kendall trend test

The long-term trend analysis was also carried out for temperature and rainfall data on a monthly, seasonal, and annual basis within the study area using the Mann–Kendall trend test (Mann, 1945; Kendall, 1948; Animashaun *et al.*, 2020). In this study, the MK test was used to detect the presence of monotonic (decreasing or increasing) trends and determine whether they are statistically significant or not. The MK test is a nonparametric test that has been widely used to determine temporal variations in hydrometeorological variables (Zhang *et al.*, 2014; Li *et al.*, 2016). Rather than assuming no trend, the null hypothesis assumes the data are independently ordered and random and compared with the alternative hypothesis (H1). A summary of the test statistics of the Mann–Kendall (S_{MK}) is presented using the below equation,

$$S_{MK} = \sum_{i=1}^{n-1} \sum_{j=1}^n \text{sign}(x_j - x_i), \quad (1)$$

where x_i and x_j are the sequential data points in a given time series, and n is the data set length,

$$\text{sign}(x_j - x_i) = \begin{cases} +1 & (x_j - x_i) > 0 \\ 0 & (x_j - x_i) = 0 \\ -1 & (x_j - x_i) < 0 \end{cases} \quad (2)$$

The S_{MK} is computed as the sum of the integers, and Equation (1) indicates negative, no, and positive differences, respectively. For series without a trend, the expected value of S is zero ($E[S] = 0$), and the variance (σ^2) is computed as below,

$$\sigma^2(S_{MK}) = \frac{1}{18} \left\{ n(n-1)(2n+5) - \sum_{i=1}^q t_i(t_i-1)(2t_i+5) \right\}. \quad (3)$$

In Equation (3), the number of tied groups in a given time series is provided by q , while the number of data items in the i th ties group is given by t_i . The standardized MK statistics Z is computed as

$$Z = \begin{cases} \frac{(S_{MK} - 1)}{\sqrt{\sigma^2(S_{MK})}} & \text{if } S_{MK} > 0 \\ 0 & \text{if } S_{MK} = 0 \\ \frac{(S_{MK} + 1)}{\sqrt{\sigma^2(S_{MK})}} & \text{if } S_{MK} < 0 \end{cases} \quad (4)$$

A decreasing (increasing) trend can be considered a negative (positive) Z value.

3.4 | Sen's slope estimator

Using the Sen's slope estimator (Sen, 1968) to calculate the true slope of an existing trend, such as the amount of change per year, this nonparametric method is used, and the test was performed using XLSTAT 2017 software. Sen's slope negative (positive) value indicates the decreasing (increasing) trend in the given time series. In order to compute the Sen's slope, the slopes between all consecutive data points are estimated $[(X_i - X_j) / j - i]$, and then the calculated median of all slopes. The Sen's slope can be calculated using the following equation:

$$\beta = \text{median} \left(\frac{X_j - X_i}{j - i} \right) \text{ for } i = 1, 2, 3, \dots, M, \text{ where } j > i, \quad (5)$$

where X_i and X_j are the consecutive values of time series data. The test results from Sen's slope estimator are shown in Tables 3 and 4.

TABLE 3 Mann–Kendall trend test coefficient and Sen's slope results of monthly, seasonal, annual T_{\max} , T_{\min} , T_{mean} , and rainfall from 2001 to 2020

	T_{\max}				T_{\min}				T_{mean}				Rainfall			
	MK statistics	Kendall tau (t)	Sen's slope (S)	MK statistics	Kendall tau (t)	Sen's slope (S)	MK statistics	Kendall tau (t)	Sen's slope (S)	MK statistics	Kendall tau (t)	Sen's slope (S)	MK statistics	Kendall tau (t)	Sen's slope (S)	
January	-58	-1.8493	-0.1438	-20	-0.6164	-0.1297	-38	-1.2004	-0.0784	44	1.64736	0				
February	-10	-0.292	-0.048	-18	-0.5516	-0.146	-18	-0.5516	-0.0228	-34	-1.2169	0				
March	-48	-1.5249	-0.1587	-25	-0.7791	-0.2984	-26	-0.8111	-0.0644	-32	-1.1416	0				
April	-48	-1.5249	-0.1442	-20	-0.6164	-0.200d9	-50	-1.5898	-0.105	33	1.04801	0.52917				
May	-37	-1.1686	-0.0907	-22	-0.6813	-0.2175	-24	-0.7462	-0.0388	30	0.94088	1.63214				
June	-36	-1.1355	-0.0789	-26	-0.8111	-0.1284	8	0.22711	0.01536	70	2.24102	3.05275				
July	-36	-1.1355	-0.0871	-16	-0.4867	-0.0747	12	0.35689	0.00983	26	0.81196	0.5875				
August	-20	-0.6164	-0.0558	-16	-0.4867	-0.0876	22	0.68133	0.02577	-4	-0.0973	-0.1661				
September	-26	-0.8111	-0.0569	-14	-0.4218	-0.0545	6	0.16222	0.02405	35	1.10369	5.20238				
October	-55	-1.7529	-0.0772	-4	-0.0973	-0.0114	12	0.35689	0.01565	-18	-0.5516	-1.6844				
November	-12	-0.3569	-0.0147	14	0.42178	0.09	38	1.20044	0.06965	-9	-0.2597	-0.1833				
December	-50	-1.5914	-0.1171	26	0.81196	0.1029	16	0.48718	0.03951	67	2.16695	0.255				
Winter	-42	-1.3302	-0.1198	-16	-0.4867	-0.1261	-28	-0.876	-0.0694	46	1.47297	0.5				
Summer	-56	-1.7844	-0.1857	-26	-0.8111	-0.2082	-46	-1.46	-0.0818	32	1.00577	2.13706				
Monsoon	-38	-1.2004	-0.0739	-16	-0.4867	-0.0851	4	0.09733	0.01222	22	0.68133	6.90152				
Postmonsoon	-30	-0.9409	-0.0271	-6	-0.1622	-0.0252	22	0.68133	0.03487	-24	-0.7462	-2.2763				
Annual	-54	-1.7195	-0.1233	-28	-0.876	-0.1212	-6	-0.1622	-0.022	34	1.07066	8.97938				

Note: Sen's slope is $^{\circ}\text{C year}^{-1}$ for temperature and mm year^{-1} for rainfall.

Different timescales		MK statistics	Kendall tau (<i>t</i>)	Sen's slope (<i>S</i>)
SPI	1 month	2,570	2.068	0.00150
	3 months	2,615	2.129	0.00198
	6 months	1,687	1.400	0.00142
	12 months	900	0.776	0.00090
	24 months	922	0.861	0.00086
SPEI	1 month	3,578	2.8773	0.0030
	3 months	3,303	2.6895	0.0031
	6 months	3,249	2.6963	0.0035
	12 months	3,450	2.9761	0.0040
	24 months	3,348	3.1304	0.0045

Note: The significance of trends was assessed at $p < .05$. Sen's slope is /month.

TABLE 4 Mann–Kendall trend test coefficient and Sen's slope results during the study period (2001–2020)

3.5 | Change point detection using Pettit's test

This statistical test is a nonparametric rank test developed by Pettitt (1979) to assess the presence of sudden changes in the time series of meteorological data and detect the change year (shifting) in the time series (Buishand, 1982). It identifies the change point in the middle of the series. It detects the change points in the middle of any time series (Jaiswal *et al.*, 2015) and detects a significant change in the mean of a time series. This test is based on the rank of the series and ignores the normality of the series (Srilakshmi *et al.*, 2022)

$$Q = \max |X_k| \text{ for } 1 \leq k \leq n, \quad (6)$$

where Q is the test statistics, n is the sample length, and r is the rank of the time series,

$$X_k = \sum_{i=1}^k r_i - k(n+1) \text{ where, } i=1, \dots, n. \quad (7)$$

According to the test, if the time series breaks or shifts in year E , the statistic value is maximal or minimal near the year $k = E$.

3.6 | Deviation analysis of rainfall

The percentage deviation ($D\%$) of yearly rainfall is computed to understand dry years. The number of excess, deficit, scanty and no rain years, and the percentage departure of annual rainfall were calculated using Equation (8). Rainfall deviations included negative (positive) deviations indicating that the actual rainfall is less than (greater than) the normal rainfall. Therefore, the departure analysis of the annual rainfall time series can identify drought years. Meteorological drought is

TABLE 5 Classification of droughts based on percentage departure (as per IMD)

Climatic moisture categories	% departure of realized rainfall from normal rainfall	No. of years (% contribution)
Excess	$\geq +20$	5 (25)
Normal	-19 to +19	7 (35)
Deficit	-20 to -59	5 (25)
Scanty	-60 to -99	2 (10)
No rain	-100	1 (5)

described as a scenario in which seasonal/annual rainfall over a specific area is less than 75% of normal, according to the Indian Meteorological Department (IMD). The classification of droughts is mentioned in Table 5 (Thomas and Prasannakumar, 2016). The rainfall deviation can be calculated using the following equation:

$$D_i(\%) = \frac{Rf_i - Rf_m}{Rf_i} \times 100, \quad (8)$$

where D_i , Rf_i , Rf_m are the annual rainfall departure, annual rainfall series, and mean annual rainfall, respectively. Based on departure analysis of annual rainfall in a given time series, data are presented in Table 5.

3.7 | Standardized precipitation index

The SPI is one of the most widely used meteorological drought indicators, indicating the rainfall occurrence probability in a given area over a given period (McKee *et al.*, 1993). It is one of the ways to express precipitation in a given period, and it is very useful to monitor drought conditions and assess the climatic conditions on a monthly scale. The World Meteorological Organization (WMO) recommends the use of SPI as the essential

drought index to monitor meteorological drought conditions due to its simplicity and use (Svoboda *et al.*, 2012). The SPI is flexible and designed to quantify the rainfall deficit and calculate droughts in different time windows, such as 1, 3, 6, 12, 24, and 48 months. Naresh Kumar *et al.* (2009) also reported the SPI over the Anantapur region from 1969 to 2007. An analytical solution is provided for rainfall data with a gamma distribution function (McKee *et al.*, 1993; Edwards, 1997; Anteneh *et al.*, 2019). The specific calculation method (Liu *et al.*, 2021) is as follows:

$$g(x) = \frac{1}{\beta^\alpha \Gamma(\alpha)} x^{\alpha-1} e^{-\frac{x}{\beta}}, x > 0, \quad (9)$$

where α and β are the shape, the scale parameters, and x is the amount of rainfall and thus, the gamma function can be written as

$$\Gamma(\alpha) = \int_0^\infty x^{\alpha-1} e^{-x} dx, \quad (10)$$

where the α and β values are greater than zero, and these are estimated for n is the number of rainfall series given by the following method:

$$\hat{\alpha} = \frac{1}{4A} \left(1 + \sqrt{1 + \frac{4A}{3}} \right), \hat{\beta} = \frac{\bar{A}}{\hat{\alpha}} \text{ and } A = \ln(\bar{x}) - \frac{\sum \ln(x)}{n}. \quad (11)$$

The following equation can be used to calculate the cumulative probability for a given month,

$$G(x) = \int_0^x g(x) dx = \frac{1}{\beta^\alpha \Gamma(\alpha)} \int_0^x x^{\alpha-1} e^{-\frac{x}{\beta}} dx. \quad (12)$$

The SPI can be calculated as follows:

$$\text{SPI} = S \frac{t - (a_2 t - a_1) + a_0}{[(b_3 + b_2)t + b_1]t + 1.0}, t = \sqrt{\ln \frac{1}{G(x)}}. \quad (13)$$

In Equation (13), $G(x)$ is gamma function related rainfall probability distribution, S is the probability density negative coefficient (if $G(x) \leq 0.5$, $S = -1$) and positive coefficient (if $G(x) > 0.5$, $S = 1$), and x is the amount of rainfall and the constant values are given as $a_0 = 2.5155$, $a_1 = 0.8028$, $a_2 = 0.0103$, $b_1 = 1.4327$, $b_2 = 0.1892$, $b_3 = 0.0013$.

3.8 | Standardized precipitation evapotranspiration index

The difference between monthly precipitation (P) and monthly potential evapotranspiration (PET) gives the SPEI; it replaces SPI and accounts for the temperature factor. Global warming stimulates changes in surface evaporation, which is more sensitive to drought reactions. The SPEI was proposed based on the SPI by C. W. Thornthwaite in 2010 (Thornthwaite, 1948; Vicente-Serrano *et al.*, 2010). The complete SPEI theory can be described and calculated as follows:

$$\text{PET} = 16 \times \left(\frac{N}{12} \right) \times \left(\frac{m}{30} \right) \times \left(10 \times \frac{T_i}{I_h} \right)^a, \quad (14)$$

$$I_h = \sum_{i=1}^{12} i, i = [\max(T_i, 0)]^{1.514}, \quad (15)$$

where T_i , m , and N are the monthly mean temperature ($^{\circ}\text{C}$), the number of days in a month, and the monthly mean sunshine hour, and I is the 12-month thermal indexes calculated as Equation (15), and a can be calculated as the following formula:

$$a = 6.75 \times 10^{-7} I^3 - 7.71 \times 10^{-5} I^2 + 1.79 \times 10^{-5} I + 0.492, \quad (16)$$

and the difference ($D_i = P_i - \text{PET}_i$) between precipitation (P_i) and potential evapotranspiration (PET_i).

In order to calculate the value of SPEI, the three-parameter log-logistic probability density function is calculated as follows:

$$f(x) = \frac{\beta}{\alpha} \left(\frac{x - \gamma}{\alpha} \right) \left[1 + \left(\frac{x - \gamma}{\alpha} \right) \right]^{-2}, \quad (17)$$

where γ represents the origin parameters and thus the P log-logistic probability distribution function is given by

$$P = \left[1 + \left(\frac{\alpha}{x - \gamma} \right) \right]^{-1}. \quad (18)$$

The SPEI can easily be calculated as the standardized values of $F(x)$ (Vicente-Serrano *et al.*, 2010) with the following formula: where the values of a_0 , a_1 , a_2 , b_1 , b_2 , and b_3 are the same as those for the SPI.

$$\text{SPEI} = \begin{cases} + \left(W - \frac{a_0 + a_1 W + a_2 W^2}{1 + b_1 W + b_2 W^2 + b_3 W^3} \right), & P > 0.5 \text{ and } W = \sqrt{-2 \ln(1-P)} \\ - \left(W - \frac{a_0 + a_1 W + a_2 W^2}{1 + b_1 W + b_2 W^2 + b_3 W^3} \right), & P \leq 0.5 \text{ and } W = \sqrt{-2 \ln(P)} \end{cases}, \quad (19)$$

TABLE 6 Monthly, seasonal, and annual means of T_{\max} , T_{\min} , and T_{mean} and rainfall distribution over Anantapur during 2001–2020

	Rainfall (mm)				T_{\max}	T_{\min}		T_{mean}		
	Mean	SD	CV (%)	% contribution to annual rainfall		Mean	SD	Mean	SD	
January	10	11	113	2	35.62	2.79	25.80	2.54	30.71	2.49
February	7	8	116	1	34.03	3.21	24.09	2.82	29.06	2.84
March	11	10	95	2	34.38	3.76	24.87	3.16	29.63	3.37
April	26	22	84	5	33.17	3.29	23.38	2.90	28.27	2.94
May	55	35	64	10	33.48	3.96	23.72	2.96	28.60	3.33
June	58	49	83	11	33.75	3.58	23.73	3.35	28.74	3.31
July	52	52	100	10	33.20	3.34	24.01	3.04	28.61	3.05
August	88	80	90	17	34.43	7.67	22.80	2.69	28.62	4.95
September	122	82	67	23	32.88	3.29	22.40	2.96	27.64	2.77
October	95	53	56	18	32.28	4.00	22.60	2.99	27.44	3.18
November	28	30	107	5	32.01	2.63	21.08	2.72	26.55	2.38
December	5	7	122	1	32.73	2.78	21.32	3.38	27.03	2.73
Winter	22	8	37	4	31.49	1.69	19.41	2.79	25.45	1.01
Summer	92	45	49	18	38.59	2.37	25.80	2.76	32.20	1.36
Monsoon	321	164	51	61	33.41	1.87	24.75	1.76	29.08	1.02
Postmonsoon	123	59	48	24	30.81	1.83	22.08	2.42	26.45	1.29
Annual	523	193	37	100	35.34	4.90	22.39	3.05	28.86	2.44

Abbreviations: CV, coefficient of variation; T_{\max} , maximum temperature; T_{\min} , minimum temperature; T_{mean} , mean temperature; SD, standard deviation.

According to the SPEI definition, if the SPEI value is above 0, it suggests a wet climate process, and if it is below 0, it indicates a dry climatic process. The dry and the wet climate processes alternate more frequently at short timescales than at long timescales based on the criterion above. The SPEI can be calculated at multiple timescales based on meteorological data, that is, 1, 3, 6, 12, and 24 months. The 1-month SPEI indicated short-term water deficit and excess, while the 3-month SPEI showed seasonal moisture conditions that provide climatic balance. The 6-month SPEI show the intermediate-term wet and dry climate events. The long-term dry and wet climate process can be observed in 12- and 24-month SPEI droughts. Thus, the duration of the wet and dry climate process is longer in long-term timescales and shorter in short-term timescales. The climatic trend and slope values of SPI/SPEI at the multiple timescales, the Mann-Kendall statistical test and Sen's slope estimator are used. The drought indices had significant trends at multiple timescales. The corresponding results are summarized in Table 4.

4 | RESULTS AND DISCUSSION

4.1 | Preliminary analysis

Long-term rainfall, min, max, and daily mean temperature and their SD and CV on monthly, seasonal and

annual basis were analysed in the preliminary analysis from 2001 to 2020 and the results are presented in Table 6. The long-term monthly rainfall CV ranged from 37 to 122%, with a monthly mean of 78%, indicating that rainfall over Anantapur is highly variable. The observed monthly mean and SD of maximum rainfall for the study period is 122 ± 82 mm, with a CV of 67% in September, whereas the minimum rainfall is 5 ± 7 mm with 122% of CV in December. A high significant variation of rainfall CV was observed in December (122%), followed by February (116%) and January (113%). The annual rainfall varies from 218 to 957 mm, with monsoon (46–793 mm) being the highest, followed by postmonsoon contributes (33–217 mm), summer (7–161 mm) and winter (1–27 mm). During the study period, Anantapur receives an average annual rainfall of 523 ± 193 mm, with a CV of 37%. The seasonal contribution of annual rainfall is maximum during monsoon (58%) followed by postmonsoon (22%), summer (16%), and winter (4%). The monsoon and postmonsoon seasons were considered as the wet seasons, and the winter and summer as the dry seasons. On the annual basis, the extreme wettest and driest years were observed in 2007 (957 mm) and 2003 (218 mm) during the study period. Those living in drought-prone and flood-prone regions experience drastic impacts from weather extremes (droughts and floods). The seasonal maximum mean temperature (T_{mean}) were observed

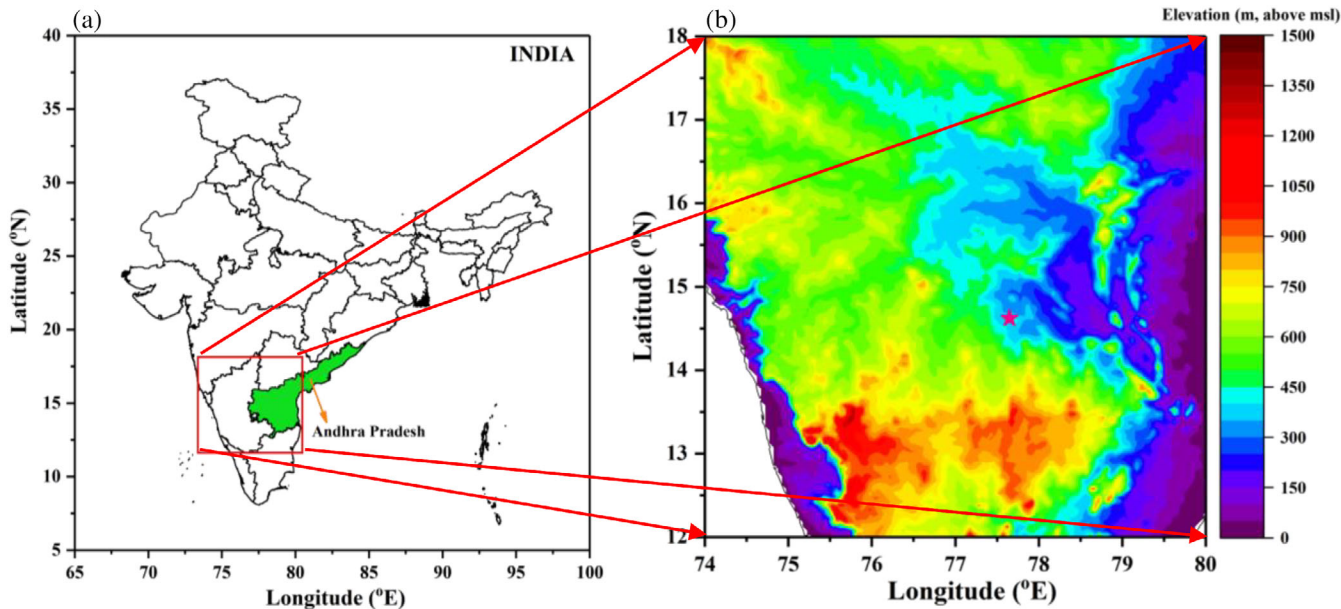


FIGURE 1 (a) Location of Andhra Pradesh State (shaded area in the red square) in India (b) the elevation (m) map of southern peninsular India (SRTM DEM, 3 arcsec) and the pink “*” represents the geographical location of the measurement site

during summer is 32.20 ± 1.36 , followed by the monsoon, postmonsoon, and winter is 29.08 ± 1.02 , 26.45 ± 2.44 , and $25.45 \pm 1.01^\circ\text{C}$, respectively.

4.2 | Temporal trends of temperature and rainfall

The monthly, seasonal, and annual variations of meteorological parameters, particularly temperature (maximum, minimum, and mean) and rainfall data over 20 years (2001–2020), were analysed. In the MK nonparametric regression test, parameters like MK statistic, Kendall's tau, and Sen's slope are portrayed in Table 3. The monthly mean maximum temperature (T_{max}) showed statistically decreasing trends during the study period. The monthly mean minimum temperature (T_{min}) also shows a decreasing trend in all the months except in November ($0.09^\circ\text{C}\cdot\text{year}^{-1}$) and December ($0.102^\circ\text{C}\cdot\text{year}^{-1}$). Overall, the T_{mean} indicates an increasing trend from June to December ($0.015\text{--}0.069^\circ\text{C}\cdot\text{year}^{-1}$) and a decreasing trend from January to May (-0.022 to $-0.078^\circ\text{C}\cdot\text{year}^{-1}$). The rainfall shows an increasing trend in the months of April, May, June, July, September, and December, whereas a decreasing trend was observed in the months of August, October, and November. No trends were observed in the months of January, February, and March. The increasing trend of rainfall ranges from 0.255 to $5.202 \text{ mm}\cdot\text{year}^{-1}$, whereas the decreasing trend values range from -0.166 to $-1.684 \text{ mm}\cdot\text{year}^{-1}$ during the study period (Figures 1 and 2).

The time series of seasonal temperature (T_{max} , T_{min} , and T_{mean}) and rainfall with linear regression trend lines are shown in Figure 3. The seasonal trend statistics of T_{max} show a decreasing trend during all seasons at a 90% significance level. The significant decrease trend of T_{max} was observed during the summer ($-0.185^\circ\text{C}\cdot\text{year}^{-1}$), followed by winter ($-0.119^\circ\text{C}\cdot\text{year}^{-1}$), monsoon ($-0.073^\circ\text{C}\cdot\text{year}^{-1}$), and postmonsoon ($-0.027^\circ\text{C}\cdot\text{year}^{-1}$) seasons. Thus, the results show that the T_{max} decreases over the study region, which indicates that the region is experiencing a cooling effect. The T_{min} linear fit also shows a decreasing trend during all seasons. During the winter, summer, monsoon, and postmonsoon, the trend magnitudes were -0.126 , -0.208 , -0.085 , and $-0.025^\circ\text{C}\cdot\text{year}^{-1}$, respectively (Figure 3b). The overall T_{mean} experiences no significant decreasing trend during winter ($-0.069^\circ\text{C}\cdot\text{year}^{-1}$) and summer ($-0.081^\circ\text{C}\cdot\text{year}^{-1}$) seasons and an increasing trend during monsoon ($0.012^\circ\text{C}\cdot\text{year}^{-1}$) and postmonsoon ($0.034^\circ\text{C}\cdot\text{year}^{-1}$) seasons (Figure 3c), which implies that monsoon and premonsoon seasons are becoming warmer. It indicates that the dry seasons are experiencing the cooling effect, and the wet seasons are experiencing the warming effect. The noticeable increasing trend in the rainfall time series is observed on the seasonal scale in all the seasons except the postmonsoon season, and the linear fits are represented in Figure 3d. During the winter, summer, monsoon, and postmonsoon seasons, the magnitudes of rainfall trends with a corresponding value of Sen's estimator are 0.5 , 2.137 , 6.901 , and $-2.276 \text{ mm}\cdot\text{year}^{-1}$,

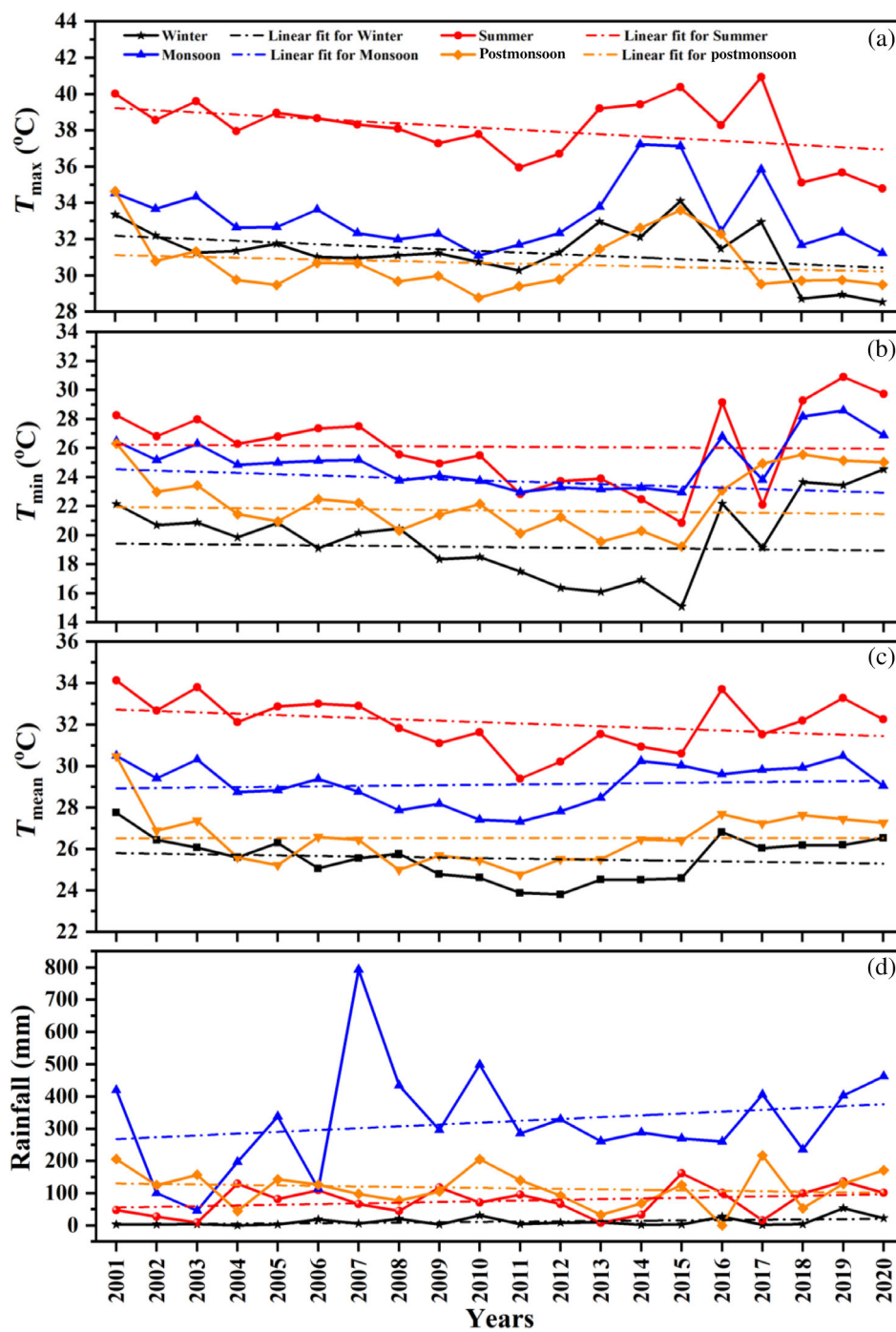


FIGURE 2 Seasonal time series of (a) maximum temperature (T_{\max}), maximum temperature (T_{\min}) and mean temperature (T_{mean}) and (b) rainfall (RF) from 2001 to 2020

respectively, with a 90% of the significance level. The variability in rainfall affects water supply at different stages of crop development to meet the crop water demand (Krishan *et al.*, 2018).

The MK trend test and Sen's slope estimator result indicates that the annual time series of T_{\max} , T_{\min} , and T_{mean} shows a decreasing trend; however not statistically significant with a magnitude of -0.123 , -0.121 , and $-0.022^{\circ}\text{C}\cdot\text{year}^{-1}$, respectively, and the results are plotted in Figure 4a. Reductions in T_{\min} and T_{\max} in the study area were attributed to the overall decrease in T_{mean} .

Therefore, the long-term decreasing trend in the annual temperature time series is evident of a cooling in the study location. The rainfall linear fit shows an increasing trend of $8.979 \text{ mm}\cdot\text{year}^{-1}$ with a 90% significance level.

Table 7 represents the change point detection results obtained using the Pettit test. To identify the breakpoint year, change point detection of T_{\max} , T_{\min} , T_{mean} , and rainfall series were analysed. The monthly rainfall shows the change point year in most of the months observed between 2003 and 2009, while others show 2011 (November), 2015 (January), and 2019 (April). Change

FIGURE 3 Annual time series of (a) maximum temperature (T_{\max}), minimum temperature (T_{\min}) and mean temperature (T_{mean}) and (b) rainfall (RF) from 2001 to 2020. The dashed lines black, red, blue, and orange indicate the trend lines of winter, summer, monsoon, and postmonsoon seasons

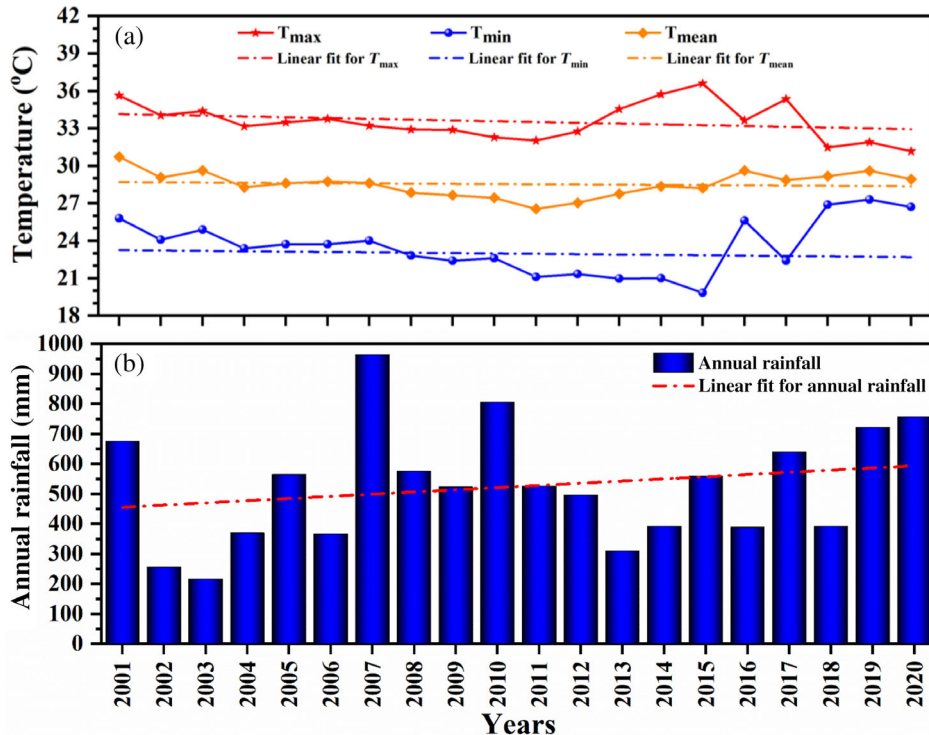
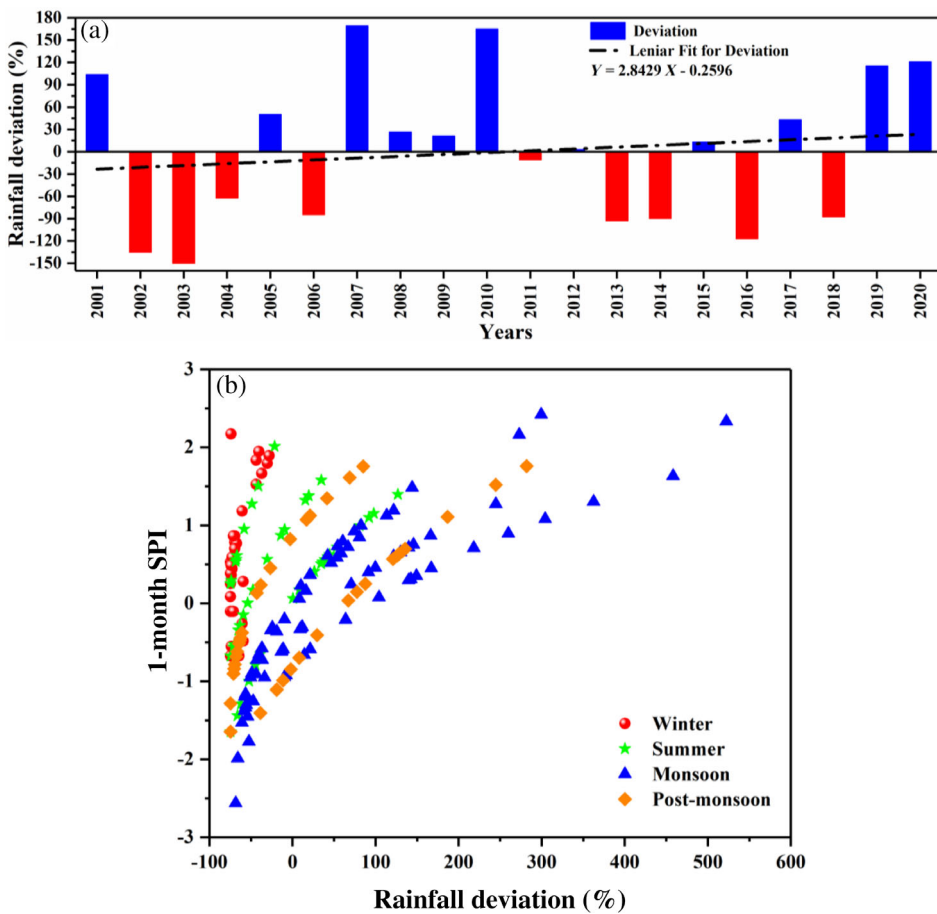


FIGURE 4 (a) Annual rainfall deviation with the linear trend and the black dashed line indicates the trend of the series, the positive deviations (blue bars) indicating excess rainfall and negative deviations (red bars) indicating deficit rainfall. (b) Scatter plots between rainfall deviation and 1-month SPI over Anantapur for the study period



point year of T_{\max} was observed between 2004 and 2008 while a few months shown between 2016 and 2019 and

T_{\min} were observed between 2003 and 2010 except in December (2018), while T_{mean} were observed between

TABLE 7 Result of the change point detection in different timescales of rainfall, T_{\max} , T_{\min} , and T_{mean}

	Rainfall	T_{\max}	T_{\min}	T_{mean}
January	2015	2017	2008	2008
February	2008	2017	2010	2010
March	2008	2007	2011	2007
April	2019	2019	2011	2008
May	2003	2019	2010	2008
June	2015	2006	2010	2006
July	2006	2008	2009	2003
August	2006	2007	2009	2014
September	2019	2004	2007	2006
October	2003	2016	2007	2003
November	2011	2004	2003	2017
December	2009	2018	2018	2007
Winter	2019	2017	2010	2010
Summer	2003	2019	2010	2008
Monsoon	2006	2006	2010	2003
Postmonsoon	2011	2007	2007	2003
Annual	2006	2019	2010	2007

2003 and 2010 except in August, November, and December (2018). The seasonal change point of rainfall was observed during winter (2019), summer (2003), monsoon (2006), and postmonsoon (2011). T_{\max} was observed during winter (2017), summer (2019), monsoon (2006), and postmonsoon (2007), whereas T_{\min} was observed during winter, summer, and monsoon seasons in the year 2010 and postmonsoon in the year 2007. Finally, the T_{mean} were observed during winter (2010), summer (2008), monsoon, and postmonsoon in 2003. The annual change point of rainfall, T_{\max} , T_{\min} , and T_{mean} , was observed in 2006, 2019, 2010, and 2007, respectively.

4.3 | Deviation of annual rainfall trend and comparison with 1-month SPI

Over the last two decades, Anantapur rainfall indices characterized by high annual variability from 2001 to 2021 are shown in Figure 5a. Thus, two significant excess rainfall years were noticed in 2007 and 2010 (wettest years), and the two high deficit rainfall years were detected in 2002 and 2003 (driest years). The trend line of rainfall deviation shows an increasing trend with a magnitude of 2.84% per year for the period 2001–2020. It indicates that the region is shifting from drier to wetter conditions.

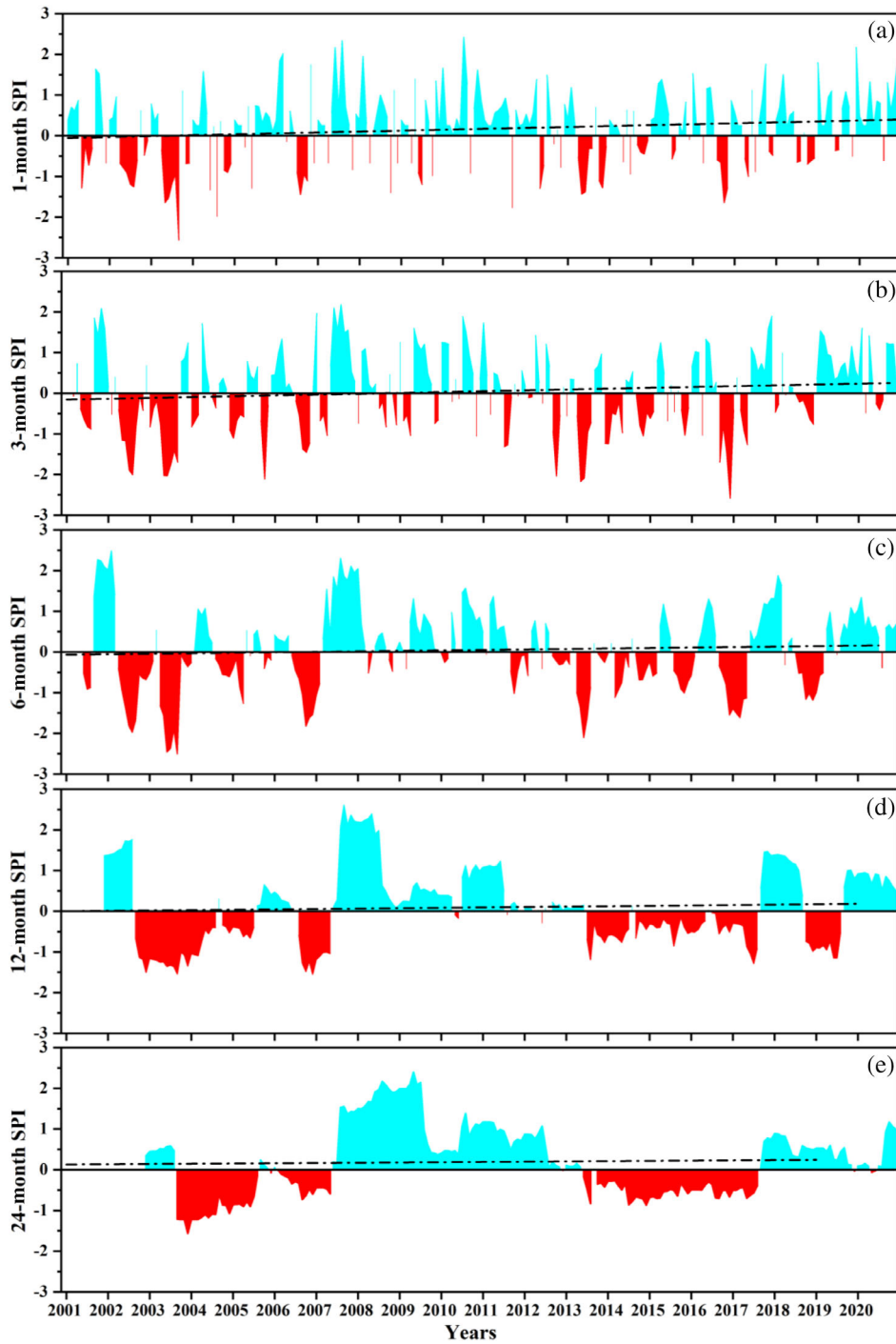
Figure 5b shows the scatter plots between rainfall deviation and 1-month SPI for different seasons. It

showed a wider range in negative and positive directions. It is evident that particularly in the low rainfall in a study region, a very high negative deviation of -20 to -80% represents deficient rainfall, corresponding to the SPI values of 2 to -0.75 during the winter season. On the other hand, most of the negative rainfall deviation lies between -20 and -80% during the summer. The SPI values vary from -1.5 to 2, whereas a few points deviated towards positive SPI values ranging from 0 to 1.5 with a -20 to 110% rainfall deviation. The monsoon season is majorly responsible for the excess rainfall over the study region, and the rainfall deviation varies from -80 to 500%. Most of the monsoon months show excess rainfall, corresponding SPI values indicating near-normal rainfall to extremely wet. The second-highest precipitation was observed in the postmonsoon season discussed in the second-highest precipitation. During this postmonsoon season, the negative SPI values were less than -0.2; a negative deviation was observed at less than -20% rainfall. The positive rainfall deviation was observed on the higher side, ranging from 0 to 500%, and the corresponding SPI values also show greater than 0.1. These results are in good agreement with Naresh Kumar *et al.*, 2009, who studied the SPI index for the Anantapur and Khammam districts from 1969 to 2007. The above results show that some monsoon and postmonsoon months show excess rainfall while others show deficit rainfall. From an agricultural point of view, the monsoon and postmonsoon seasons play a vital role in the growth of different crops in these seasons.

4.4 | Temporal evolution droughts by SPI and SPEI

Figures 6 represents the temporal distribution of drought conditions by the monthly SPI using rainfall measurements at various timescales 1, 3, 6, 12, and 24 months from 2001 to 2020 over the study region. The temporal variations of 1-month SPI (Figure 6a) values indicate 23 short-term drought events were identified with 1 “extremely dry” (-2.55 in September 2003), 5 “severely dry,” and 17 “moderately dry” droughts and had more intense droughts with the duration of 2–4 months. As can be seen from the 3-month SPI (Figure 6b), 31 seasonal droughts events were identified during the period with 8 “extremely dry,” 4 “severely dry,” and 19 “moderately dry” droughts and most of the events lasted for about 2–3 months. Thus, on a 3-month scale, dry and wet periods are highly frequent. Figure 6c shows the temporal distribution of 6-month SPI, similar to the 3-month SPI. It shows that 33 drought intermediate-term drought events with 4 “extremely dry,” 12 “severely dry,” and

FIGURE 5 Long-term temporal patterns of standardized precipitation index (SPI) at the (a) 1-, (b) 3-, (c) 6-, (d) 12-, and (e) 24-month timescales in Anantapur during 2001–2020. The black dashed line indicates the trend of the series, with the positive (cyan shaded area) values indicating wetness and negative (red shaded area) values representing dryness



17 “moderately dry” droughts were observed during the period. The distribution of 12-month SPI shows that more intense groundwater droughts characterize earlier decades. The temporal variation of 12-month SPI values (Figure 6d), 3 “severely dry” and 29 “moderately dry” long-term drought events have occurred for 3–11 months. Similar to the 12-month SPI, the 24-month SPI (Figure 6e) values indicate the 1 “severely dry” (-1.55 in December 2003) and 29 “moderately dry” long-term drought events. These results indicate that extreme

droughts occurred in 2002, 2003, 2005, 2012, 2013, and 2016 with a maximum of -2.5822 in December 2016, severely affecting the study region’s agriculture. The SPI drought trend over the study regions shows a significant ($p < .05$) increasing trend on all timescales, such as 0.0015 , 0.0019 , 0.0014 , 0.0009 , and $0.0008 \text{ month}^{-1}$ for 1-, 3-, 6-, 12-, and 24-month SPI, respectively.

According to the temporal distribution of 1-month SPEI (Figure 7a), 41 short-term drought events were identified with 4 “extremely dry,” 9 “severely dry,” and

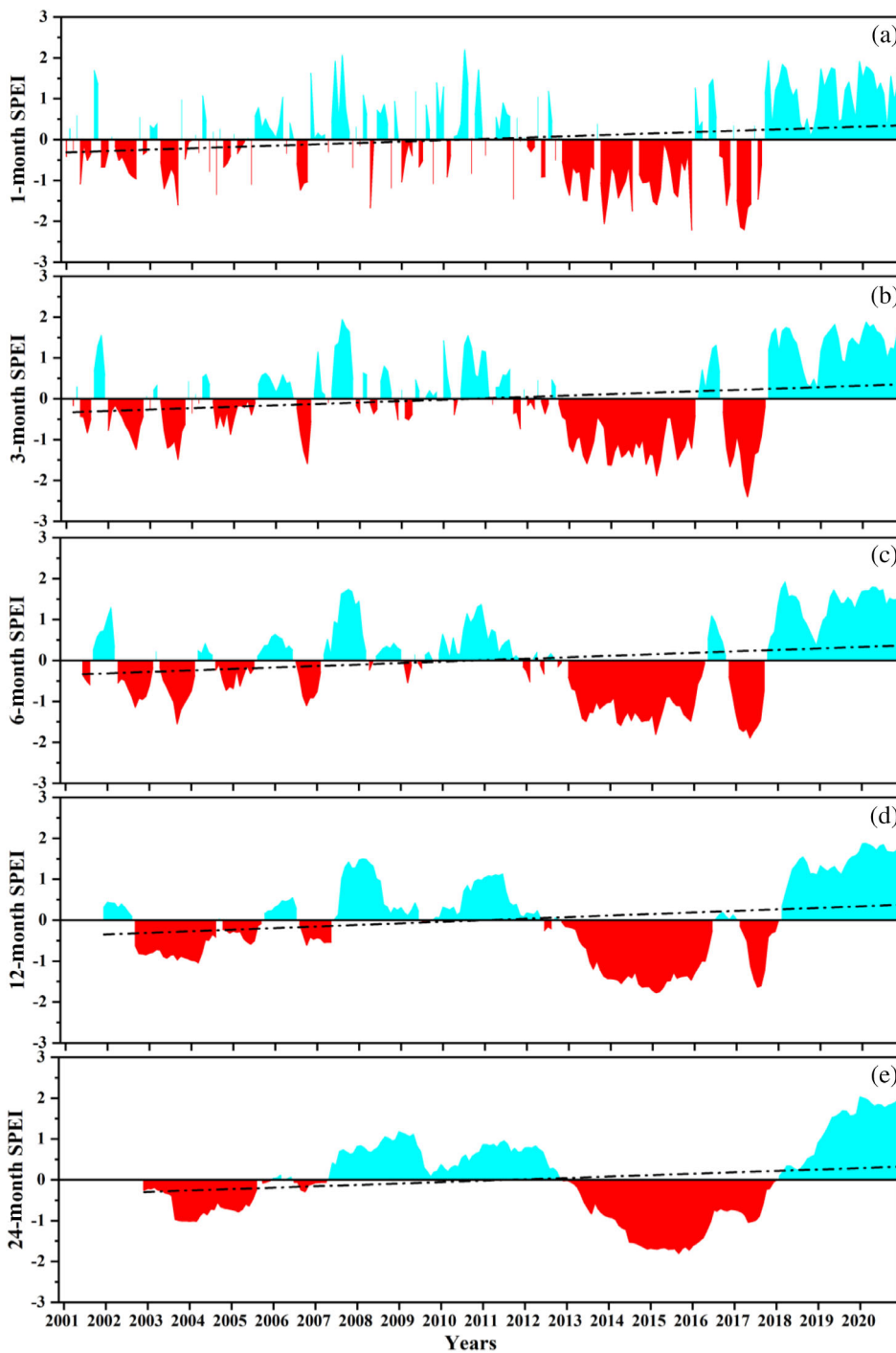


FIGURE 6 Long-term temporal patterns of standardized precipitation evapotranspiration index (SPEI) at the (a) 1-, (b) 3-, (c) 6-, (d) 12-, and (e) 24-month timescales in Anantapur during 2001–2020. The black dashed line indicates the trend of the series, with the positive (cyan shaded area) values indicating wetness and negative (red shaded area) values representing dryness

28 “moderately dry” droughts and are more intense (−2.209 in December 2015) droughts. Thus, most of the drought’s duration is 3–6 months. From Figure 7b, the 3-month SPEI indicates the dry and the wet climate process were identified alternatively at least 40 times during the study period. From 6-month SPEI (Figure 7c), we have identified 45 intermediate-term wet and dry climate events with 12 “severely dry” and 33 “moderately dry” droughts; thus, the duration of most of the drought events is 6–9 months. Monitoring interannual droughts

were achieved better with the long-term 12- and 24-month SPEI. The temporal distribution of 12-month SPEI is shown in Figure 7d, and 39 long-term wet and dry climate events were identified with 12 “severely dry” and 27 “moderately dry” droughts with a duration of 5–7 months. Similar to the temporal distribution of 12-month SPEI, the 24-month SPEI is presented in Figure 7e; a total of 35 long-term wet and dry climate events were identified from 2014 to 2016, with 15 “severely dry” occurring in 2003, 2004, 2014, 2016, and

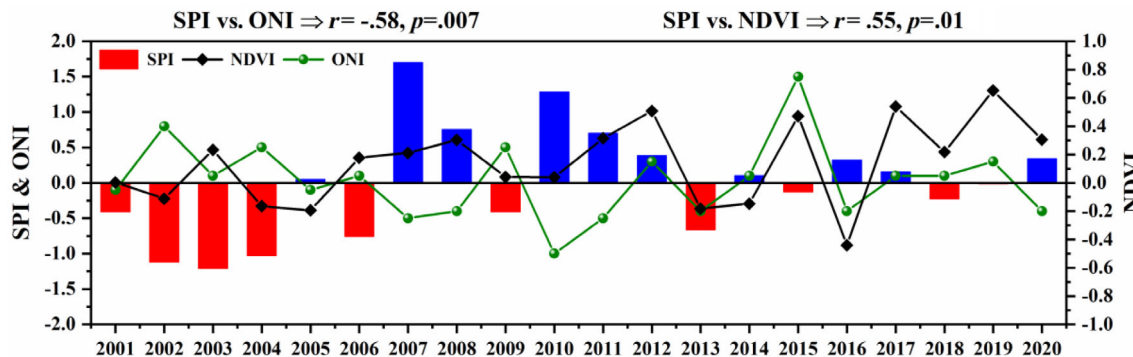


FIGURE 7 The time series plot shows the relations between 1-month SPI vs. El Niño/La Niña events and 1-month SPI vs. NDVI during 2001–2020. The black dashed line indicates the trend of the series, the positive (blue bars) values indicating wetness and negative (red bars) values representing dryness

2017, and 20 “moderately dry” droughts occurred between 2014 and 2016. The Sen's slope trend values of SPEI at 1-, 3-, 6-, 12-, and 24-month timescales show a significant ($p < .05$) increasing trend as temporally with magnitudes of 0.003, 0.0031, 0.0035, 0.004, 0.0045 month $^{-1}$, respectively.

The results from both SPI and SPEI indicates alternating drought and wet periods and consistency on the different timescales. From 12-month SPI values, two wetting and two drying periods are noticed, and the drying period started in September 2003 and continued till June 2004. In addition, the drought ended, and a wetting period began from August 2008 to June 2012. Again, the drying period started with low magnitudes from August 2013 to July 2017, while the wetting period from September 2017 continued till the end of the study period. The drying and wetting period from the 12-month SPEI is observed during the same period with a lower magnitude from 2001 to 2010 and higher from 2011 to 2020 than the SPI. Interestingly, the study region has been experiencing the alternating 5 years wetting and 5 years drying periods. From 24-month SPI and SPEI, the long-term droughts are identified in both the indexes with different magnitudes, showing moderate drought years in 2003 and 2004. The 24-month SPEI identified the severe droughts in 2014, 2015, and 2016, but the SPI drought index uses precipitation-based metrics only and did not recognize these drought conditions. On the other hand, the SPEI considers both precipitation and temperature. Despite this, SPEI is more sensitive to drought changes since it considers evapotranspiration. Using SPEI as a drought index was more accurate and sensitive than using SPI, as it could figure out more complex dry/wet conditions. Based on historical drought data, the SPEI results were more appropriate for monitoring interannual droughts due to the longer timescales of the SPEI. Figures 6 and 7 show that the droughts were more severe

during 2002–2006 and 2013–2017 than during the other periods. Extreme, severe, and mild droughts are more likely to occur over long-term, short-term, and medium-term periods. The significant increasing trend in all SPI and SPEI timescales indicates reducing drought severity and shows the study region changing from drying to wetting.

The frequency of occurrence probability of droughts is mentioned in Table 8. Different timescales of the SPI and SPEI show changes in drought frequency. Droughts persist longer, and short-term droughts show abrupt transitions between dry and wet conditions, even though the number of occurrences decreases with increasing timescale. From SPI, 10, 13, 14, and 14, 6% of droughts are identified by 1-, 3-, 6-, 12-, and 24-month timescales, respectively, while 17, 18, 19, 17, and 16% of droughts are identified by 1-, 3-, 6-, 12-, and 24-month SPEI timescales during the study period.

4.5 | Temporal variations and correlation between the monsoon SPI, NDVI, and ENSO

The comparison of the time series of 1-month SPI and El Niño (drying)/La Niña (wetting) events, 1-month SPI and NDVI during the study period (2001–2020) is shown in Figure 7. The drought index (SPI < 0) is shown for multiple years (e.g., 2001, 2002, 2003, 2004, 2006, 2009, 2013, 2015, 2018, 2019), which indicated an El Niño (e.g., 2002, 2004, 2006, 2009, 2014, 2015, 2018) event and NDVI decline (e.g., 2002, 2004, 2005, 2013, 2014, 2016) occurred during this period. The very strong El Niño was observed in 2015 with a magnitude of 1.5, while the strong La Niña was observed in 2007 and 2010 with magnitudes of -0.5 and -1 , respectively. In addition, the SPI > 0 shows that very wet (0.327), moderately wet (0.365), and near

TABLE 8 Occurrence probability (%) of droughts

Drought severity class	SPI			SPEI						
	1 month	3 months	6 months	12 months	24 months	1 month	3 months	6 months	12 months	24 months
Extremely wet	2	1	3	4	3	1	9	9	7	9
Very wet	5	5	4	3	6	7	9	9	7	9
Moderately wet	8	11	9	11	8	11	11	9	14	5
Near normal	75	69	70	67	77	64	62	63	62	70
Moderately dry	7	8	7	13	6	12	13	14	12	7
Severely dry	2	2	5	1	4	4	4	5	5	9
Extremely dry	3	2			2	1				

normal (0.292) were observed in 2007, 2010, and 2015, respectively. According to these results, ENSO impacts on vegetation declines over the study region are partly related to compound dry and wet events. Hao *et al.* (2020) analysed the comparison of the time series of Niño3.4, SPI, and NDVIA from 1982 to 2015. To further explore these impacts of ENSO on dry/wet conditions over the measurement location, the Pearson's correlation coefficients between SPI and ONI, SPI and NDVI were estimated during JJA from 2001 to 2020. The significant negative correlation between SPI and ONI is -0.58 , with a *p*-value of .007. The Pearson correlation coefficient between SPI and NDVI is 0.55, which is insignificant. The reason is that precipitation does not affect vegetation instantly (Dutta *et al.*, 2013). The effects of precipitation in a given month do not affect vegetation during the same month, but their effects become evident over longer periods. Since the longer-scale SPIs tend to smooth the SPI values and diminish the variances in precipitation data, correlations did not improve from 6 to 12 months (Ji and Peters, 2003). Bhavani *et al.* (2017) found that the Pearson correlation coefficient between NDVI and SPI was 0.49 over the Anantapur region. Table 9 presents the comparison data of the time series of 1-month SPI, NDVI, and ENSO from 2001 to 2020.

5 | SUMMARY AND CONCLUSIONS

The present study uses Mann–Kendall and Sen's slope estimators to analyse the long-term variations and trends in monthly temperatures and precipitation from 2001 to 2020. These results demonstrate the pattern of changes in temperature and rainfall as the most significant climate factors. The main conclusions are listed as follows:

- The mean temperature analysis over Anantapur implies a decreasing trend in winter and summer, which means that these seasons are becoming cooling, while the monsoon and postmonsoon rainfall have increasing trends, which implies warmer. However, it was also found that rainfall does vary significantly depending on the season. Hence, there was an increasing trend in winter, summer, and monsoon seasons, while a decreasing trend was observed during the postmonsoon season.
- The annual time series of T_{mean} shows the decreasing trend, whereas rainfall was noticed as an increasing trend over the study location. Therefore, the measurement location is shifted from the drying to the wetting region.
- The rainfall departure analysis gives the 25% experiencing the excess, 35% normal, and 40% deficit

TABLE 9 The comparison of the time series of 1-month SPI, NDVI, and ENSO from 2001 to 2020

Year	1-month SPI	NDVI	ENSO
2001	-0.409	0.251	-0.1
2002	-1.119	0.287	0.8
2003	-1.213	0.237	0.1
2004	-1.031	0.306	0.5
2005	0.050	0.299	-0.1
2006	-0.761	0.287	0.1
2007	1.702	0.359	-0.5
2008	0.757	0.313	-0.4
2009	-0.411	0.287	0.5
2010	1.286	0.386	-1.0
2011	0.702	0.333	-0.5
2012	0.387	0.274	0.3
2013	-0.667	0.280	-0.4
2014	0.100	0.288	0.1
2015	-0.128	0.317	1.5
2016	0.324	0.384	-0.4
2017	0.159	0.296	0.1
2018	-0.227	0.312	0.1
2019	-0.016	0.290	0.3
2020	0.345	0.448	-0.4

rainfall years were observed, and the two severely dry years observed in the study period were 2002 and 2003. In addition, the rainfall deviation shows an increasing trend, indicating that the region is shifting from drier to wetter conditions.

- The SPI and SPEI, a climatological drought index show that, the droughts were more severe from 2002 to 2006 and from 2013 to 2017 than the rest periods of both indices.
- Statistical significance for trends in SPI and SPEI time series and drought characteristics were also examined using the Mann–Kendall test and noticed a significant increasing trend with different magnitudes over all timescales. It indicates that the study region changes from drying to wetting.
- The assessment of the droughts and the response of vegetation based on SPI, ENSO and NDVI are observed during the study period. A significant negative correlation (-0.58) was obtained between SPI and ONI, and no significant positive correlation (0.55) was obtained between SPI and NDVI.

From the above findings of this study, it is necessary to pursue further studies in order to explore how changes

in these factors, especially the intersections of rainfall variability and temperature variations, have affected Anantapur's crop production and consequently impacted the livelihoods and well-being of the rural population, especially marginalized rural communities that depend mainly on subsistence agriculture.

AUTHOR CONTRIBUTIONS

Rama Gopal Kotalo: Review and editing (equal). **Lokeswara Reddy Thotli:** Conceptualization (lead); writing – original draft (lead); formal analysis (lead); writing – review and editing (equal). **Balakrishnaiah Gugamsetty:** Software (lead); writing – review and editing (equal). **Raja Obul Reddy Kalluri:** Methodology (lead); writing – review and editing (equal). **Bhavyasree Akkiraju:** Designed the study; data collection (equal). **Chakradhar Rao Tandule** and **Siva Sankara Reddy Lingala:** Conceptualization (supporting); writing – original draft (supporting); writing – review and editing (equal).

ACKNOWLEDGEMENT

The authors want to express gratitude to the ISRO for their financial support under ISRO-GBP (NOBLE) project.

ORCID

Lokeswara Reddy Thotli  <https://orcid.org/0000-0002-4627-9639>

Rama Gopal Kotalo  <https://orcid.org/0000-0001-9065-0856>

REFERENCES

- Agilan, V. and Umamahesh, N.V. (2017) What are the best covariates for developing non-stationary rainfall intensity–duration–frequency relationship? *Advances in Water Resources*, 101, 11–22. <https://doi.org/10.1016/j.advwatres.2016.12.016>.
- Alam, N.M., Sharma, G.C., Moreira, E., Jana, C., Mishra, P.K., Sharma, N.K. and Mandal, D. (2017) Evaluation of drought using SPEI drought class transitions and log-linear models for different agro-ecological regions of India. *Physics and Chemistry of the Earth*, 100, 31–43. <https://doi.org/10.1016/j.pce.2017.02.008>.
- Allen, P. (2011) Professional artist management and its principles. In: Allen, P. (Ed.) *Artist Management for the Music Business*, 2nd edition. Boston: Focal Press, pp. 1–11.
- Animashaun, I.M., Oguntunde, P.G., Akinwumiju, A.S. and Olubanjo, O.O. (2020) Rainfall analysis over The Niger central hydrological area, Nigeria: variability, trend, and change point detection. *Scientific African*, 8, e00419. <https://doi.org/10.1016/j.sciaf.2020.e00419>.
- Animesh, C., Dutta, D., Bera, D. and Kundu, A. (2021) Regional variation of drought parameters and long-term trends over India using standardized precipitation evapotranspiration index. *Journal of Environmental Management*, 296, 113056.

- Anteneh, A.Z., Melesse, A.M., Abtew, W. and Whitman, D. (2019) Rainfall trend and variability in Southeast Florida: implications for freshwater availability in the Everglades. *PLoS One*, 14(2), 1–20. <https://doi.org/10.1371/journal.pone.0212008>.
- Asfaw, A., Simane, B., Hassen, A. and Bantider, A. (2018) Variability and time series trend analysis of rainfall and temperature in northcentral Ethiopia: a case study in Woleka sub-basin. *Weather and Climate Extremes*, 19, 29–41. <https://doi.org/10.1016/j.wace.2017.12.002>.
- Bhavani, P., Chakravarthi, V., Roy, P.S., Joshi, P.K. and Chandrasekar, K. (2017) Long-term agricultural performance and climate variability for drought assessment: a regional study from Telangana and Andhra Pradesh states, India. *Geomatics, Natural Hazards and Risk*, 8(2), 822–840. <https://doi.org/10.1080/19475705.2016.1271831>.
- Buishand, T.A. (1982) Some methods for testing the homogeneity of rainfall records. *Journal of Hydrology*, 58(1–2), 11–27. [https://doi.org/10.1016/0022-1694\(82\)90066-X](https://doi.org/10.1016/0022-1694(82)90066-X).
- Celso, S.A.G., Brasil Neto, R.M., do Nascimento, T.V.M., da Silva, R.M., Mishra, M. and Frade, T.G. (2021) Geospatial drought severity analysis based on PERSIANN-CDR-estimated rainfall data for Odisha state in India (1983–2018). *Science of the Total Environment*, 750, 141258.
- Chakraborty, D., Saha, S., Singh, R.K., Sethy, B.K., Kumar, A., Saikia, U.S., Das, S.K., Makdoh, B., Borah, T.R., Nomita Chanu, A., Walling, I., Rolling Anal, P.S., Chowdhury, S. and Daschaudhuri, D. (2017) Trend analysis and change point detection of mean air temperature: a spatio-temporal perspective of north-eastern India. *Environmental Processes*, 4(4), 937–957. <https://doi.org/10.1007/s40710-017-0263-6>.
- Cook, B.I., Smerdon, J.E., Seager, R. and Coats, S. (2014) Global warming and 21st century drying. *Climate Dynamics*, 43(9), 2607–2627. <https://doi.org/10.1007/s00382-014-2075-y>.
- Dabanhı, İ., Mishra, A.K. and Şen, Z. (2017) Long-term spatio-temporal drought variability in Turkey. *Journal of Hydrology*, 552, 779–792. <https://doi.org/10.1016/j.jhydrol.2017.07.038>.
- Danandeh Mehr, A. and Vaheddoost, B. (2020) Identification of the trends associated with the SPI and SPEI indices across Ankara, Turkey. *Theoretical and Applied Climatology*, 139(3–4), 1531–1542. <https://doi.org/10.1007/s00704-019-03071-9>.
- de Bodas Terassi, P.M., de Oliveira-Júnior, J.F., de Góis, G. and Galvani, E. (2018) Variabilidade do Índice de Precipitação Padronizada na Região Norte do Estado do Paraná Associada aos Eventos de El Niño-Oscilação Sul. *Revista Brasileira de Meteorologia*, 33(1), 11–25. <https://doi.org/10.1590/0102-7786331002>.
- Dong, C., MacDonald, G.M., Willis, K., Gillespie, T.W., Okin, G.S. and Williams, A.P. (2019) Vegetation responses to 2012–2016 drought in Northern and Southern California. *Geophysical Research Letters*, 46(7), 3810–3821. <https://doi.org/10.1029/2019GL082137>.
- Dutta, D., Kundu, A. and Patel, N.R. (2013) Predicting agricultural drought in eastern Rajasthan of India using NDVI and standardized precipitation index. *Geocarto International*, 28(3), 192–209. <https://doi.org/10.1080/10106049.2012.679975>.
- Edwards, D.C. (1997) Characteristics of 20th century drought in the United States at multiple time scales. *Atmospheric Sciences*, 298, 174.
- Eyring, V., Gillett, N.P., Achuta Rao, K.M., Barimalala, R., Barreiro Parrillo, M., Bellouin, N., Cassou, C., Durack, P.J., Kosaka, Y., McGregor, S., Min, S., Morgenstern, O. and Sun, Y. (2021) Human influence on the climate system. In: *Climate Change 2021: The Physical Science Basis. Contribution of Working Group I to the Sixth Assessment of the Intergovernmental Panel on Climate Change*. Cambridge and New York, NY: Cambridge University Press, pp. 423–552.
- Fang, G., Li, X., Xu, M., Wen, X. and Huang, X. (2021) Spatiotemporal variability of drought and its multi-scale linkages with climate indices in the huaihe river basin, central China and east China. *Atmosphere*, 12(11), 1446. <https://doi.org/10.3390/atmos12111446>.
- Gocic, M. and Trajkovic, S. (2013) Analysis of changes in meteorological variables using Mann–Kendall and Sen's slope estimator statistical tests in Serbia. *Global and Planetary Change*, 100, 172–182. <https://doi.org/10.1016/j.gloplacha.2012.10.014>.
- Godfray, H.C.J., Beddington, J.R., Crute, I.R., Haddad, L., Lawrence, D., Muir, J.F., Pretty, J., Robinson, S., Thomas, S.M. and Toulmin, C. (2010) Food security: the challenge of feeding 9 billion people. *Science*, 327(5967), 812–818. <https://doi.org/10.1126/science.1185383>.
- Gopal, K.R., Obul Reddy, K.R., Balakrishnaiah, G., Arafath, S.M.D., Kumar Reddy, N.S., Rao, T.C., Reddy, T.L. and Reddy, R.R. (2016) Regional trends of aerosol optical depth and their impact on cloud properties over southern India using MODIS data. *Journal of Atmospheric and Solar-Terrestrial Physics*, 146, 38–48. <https://doi.org/10.1016/j.jastp.2016.05.005>.
- Haile, G.G., Tang, Q., Leng, G., Jia, G., Wang, J., Cai, D., Sun, S., Baniya, B. and Zhang, Q. (2020) Long-term spatiotemporal variation of drought patterns over the Greater Horn of Africa. *Science of the Total Environment*, 704, 135299. <https://doi.org/10.1016/j.scitotenv.2019.135299>.
- Hao, Y., Hao, Z., Feng, S., Zhang, X. and Hao, F. (2020) Response of vegetation to El Niño–Southern Oscillation (ENSO) via compound dry and hot events in southern Africa. *Global and Planetary Change*, 195(19), 103358. <https://doi.org/10.1016/j.gloplacha.2020.103358>.
- Hare, W. (2003) *Assessment of Knowledge on Impacts Of Climate Change—Contribution to the Specification of Art. 2 of the UNFCCC*. Berlin: WBGU.
- Islam, A.R.M.T., Salam, R., Yeasmin, N., Kamruzzaman, M., Shahid, S., Fattah, M.A., Uddin, A.S., Shahariar, M.H., Mondol, M.A.H., Jhajharia, D. and Techato, K. (2021) Spatio-temporal distribution of drought and its possible associations with ENSO indices in Bangladesh. *Arabian Journal of Geosciences*, 14(23), 2681. <https://doi.org/10.1007/s12517-021-08849-8>.
- Jaiswal, R.K., Lohani, A.K. and Tiwari, H.L. (2015) Statistical analysis for change detection and trend assessment in climatological parameters. *Environmental Processes*, 2(4), 729–749. <https://doi.org/10.1007/s40710-015-0105-3>.
- Jeongeun, W., Choi, J., Lee, O. and Kim, S. (2020) Copula-based joint drought index using SPI and EDDI and its application to climate change. *Science of the Total Environment*, 744, 140701.
- Jhajharia, D., Dinpashoh, Y., Kahya, E., Choudhary, R.R. and Singh, V.P. (2014) Trends in temperature over Godavari River basin in southern peninsular India. *International Journal of Climatology*, 34(5), 1369–1384. <https://doi.org/10.1002/joc.3761>.
- Jhajharia, D., Gupta, S., Mirabbasi, R., Kumar, R. and Patle, G.T. (2021) Pan evaporative changes in transboundary Godavari

- River basin, India. *Theoretical and Applied Climatology*, 145(3–4), 1503–1520. <https://doi.org/10.1007/s00704-021-03707-9>.
- Ji, L. and Peters, A.J. (2003) Assessing vegetation response to drought in the northern Great Plains using vegetation and drought indices. *Remote Sensing of Environment*, 87(1), 85–98. [https://doi.org/10.1016/S0034-4257\(03\)00174-3](https://doi.org/10.1016/S0034-4257(03)00174-3).
- Kalluri, R.O.R., Gugamsetty, B., Kotalo, R.G., Nagireddy, S.K.R., Tandule, C.R., Thotli, L.R., Shaik, N.H., Maraka, V.R., Rajuru, R.R. and Surendran Nair, S.B. (2017) Seasonal variation of near surface black carbon and satellite derived vertical distribution of aerosols over a semi-arid station in India. *Atmospheric Research*, 184, 77–87. <https://doi.org/10.1016/j.atmosres.2016.09.003>.
- Kalluri, R.O.R., Gugamsetty, B., Kotalo, R.G., Thotli, L.R., Tandule, C.R. and Akkiraju, B. (2020) Long-term (2008–2017) analysis of atmospheric composite aerosol and black carbon radiative forcing over a semi-arid region in southern India: model results and ground measurement. *Atmospheric Environment*, 240, 117840. <https://doi.org/10.1016/j.atmosenv.2020.117840>.
- Kalluri, R.O.R., Thotli, L.R., Gugamsetty, B., Kotalo, R.G., Akkiraju, B., Virupakshappa, U.K. and Lingala, S.S.R. (2022) An assessment of the impact of Indian summer monsoon droughts on atmospheric aerosols and associated radiative forcing at a semi-arid station in peninsular India. *Science of the Total Environment*, 813, 152683. <https://doi.org/10.1016/j.scitotenv.2021.152683>.
- Kang, H. and Sridhar, V. (2017) Combined statistical and spatially distributed hydrological model for evaluating future drought indices in Virginia. *Journal of Hydrology: Regional Studies*, 12, 253–272. <https://doi.org/10.1016/j.ejrh.2017.06.003>.
- Kendall, M.G. (1948) *Rank Correlation Methods*. New York, NY: Oxford University Press.
- Kisi, O., Docheshmeh Gorgij, A., Zounemat-Kermani, M., Mahdavi-Meymand, A. and Kim, S. (2019) Drought forecasting using novel heuristic methods in a semi-arid environment. *Journal of Hydrology*, 578, 124053. <https://doi.org/10.1016/j.jhydrol.2019.124053>.
- Krishan, R., Nikam, B.R., Pingale, S.M., Chandrakar, A. and Khare, D. (2018) Analysis of trends in rainfall and dry/wet years over a century in the eastern Ganga Canal command. *Meteorological Applications*, 25(4), 561–574. <https://doi.org/10.1002/met.1721>.
- Kumar, P., Wiltshire, A., Mathison, C., Asharaf, S., Ahrens, B., Lucas-Picher, P., Christensen, J.H., Gobiet, A., Saeed, F., Hagemann, S. and Jacob, D. (2013) Downscaled climate change projections with uncertainty assessment over India using a high resolution multi-model approach. *Science of the Total Environment*, 468–469, S18–S30. <https://doi.org/10.1016/j.scitotenv.2013.01.051>.
- Kumar, V., Jain, S.K. and Singh, Y. (2010) Analysis of long-term rainfall trends in India. *Hydrological Sciences Journal*, 55(4), 484–496. <https://doi.org/10.1080/02626667.2010.481373>.
- Li, X. and Huang, W.R. (2021) How long should the pre-existing climatic water balance be considered when capturing short-term wetness and dryness over China by using SPEI? *Science of the Total Environment*, 786, 147575.
- Li, Z., Huang, G., Wang, X., Han, J. and Fan, Y. (2016) Impacts of future climate change on river discharge based on hydrological inference: a case study of the Grand River watershed in Ontario, Canada. *Science of the Total Environment*, 548–549, 198–210. <https://doi.org/10.1016/j.scitotenv.2016.01.002>.
- Liu, C., Yang, C., Yang, Q. and Wang, J. (2021) Spatiotemporal drought analysis by the standardized precipitation index (SPI) and standardized precipitation evapotranspiration index (SPEI) in Sichuan Province, China. *Scientific Reports*, 11(1), 1–14. <https://doi.org/10.1038/s41598-020-80527-3>.
- Liu, X., Pan, Y., Zhu, X., Yang, T., Bai, J. and Sun, Z. (2018) Drought evolution and its impact on the crop yield in the North China Plain. *Journal of Hydrology*, 564, 984–996. <https://doi.org/10.1016/j.jhydrol.2018.07.077>.
- Loo, Y.Y., Billa, L. and Singh, A. (2015) Effect of climate change on seasonal monsoon in Asia and its impact on the variability of monsoon rainfall in Southeast Asia. *Geoscience Frontiers*, 6(6), 817–823. <https://doi.org/10.1016/j.gsf.2014.02.009>.
- Mallya, G., Mishra, V., Niyogi, D., Tripathi, S. and Govindaraju, R. S. (2016) Trends and variability of droughts over the Indian monsoon region. *Weather and Climate Extremes*, 12, 43–68. <https://doi.org/10.1016/j.wace.2016.01.002>.
- Mann, H.B. (1945) Nonparametric tests against trend. *Econometrica*, 13(3), 245–259. <https://doi.org/10.2307/1907187>.
- McKee, T. B., Doesken, N. J. and Kleist, J. R. (1993) *The relationship of drought frequency and duration to time scales*. Paper presented at: Eighth Conference on Applied Climatology, January 17–22, 1993, Anaheim, CA.
- Mishra, A.K. and Singh, V.P. (2010) A review of drought concepts. *Journal of Hydrology*, 391(1), 202–216. <https://doi.org/10.1016/j.jhydrol.2010.07.012>.
- Mishra, A.K. and Singh, V.P. (2011) Drought modeling—a review. *Journal of Hydrology*, 403(1), 157–175. <https://doi.org/10.1016/j.jhydrol.2011.03.049>.
- Mishra, V., Tiwari, A.D., Aadhar, S., Shah, R., Xiao, M., Pai, D.S. and Lettenmaier, D. (2019) Drought and famine in India, 1870–2016. *Geophysical Research Letters*, 46(4), 2075–2083. <https://doi.org/10.1029/2018GL081477>.
- Mooley, D.A. and Parthasarathy, B. (1983) Indian summer monsoon and El Niño. *Pure and Applied Geophysics*, 121(2), 339–352. <https://doi.org/10.1007/BF02590143>.
- Mumo, L., Yu, J. and Ayugi, B. (2019) Evaluation of spatiotemporal variability of rainfall over Kenya from 1979 to 2017. *Journal of Atmospheric and Solar-Terrestrial Physics*, 194, 105097. <https://doi.org/10.1016/j.jastp.2019.105097>.
- Murphy, B.F. and Timbal, B. (2008) A review of recent climate variability and climate change in southeastern Australia. *International Journal of Climatology*, 28(7), 859–879. <https://doi.org/10.1002/joc.1627>.
- Murthy, C.S., Laxman, B. and Sesha Sai, M.V.R. (2015) Geospatial analysis of agricultural drought vulnerability using a composite index based on exposure, sensitivity and adaptive capacity. *International Journal of Disaster Risk Reduction*, 12, 163–171. <https://doi.org/10.1016/j.ijdrr.2015.01.004>.
- Naresh Kumar, M., Murthy, C.S., Sesha Sai, M.V.R. and Roy, P.S. (2009) On the use of standardized precipitation index (SPI) for drought intensity assessment. *Meteorological Applications*, 16(3), 381–389. <https://doi.org/10.1002/met.136>.
- Nicholson, S.E. (2017) Climate and climatic variability of rainfall over eastern Africa. *Reviews of Geophysics*, 55(3), 590–635. <https://doi.org/10.1002/2016RG000544>.

- Ogunrinde, A.T., Oguntunde, P.G., Akinwumiju, A.S. and Fasimmirin, J.T. (2019) Analysis of recent changes in rainfall and drought indices in Nigeria, 1981–2015. *Hydrological Sciences Journal*, 64(14), 1755–1768. <https://doi.org/10.1080/02626667.2019.1673396>.
- Parthasarathy, B. and Pant, G.B. (1985) Seasonal relationships between Indian summer monsoon rainfall and the southern oscillation. *Journal of Climatology*, 5(4), 369–378. <https://doi.org/10.1002/joc.3370050404>.
- Pei, Z., Fang, S., Wang, L. and Yang, W. (2020) Comparative analysis of drought indicated by the SPI and SPEI at various time-scales in inner Mongolia, China. *Water (Switzerland)*, 12(7), 1925. <https://doi.org/10.3390/w12071925>.
- Pettitt, A.N. (1979) A non-parametric test for the approach problem. *Applied Statistics*, 28(2), 126–135.
- Polong, F., Chen, H., Sun, S. and Ongoma, V. (2019) Temporal and spatial evolution of the standard precipitation evapotranspiration index (SPEI) in the Tana River basin, Kenya. *Theoretical and Applied Climatology*, 138(1), 777–792. <https://doi.org/10.1007/s00704-019-02858-0>.
- Raja Obul Reddy, K., Balakrishnaiah, G., Rama Gopal, K., Siva Kumar Reddy, N., Chakradhar Rao, T., Lokeswara Reddy, T., Nazeer Hussain, S., Vasudeva Reddy, M., Reddy, R.R., Boreddy, S.K.R. and Suresh, B.S. (2016) Long term (2007–2013) observations of columnar aerosol optical properties and retrieved size distributions over Anantapur, India using multi wavelength solar radiometer. *Atmospheric Environment*, 142, 238–250. <https://doi.org/10.1016/j.atmosenv.2016.07.047>.
- Rama Gopal, K., Balakrishnaiah, G., Arafath, S.M., Raja Obul Reddy, K., Siva Kumar Reddy, N., Pavan Kumari, S., Raghavendra Kumar, K., Chakradhar Rao, T., Lokeswara Reddy, T., Reddy, R.R., Nazeer Hussain, S., Vasudeva Reddy, M., Suresh Babu, S. and Mallikarjuna, R.P. (2017) Measurements of scattering and absorption properties of surface aerosols at a semi-arid site, Anantapur. *Atmospheric Research*, 183, 84–93. <https://doi.org/10.1016/j.atmosres.2016.08.016>.
- Ramaoe, C.S. (1983) Teleconnections and the siege of time. *Journal of Climatology*, 3(3), 223–231. <https://doi.org/10.1002/joc.3370030302>.
- Rasmusson, E.M. and Carpenter, T.H. (1983) The relationship between eastern equatorial Pacific sea surface temperatures and rainfall over India and Sri Lanka. *Monthly Weather Review*, 111(3), 517–528.
- Satish Kumar, K., Venkata Rathnam, E. and Sridhar, V. (2021) Tracking seasonal and monthly drought with GRACE-based terrestrial water storage assessments over major river basins in south India. *Science of the Total Environment*, 763, 142994.
- Schepen, A., Wang, Q.J. and Robertson, D. (2012) Evidence for using lagged climate indices to forecast Australian seasonal rainfall. *Journal of Climate*, 25(4), 1230–1246. <https://doi.org/10.1175/JCLI-D-11-00156.1>.
- Sen, P.K. (1968) Estimates of the regression coefficient based on Kendall's tau. *Journal of the American Statistical Association*, 63(324), 1379–1389. <https://doi.org/10.1080/01621459.1968.10480934>.
- Setti, S., Maheswaran, R., Radha, D. and Sridhar, V. (2020) Attribution of hydrologic changes in a tropical river basin to rainfall variability and land-use change: case study from India. *Journal of Hydrologic Engineering*, 25(8), 5020015. [https://doi.org/10.1061/\(ASCE\)HE.1943-5584.0001937](https://doi.org/10.1061/(ASCE)HE.1943-5584.0001937).
- Sharma, A.P.M., Jhajharia, D., Gupta, S. and Yurembam, G.S. (2022) Multiple indices based agricultural drought assessment in Tripura, northeast India. *Arabian Journal of Geosciences*, 15(7), 1–13. <https://doi.org/10.1007/s12517-022-09855-0>.
- Sharma, A.P.M., Jhajharia, D., Yurembam, G.S. and Gupta, S. (2021) Assessment of meteorological drought with application of standardized precipitation evapotranspiration index (SPEI) for Tripura, northeast India. *International Journal of Environment and Climate Change*, 11(3), 126–135. <https://doi.org/10.9734/ijecc/2021/v11i330383>.
- Sheffield, J., Wood, E.F. and Roderick, M.L. (2012) Little change in global drought over the past 60 years. *Nature*, 491(7424), 435–438. <https://doi.org/10.1038/nature11575>.
- Shrestha, S., Yao, T. and Adhikari, T.R. (2019) Analysis of rainfall trends of two complex mountain river basins on the southern slopes of the Central Himalayas. *Atmospheric Research*, 215(16), 99–115. <https://doi.org/10.1016/j.atmosres.2018.08.027>.
- Sivakumar, M.V.K., Stefanski, R., Bazzza, M., Zelaya, S., Wilhite, D. and Magalhaes, A.R. (2014) High level meeting on national drought policy: summary and major outcomes. *Weather and Climate Extremes*, 3, 126–132. <https://doi.org/10.1016/j.wace.2014.03.007>.
- Smakhtin, V.U. and Hughes, D.A. (2007) Automated estimation and analyses of meteorological drought characteristics from monthly rainfall data. *Environmental Modelling & Software*, 22(6), 880–890. <https://doi.org/10.1016/j.envsoft.2006.05.013>.
- Srilakshmi, M., Jhajharia, D., Gupta, S., Yurembam, G.S. and Patle, G.T. (2022) Analysis of spatio-temporal variations and change point detection in pan coefficients in the northeastern region of India. *Theoretical and Applied Climatology*, 147(3–4), 1545–1559. <https://doi.org/10.1007/s00704-021-03888-3>.
- Srinivasa Reddy, M., Sanjith Kumar, R. and Uday Bhaskar Reddy, E.B. (2008) Drought in Annntapur District: an overview. *Asian Economic Reviews*, 50(3), 539–560.
- Svoboda, M., Michael, H. and Wood, D.A. (2012) Standardized precipitation index user guide. *Journal of Applied Bacteriology*, 63(3), 1–16.
- Tehseen, J., Li, Y., Rashid, S., Li, F., Hu, Q., Feng, H., Chen, X., Ahmad, S., Liu, F. and Pulatov, B. (2021) Performance and relationship of four different agricultural drought indices for drought monitoring in China's mainland using remote sensing data. *Science of the Total Environment*, 759, 143530. <https://doi.org/10.1016/j.scitotenv.2020.143530>.
- Thilakarathne, M. and Sridhar, V. (2017) Characterization of future drought conditions in the lower Mekong River basin. *Weather and Climate Extremes*, 17, 47–58.
- Thomas, J. and Prasannakumar, V. (2016) Temporal analysis of rainfall (1871–2012) and drought characteristics over a tropical monsoon-dominated State (Kerala) of India. *Journal of Hydrology*, 534, 266–280. <https://doi.org/10.1016/j.jhydrol.2016.01.013>.
- Thorntwaite, C.W. (1948) An approach toward a rational classification of climate. *Geographical Review*, 38(1), 55–94. <https://doi.org/10.2307/210739>.
- Thotli, L.R., Balakrishnaiah, G., Kalluri, R.O.R., Nagireddy, S.K.R., Tandule, C.R., Kotolo, R.G. and Akkiraju, B. (2020) Perturbations of atmospheric surface layer characteristics during the annular solar eclipse on December 26, 2019 over a semi-arid region Anantapur in southern India. *Journal of Atmospheric and Solar-Terrestrial Physics*, 211, 105467. <https://doi.org/10.1016/j.jastp.2020.105467>.

- Vicente-Serrano, S.M., Beguería, S. and López-Moreno, J.I. (2010) A multiscalar drought index sensitive to global warming: the standardized precipitation evapotranspiration index. *Journal of Climate*, 23(7), 1696–1718. <https://doi.org/10.1175/2009JCLI2909.1>.
- Wang, L. and Chen, W. (2014) A CMIP5 multimodel projection of future temperature, precipitation, and climatological drought in China. *International Journal of Climatology*, 34(6), 2059–2078. <https://doi.org/10.1002/joc.3822>.
- Wang, Z., Zhong, R., Lai, C., Zeng, Z., Lian, Y. and Bai, X. (2018) Climate change enhances the severity and variability of drought in the Pearl River basin in south China in the 21st century. *Agricultural and Forest Meteorology*, 249, 149–162. <https://doi.org/10.1016/j.agrformet.2017.12.077>.
- Yao, J., Zhao, Y. and Yu, X. (2018) Spatial-temporal variation and impacts of drought in Xinjiang (northwest China) during 1961–2015. *PeerJ*, 6(6), e4926. <https://doi.org/10.7717/peerj.4926>.
- Yao, N., Li, L., Feng, P., Feng, H., Li Liu, D., Liu, Y., Jiang, K., Hu, X. and Li, Y. (2020) Projections of drought characteristics in China based on a standardized precipitation and evapotranspiration index and multiple GCMs. *Science of the Total Environment*, 704, 1–18. <https://doi.org/10.1016/j.scitotenv.2019.135245>.
- Zamani, R., Mirabbasi, R., Abdollahi, S. and Jhajharia, D. (2017) Streamflow trend analysis by considering autocorrelation structure, long-term persistence, and Hurst coefficient in a semi-arid region of Iran. *Theoretical and Applied Climatology*, 129(1–2), 33–45. <https://doi.org/10.1007/s00704-016-1747-4>.
- Zhang, L., Podlasly, C., Ren, Y., Feger, K.-H., Wang, Y. and Schwärzel, K. (2014) Separating the effects of changes in land management and climatic conditions on long-term streamflow trends analyzed for a small catchment in the Loess Plateau region, NW China. *Hydrological Processes*, 28(3), 1284–1293. <https://doi.org/10.1002/hyp.9663>.
- Zhou, L., Wang, S., Du, M., Chen, Q., He, C., Zhang, J., Zhu, Y. and Gong, Y. (2021) The influence of ENSO and MJO on drought in different ecological geographic regions in China. *Remote Sensing*, 13(5), 1–19. <https://doi.org/10.3390/rs13050875>.

How to cite this article: Thotli, L. R., Gugamsetty, B., Kalluri, R. O. R., Tandule, C. R., Kotalo, R. G., Akkiraju, B., & Lingala, S. S. R. (2022). Long-term (2001–2020) trend analysis of temperature and rainfall and drought characteristics by in situ measurements at a tropical semi-arid station from southern peninsular India. *International Journal of Climatology*, 42(16), 8928–8949. <https://doi.org/10.1002/joc.7783>



An assessment of the impact of Indian summer monsoon droughts on atmospheric aerosols and associated radiative forcing at a semi-arid station in peninsular India



Raja Obul Reddy Kalluri ^a, Lokeswara Reddy Thotli ^a, Balakrishnaiah Gugamsetty ^a, Rama Gopal Kotalo ^{a,*}, Bhavyasree Akkiraju ^a, Usha Kajjer Virupakshappa ^{a,b}, Siva Sankara Reddy Lingala ^a

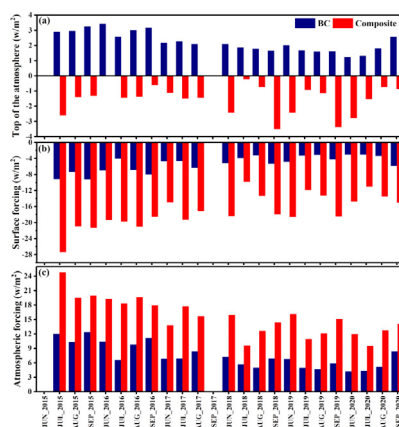
^a *Aerosol & Atmospheric Research Laboratory, Department of Physics, Sri Krishnadevaraya University, Anantapur 515 003, Andhra Pradesh, India*

^b *Member of the Legislative Assembly (MLA), Kalyandurg 515761, Andhra Pradesh, India*

HIGHLIGHTS

- A study was conducted to examine aerosols during southwest monsoon over a semi-arid site in Southern India.
- The SPI was used to identify the droughts and normal monsoon years.
- The BLH and VC were negatively correlated with BC during two measurement periods.
- The BC forcing was substantially larger during drought years than in normal monsoon years.

GRAPHICAL ABSTRACT



ARTICLE INFO

Article history:

Received 16 September 2021

Received in revised form 14 December 2021

Accepted 21 December 2021

Available online 29 December 2021

Editor: Pavlos Kassomenos

Keywords:

Aerosol optical depth

BC mass concentration

Ventilation coefficient

Radiative forcing

Semi-arid region

ABSTRACT

A continuing increase in droughts/floods in Asian monsoon regions and worsening air quality due to aerosols are the two biggest threats to the health and well being of over 60% of the world's population. This study focuses on in-situ observations of atmospheric aerosols and their impact on shortwave direct aerosol radiative forcing (SDARF) during the southwest monsoon season (June–September) from 2015 to 2020 over a semi-arid station in Southern India. The Standardized precipitation index (SPI) is used to identify the droughts and normal monsoon years. Based on the SPI index, 2015, 2016, and 2018 were considered the drought monsoon years, while 2017, 2019, and 2020 were chosen as the normal monsoon years. During the drought monsoon years (normal monsoon years), the monthly mean black carbon (BC) was 1.17 ± 0.25 (0.72 ± 0.18), 1.02 ± 0.31 (0.64 ± 0.17), 1.02 ± 0.38 (0.74 ± 0.28), and $1.28 \pm 0.35 \mu\text{g}/\text{m}^3$ ($0.88 \pm 0.21 \mu\text{g}/\text{m}^3$), for June, July, August and September respectively. The lower BC concentration during the normal monsoon years is mainly due to the enhanced wet-removal rates by high rainfall over the measurement location. In July, there was a high ventilation coefficient (VC) and low concentration of BC, while in September, low VC, and a high concentration of BC was observed in both the drought and the normal monsoon years. In addition, a plane-parallel radiative transfer model was used to estimate shortwave direct aerosol radiative forcing for composite and without BC at various surfaces, including the surface (SUF), atmosphere (ATM), and top of the atmosphere (TOA). During the drought monsoon years (normal monsoon years), the estimated monthly mean

* Corresponding author.

E-mail address: krverma@yahoo.com (R.G. Kotalo).

ATM forcing was 17.6 ± 2.4 (13.9 ± 2.1), 17.5 ± 7.5 (12.7 ± 4.4), 17.2 ± 4.0 (13.5 ± 1.9), and $17.4 \pm 2.8 \text{ Wm}^{-2}$ ($14.6 \pm 0.7 \text{ Wm}^{-2}$) for June, July, August, and September, respectively. During the drought monsoon years, the estimated BC forcing was substantially larger ($8.8 \pm 2.6 \text{ Wm}^{-2}$) than that of normal monsoon years ($6.0 \pm 1.5 \text{ Wm}^{-2}$). It indicates the important role of absorbing BC aerosols during the drought monsoon years in introducing additional heat to the lower atmosphere, particularly over peninsular India.

1. Introduction

Atmospheric aerosols are tiny particles that are emitted into the atmosphere by both natural and manmade activities. They absorb visible solar energy, which causes the Earth's surface to be dull and impact the Indian summer monsoon (Kumar et al., 2017; Manoj et al., 2010). Black carbon (BC) has a substantial absorbing component with Spatio-temporal fluctuation in its sources and emission levels (Kalluri et al., 2021, 2020a; Manoj et al., 2019; Hussain et al., 2018; Dumka et al., 2018). For example, coal and biomass burning activities account for about 60–80% of BC emissions in Asian and African countries. However, in European countries, automobile emissions account for over 70% of BC emissions (Sanap and Pandithurai, 2015). Hoesly et al. (2018) reported that emissions in the pre-industrial period were generally dominated by biofuel use in the residential sector and an industrialization progressed emissions from industrial, energy transformation, and transportation sectors became increasingly important.

Aerosol Optical Depth (AOD) is a crucial parameter for estimating direct aerosol radiative forcing, which describes the vertically integrated extinction of solar radiation in the total atmospheric column. Because of the short life time of particles, both (direct and indirect) effects of aerosols have considerable regional fluctuations, resulting in high geographical and temporal variability in aerosol loading, as well as chemical composition and optical characteristics (Tandule et al., 2020; Kalluri et al., 2020b, 2019; Manoj et al., 2019; Gopal et al., 2017; Babu et al., 2013). When BC aerosols are freshly emitted, they are generally externally mixed and hydrophobic (Willis et al., 2016; Zhang et al., 2016). However, atmospheric aging causes internal mixing of BC with hydrophilic compounds (e.g. organic acids and ammonium sulphate) (Zhang et al., 2015), increasing its hygroscopicity and size that affects the climate by changing wet scavenging efficiency and atmospheric lifetime (McMeeking et al., 2011; Liu et al., 2010; Oshima et al., 2009; Moteki and Kondo, 2007; Shiraiwa et al., 2007). Despite its short atmospheric lifetime of only 4 to 12 days, BC plays a crucial role in radiative forcing by strongly absorbing solar radiation and reducing scattering extinction (Cape et al., 2012; Schwarz et al., 2006; Ramanathan et al., 2001). Intergovernmental Panel on Climate Change (IPCC, 2021) reported that, human-caused radiative forcing of $+2.72$ [$+1.96$ to $+3.48$] Wm^{-2} in 2019 related to 1750 has warmed the climate system. Dry and wet depositions scavenge aerosol particles, which are the key processes for maintaining the balance between sources and sinks of airborne particles. The proportional importance of each process is determined by the precipitation temporal and spatial distribution. Most aerosol particles are removed mostly through precipitation. The only effective approach is to remove particles in the accumulation mode size range ($d = 0.1\text{--}0.6 \mu\text{m}$) from the atmosphere. Dry deposition at the Earth's surface can effectively remove smaller Aitken mode particles ($d = 0.01\text{--}0.1 \mu\text{m}$). Large particles will fall through the air to the surface, where they will gravitationally settle.

The arrival of the South Asian monsoon over the Indian subcontinent is indicated by changes in the lower atmosphere circulation pattern, which are caused by an intense heat low created in northern India and strong southwest winds reaching southern India. When precipitation levels are reduced over an extended period, such as a season or more in length, the result is a drought, which is usually aggravated by other climatic factors (viz. high temperatures, high winds and low relative humidity). According to drought characteristics, there are usually the following types; meteorological, agricultural, hydrological, and socioeconomic (Mishra and Singh, 2010; Mehr and Vaheddoost, 2019; Tran et al., 2019). Among them, meteorological drought is an extreme climate event. The most intuitive

cause is the reduction in precipitation, and the other three types of drought have greater human and social aspects (Wang et al., 2019a). Because of the complexity and severity of drought, it is very challenging to identify and assess drought characteristics (Tirivarombo et al., 2018; Wang et al., 2019b). According to India Meteorological Department, meteorological drought over an area is defined as a situation when the seasonal rainfall received over the area is less than 75% of its long term average value. It is further classified as "moderate drought" if the rainfall deficit is between 26 and 50% and "severe drought" when the deficit exceeds 50% of the normal (Monsoon page, imd.gov.in). Numerous researchers have developed the use of the popular index for drought monitoring; the Standardized Precipitation Index (SPI), and this index is widely used throughout the world (Shoaib et al., 2020; Zhifang et al., 2020; Dabani et al., 2017; Haroon et al., 2016; Ashraf and Routray, 2015; Gocic and Trajkovic, 2014). Aerosol-precipitation feedback has also been found in several studies, in which higher aerosols lead to less precipitation, culminating in elevated aerosol concentrations over the Indian monsoon region (Lau et al., 2017; Bollasina et al., 2008). Scattering aerosols have a very limited impact on monsoon circulation and precipitation compared to other anthropogenic aerosols. On the other hand, absorbing aerosols have a significant impact on monsoon circulation and the production of convective precipitation, with or without the co-existence of scattering aerosols (Wang et al., 2009). Levy et al. (2013) reported that BC has led to a global temperature rise of 1 °C and fluctuations in rainfall of up to 1 mm. Ramanathan et al. (2005) used a worldwide coupled climate model to investigate the influence of BC aerosols in reducing monsoon rain over the Indian subcontinent. The impact of absorbing components (BC) on a significant reduction in monsoon rainfall due to enhanced local meridional circulation was observed by Lau and Kim (2006). Bollasina et al. (2008) found significant heterogeneity in monsoon evolution over south Asia, attributed to significant aerosol loading in the spring. According to Manoj et al. (2010), aerosols emitted from artificial activities further vary the summer monsoon and stifle monsoon activity. The absorbing aerosols released from densely inhabited and industrialized areas in India, such as dust, fossil fuel biomass burning, and forest fires, have been highlighted as a hotspot for environmental research (Shalini et al., 2020; Kalluri et al., 2016; Gopal et al., 2015; Gogoi et al., 2009; Satheesh et al., 2010). Due to minimal rainfall and dry continental terrain, Anantapur, a semi-arid, rural city with around 4 million people, is a hotspot for distinct aerosol sources. During the Southwest monsoon, the primary sources of atmospheric aerosols include vehicular emission, industrial emission, and local/long-range transportation of dust aerosols. As a result, efforts are being made to understand the impact of aerosols and their related radiative properties on a typical monsoon scenario.

The present study focuses on inter-annual fluctuations of AOD and BC aerosols for different monsoon scenarios during the study period (2015–2020). In addition, the study analyzes the temporal variations in BC concentration along with mixed layer height and ventilation coefficient during the study period. Finally, we have estimated shortwave direct aerosol composite and BC aerosol radiative forcing, as well as their related atmospheric heating rates, over the measurement location using the Santa Barbara Discrete Ordinate Radiative Transfer (SBDART) model.

2. Site description

Anantapur belongs to the dry continental and rain shadow region situated in peninsular India. The measurement site is located around 10 km from the heart of the city centre, next to the Anantapur-Chennai national

route 205, and only 7 km away from the Hyderabad-Bangalore national highway 44. The aerosol particles are collected at Sri Krishnadevaraya University, Department of Physics (14.62 N, 77.65 E, 331 m asl) from around 12 m above the ground level. The map of the observation location is shown in Fig. 1. Droughts are common at this measurement location, which is India's second-lowest rainfall area after Jaisalmer. The usual rainfall during the southwest monsoon season is 350 mm, accounting for 60–70% of total rainfall; however, during the northeast monsoon season, it is only 150 mm, accounting for just 40–30% of yearly rainfall (Kalluri et al., 2016).

3. Instrumentation

3.1. MICROTOPS sunphotometer

The real-time AOD is obtained by using the portable MICROTOPS sunphotometer over the measurement location. The sunphotometer detects the intensity of solar radiation reaching the earth at five wavelengths: 380, 500, 870, 936, and 1020 nm. The filters employed in all channels have a 1.5 nm peak wavelength precision and a full width at half maximum (FWHM) and bandwidth of 2.4 ± 0.4 nm for the 380 nm channel and 10 ± 1.5 nm for the remaining channels. The sun photometer position is adjusted until light in the Sun target window with a field view of 2.5° intersects a crosshair. The photodiodes receive radiation through the collimator and band-pass filters, which produce an electrical current proportionate to the radiant power intercepted by the photodiodes. The first amplified signals transformed into digital signals are converted using a high-resolution A/D converter. The columnar AOD is calculated using the Bouguer – Lambert-Beer principle; however, the optical depth caused by Rayleigh scattering and other species such as O_3 and NO_2 is subtracted before considering optical depth. The User Guide, MICROTOPS Sun photometer version 5.6, Solar Light Company Inc., has more information on the working principle and measurement methodologies (Ichoku et al., 2002). The instruments are used on all clear-sky days for a daily minimum of more than 3 h with a 15-minute time interval. The morning and afternoon data sets are combined and treated as one single day throughout the measurement period.

3.2. Aethalometer

Using a two-channel Aethalometer, continuous real-time BC measurements are taken over a semi-arid region, Anantapur. The instrument is run at a flow rate of 4 Ltr per min for 24 h a day, with a 5-minute time base. The BC mass concentration is determined by using the optical attenuation method. The aethalometer estimates the instantaneous concentration of optically absorbing aerosols from the rate of change of the attenuation of light transmitted through the particle-laden filter.

$$BC = \left(\frac{A}{V} \right) \frac{1}{SG} \left[\frac{\Delta ATN(\lambda)}{\Delta(t)} \right] \quad (1)$$

where $SG = \frac{14625}{\lambda_{nm}} (m^2 g^{-1})$ is the specific absorption cross-section, 'A' is the spot area (sq. cm), V is the volume of air passed through the filter, and Δ (ATN) is the attenuation of light through the filter in time Δ (t) due to BC. As BC is the major absorber in the near-infrared range and has an imaginary part of refractive index >0.44 , attenuation recorded at 880 nm is generally considered the influence of BC in this study. Even though the filter-based absorption method is extensively utilized worldwide, it is plagued by several uncertainties, including multiple scattering effects in quartz filter tape and shadowing effects (Weingartner et al., 2003). As a result, the raw data collected from the Aethalometer must be required to correct the loading effect before the data can be considered for analysis. The loading effect of observed BC data is often more significant for newly released black carbon aerosols, whereas aging group aerosols, which may have a near-zero impact, are generally smaller (Virkkula et al., 2007; Arnott et al., 2005; Weingartner et al., 2003). The loading factor corrections of BC are performed using the Virkkula et al. (2007) approach in this investigation.

3.3. Satellite retrieved surface reflectance, boundary layer height and total columnar ozone

The important input for radiative transfer model calculations is the surface albedo, which can determine the sign of the TOA. MODIS provide 8-day surface reflectance readings for constituent wavelengths such as

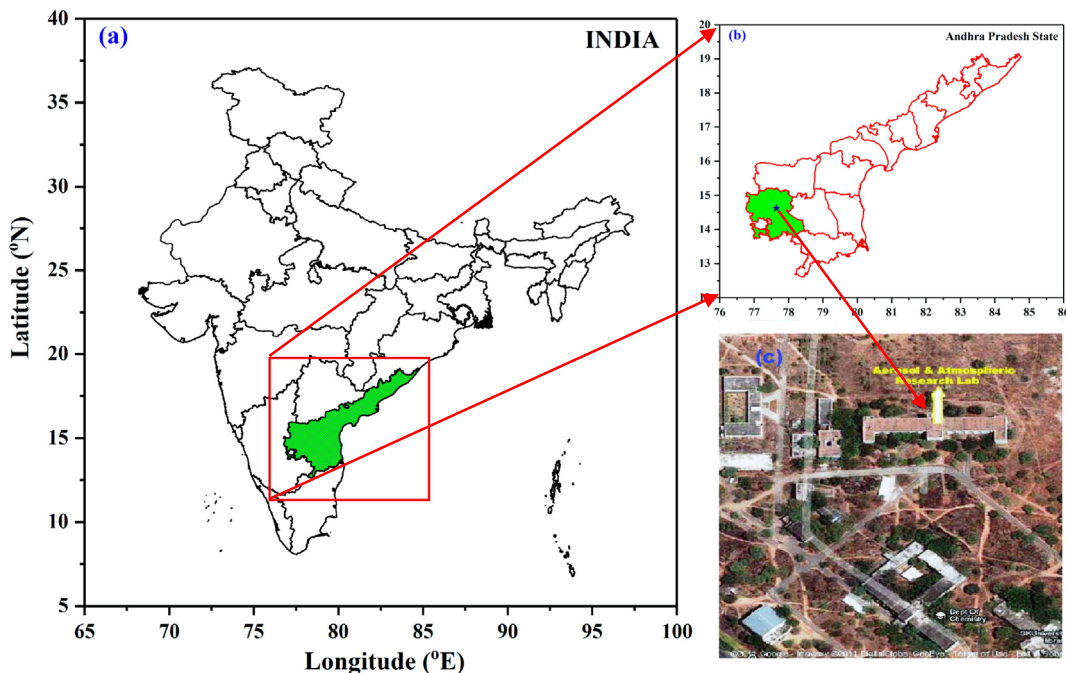


Fig. 1. Geographical location of observational site, (a) Location of the Andhra Pradesh state in India map (b) District map of Andhra Pradesh and filled green colour indicated the Anantapur district (c) Satellite aerial view of monitoring site building in the SKU campus indicated with an arrow head. (For interpretation of the references to colour in this figure legend, the reader is referred to the web version of this article.)

0.469, 0.55, 0.645, 0.859, 1.24, 1.64 and 2.13 μm all over the world. In this study, spectral reflectance values for the 8-day Level 3 Global 500 m ISIN Grid product, MOD09A1 (Terra), and MYD09A1 (Aqua) are downloaded from the Lads website during the measurement period, with the uncertainty of the retrieved reflectance values being approximately 2% (Li et al., 2009) (<http://ladsweb.nascom.nasa.gov>). ERA5 is a fifth-generation global atmospheric reanalysis product that is recently constructed utilising the 4D-Var data assimilation in CY41R2 of the European Center for Medium-Range Weather Forecasts (ECMWF) Integrated Forecasting System (IFS), which covers the period 1979 to the present (Hersbach and Dee, 2016). ERA5 will assure the most recent version of the ECMWF Earth system model data assimilation approach instead of the older ERA-Int. When comparing ERA5 to the preceding ERA-Int, two significant changes are made: the temporal resolution is updated from 3-hourly to hourly, and the spatial resolution was increased from 79 km to 25 km (Albergel et al., 2018). The ECMWF reanalysis website has further information. (<https://confluence.ecmwf.int/display/CKB/ERA5%3A+data+documentation>). The hourly near-surface 10-m u and v components of wind speed and Boundary Layer Height (BLH) are obtained from ERA-5 (<https://cds.climate.copernicus.eu/cdsapp#!/dataset/reanalysis-era5-single-levels?tab=form>) during the study period.

The Ozone Monitoring Instrument (OMI) collects total columnar ozone (TCO) data with a spatial resolution of $13 \times 24 \text{ km}^2$ based on the absorption of solar radiation in the wavelength range of 270 to 500 nm from the Earth's surface through the atmosphere. We analysed TCO level 3e global data (OMDOAO3e, Version 003) gridded at $0.25^\circ \times 0.25^\circ$ from NASA Goddard Earth Sciences Data and Information Service Center (<http://www.esrl.noaa.gov/>). In addition, Veefkind et al. (2006) provided more details on the instrument's operating principle, algorithm, and uncertainty.

3.4. Short wave direct aerosol radiative forcing and heating rates: methodology

During the study period, the Santa Barbara Discrete Ordinate Radiative Transfer (SBDART) model is utilized to estimate direct shortwave both composite and BC radiative forcing of aerosols (Ricchiazzi et al., 1998). The SBDART includes multiple scattering in a vertically inhomogeneous, non-isothermal plane-parallel media and is efficient enough in resolving radiative transfer equations (Ricchiazzi et al., 1998). The spectral AOD, Single scattering albedo (SSA), scattering phase function, surface albedo, columnar ozone, and columnar water vapor are essential inputs for determining the radiative forcing. In the wavelength range 380 to 1025 nm, spectral AOD is collected from a MICROTOPS sunphotometer, while SSA and phase function are generated from the OPAC model. The OPAC permits up to eight values of relative humidity (0%, 50%, 70%, 80%, 90%, 95%, 98%, and 99%) for calculating optical properties from given size distribution and refractive indices.

Daily mean relative humidity values were taken from the automatic weather station, which is located at the observation location. In this study, we considered near-appropriate humidity levels at the measurement site which were based on the monthly averages during the drought and normal monsoon seasons. The aethalometer is used to determine the BC mass concentration, which has a 20% uncertainty. Five aerosol types for making new aerosol mixtures based on unique topography and trajectory analysis are chosen. These include soluble, insoluble, Soot (BC), mineral accumulation, and transported mineral dust, all freely available from Hess et al. (1998), and the required aerosol optical properties are derived. The estimated AOD values closely match the ground-based obtained AOD values after creating new aerosol mixtures. Next, we have computed the relevant aerosol optical properties (SSA, Phase function, Angstrom exponent, etc.) individually as composite and without-BC mixtures. Then, we have entered them as input parameters to the SBDART for both composite and without-BC forcing. When all relevant inputs have been loaded into the model, both upwards and downwards radiative fluxes are computed within aerosol and without aerosol at different solar zenith angles (0 to 89). In order to determine aerosol radiative forcing values in terms of both composite and BC forcing, the computed radiative fluxes (composite aerosols and no aerosol) are used.

Aerosol radiative forcing either at the surface (SUF) or at the atmosphere (TOA) is defined as the change in the flux (ΔF) with an absence of aerosols in the atmosphere

$$(\Delta F) = (F_{a\downarrow} - F_{a\uparrow}) - [(F_{n\downarrow} - F_{n\uparrow})] \quad (2)$$

Where $(F_{\downarrow} - F_{\uparrow})$ denotes the net solar irradiance (downward or upward fluxes W m^{-2}) computed with aerosol (F_a) and in the absence of aerosols (F_n) at either TOA or SUF. Further, the energy absorbed in the atmosphere (ATM) is calculated as the difference between TOA and SUF forcing and is defined as,

$$(\Delta F)_{\text{ATM}} = (\Delta F)_{\text{TOA}} - (\Delta F)_{\text{SUF}} \quad (3)$$

According to Liou (2002), the atmospheric heating rate is

$$\frac{\partial T}{\partial t} = \frac{g}{C_p \Delta P} \times 24(\text{hr/day}) \times 3600(\text{sec/hr}) \quad (4)$$

where $\frac{\partial T}{\partial t}$ is the atmospheric heating rate measured in K day^{-1} , g as the acceleration due to gravity, C_p the specific heat capacity ΔP atmospheric pressure difference, and ΔF is the estimated shortwave forcing within the atmosphere.

3.5. Standardized Precipitation Index (SPI)

The Standardized Precipitation Index (SPI), which was developed by Mc Kee et al. in 1993 (McKee et al., 1993), is adaptable and may be used to calculate the precipitation deficit over a range of periods, including 1, 3, 6, 12, 24, and 48-months. In the present study, we have considered a monthly time scale of SPI because one-month SPIs provide early drought warnings and help quantify drought severity. The average SPI values are positive and negative, indicating that there are normal and drought years within the timescale (McKee et al., 1993). The specific calculation method for SPI has been mentioned in Liu et al. (2021). Based on the SPI index, 2015, 2016, and 2018 were considered drought monsoon years, whereas 2017, 2019, and 2020 were taken as normal monsoon years (Fig. 2).

4. Results and discussions

4.1. Spectral variations of aerosol optical depth and surface albedo

The monthly mean spectral fluctuation of AOD during the southwest monsoon period from 2015 to 2020 is depicted in Fig. 3. A distinct spectral variation of AOD was observed during the drought and normal monsoon years conditions, decreasing with increasing wavelength until 870 nm and then slightly increasing with a wavelength in all months. During the drought monsoon years (normal monsoon years), the monthly mean AOD (at 380 nm) was 0.31 ± 0.05 (0.28 ± 0.03), 0.33 ± 0.14 (0.26 ± 0.07), 0.32 ± 0.04 (0.26 ± 0.02), 0.30 ± 0.02 (0.29 ± 0.04), for June, July, August and September, respectively, while the respective mean values at 880 nm was 0.18 ± 0.01 (0.16 ± 0.03), 0.22 ± 0.10 (0.17 ± 0.05), 0.20 ± 0.03 (0.16 ± 0.01), 0.16 ± 0.02 (0.14 ± 0.02). The observed AOD is generally larger at shorter wavelengths, which increases irradiance scattering. The increased AOD at longer wavelengths in the drought and normal monsoon years is due to increased dust loading from stronger surface winds, reducing spectral variability. The highest AOD at longer wavelengths was seen in July and the lowest in September throughout the study period. The highest AOD at longer wavelengths in July is attributed to monsoon winds, which raise dust aerosol from dry land into the atmosphere (Ganguly et al., 2006). In contrast, September indicates the end of the monsoon season with the highest rainfall recorded, which may wash out aerosol particles from the atmosphere. Furthermore, wind direction shifts from south-westerly to northerly during September, which results in less dust aerosol contribution over the measurement site (Gopal et al., 2014).

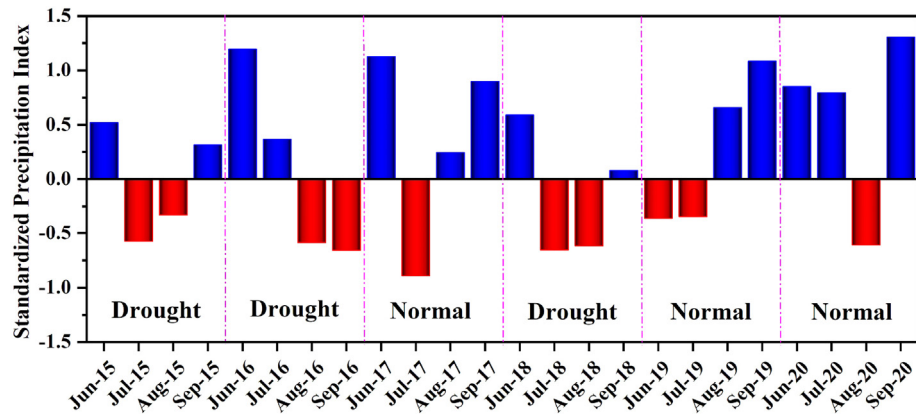


Fig. 2. Monthly variation of Standardized precipitation index (SPI) during the southwest monsoon months from 2015 to 2020.

Fig. 4 depicts the monthly variation of MODIS reflectance values at seven wavelengths during the study period. The spectral reflectance values increased significantly with wavelength increase up to $0.86\text{--}1.24\text{ }\mu\text{m}$ and then decreased in all months. Thus, the surface reflectance values are below 0.2 (for short wavelengths) and approximately 0.2 for longer wavelengths.

4.2. Temporal variation of aerosol optical depth, BC, rainfall, and temperature

The monthly mean variations of Rainfall, Temperature, AOD, and BC during the southwest monsoon from 2015 to 2020 are depicted in Fig. 5. For June, July, August, and September, the monthly cumulative rainfall ranges from 33 to 115 mm, 15–79 mm, 36–120 mm, and 52–253 mm, respectively (Fig. 5a). Furthermore, there has been a distinct variation in the rainfall patterns from 2015 to 2020 in the semi-arid station, with the lowest rainfall in July and the highest in September. During the study period, rainfall in September contributed approximately 47% to the total,

while the rainfall in June, July, and August is only 53%. During the drought monsoon years (normal monsoon years), the monthly maximum mean temperature was 36.2 ± 3.1 (35.2 ± 3.2), 34.6 ± 2.8 (33.1 ± 2.9), 34.4 ± 3.2 (32.9 ± 3.3) and 34.1 ± 2.3 °C (31.2 ± 0.3 °C) for June, July, August, and September, respectively. The lowest minimum temperature of 22 °C was observed in September 2016, while the highest maximum was 38.60 °C during June 2017.

In the drought monsoon years, the observed annual mean AOD ranges from 0.16 ± 0.02 to 0.39 ± 0.02 , and the corresponding cumulative rainfall is between 235 and 269 mm (Fig. 5a and b). While during the normal monsoon years the AOD values range from 0.19 ± 0.07 to 0.32 ± 0.06 , the associated cumulative rainfall varies between 402 and 459 mm. During the drought and normal monsoon years, the annual mean AOD was 0.30 ± 0.02 and 0.24 ± 0.01 , respectively. The largest AOD (0.39 ± 0.02) was recorded in July 2015, while the lowest AOD (0.16 ± 0.02) was noted in July 2016 (Fig. 5b). An increase in temperature causes aerosol lifting, which affects the size distribution resulting in higher quantities of AOD during

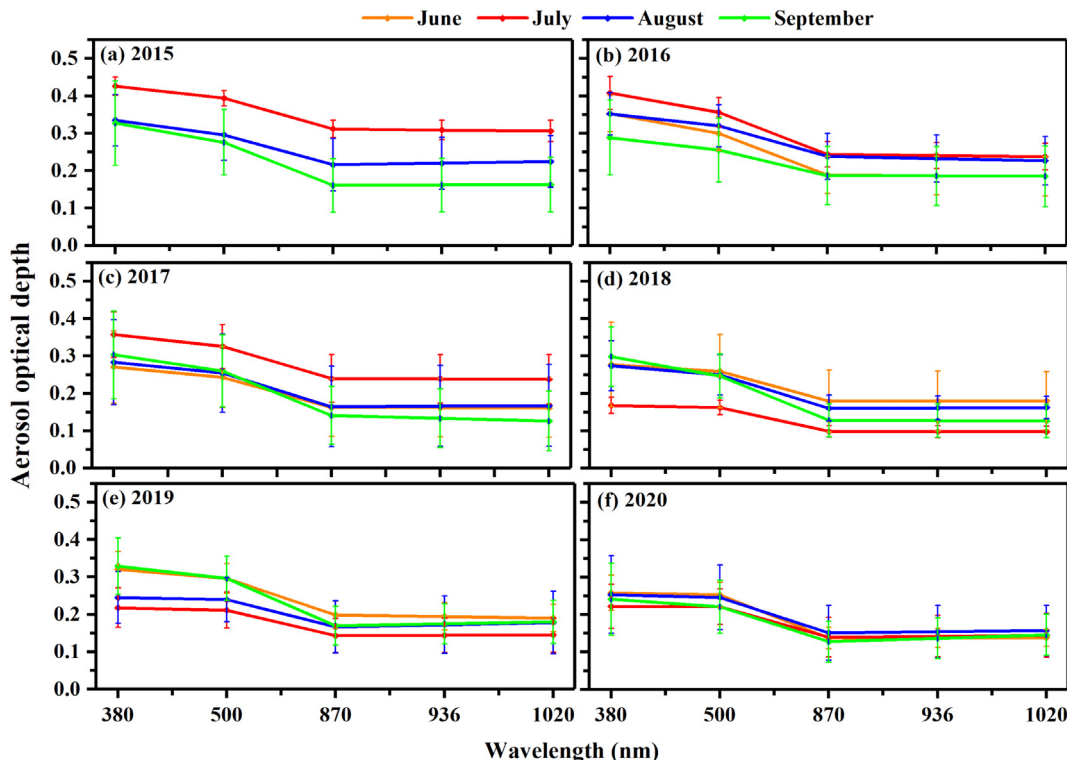


Fig. 3. Monthly variation of the spectral means AOD over Anantapur during the southwest monsoon months from 2015 to 2020. The vertical bars represent the standard deviation from the monthly mean. The gap in the data series is attributed to lack of data.

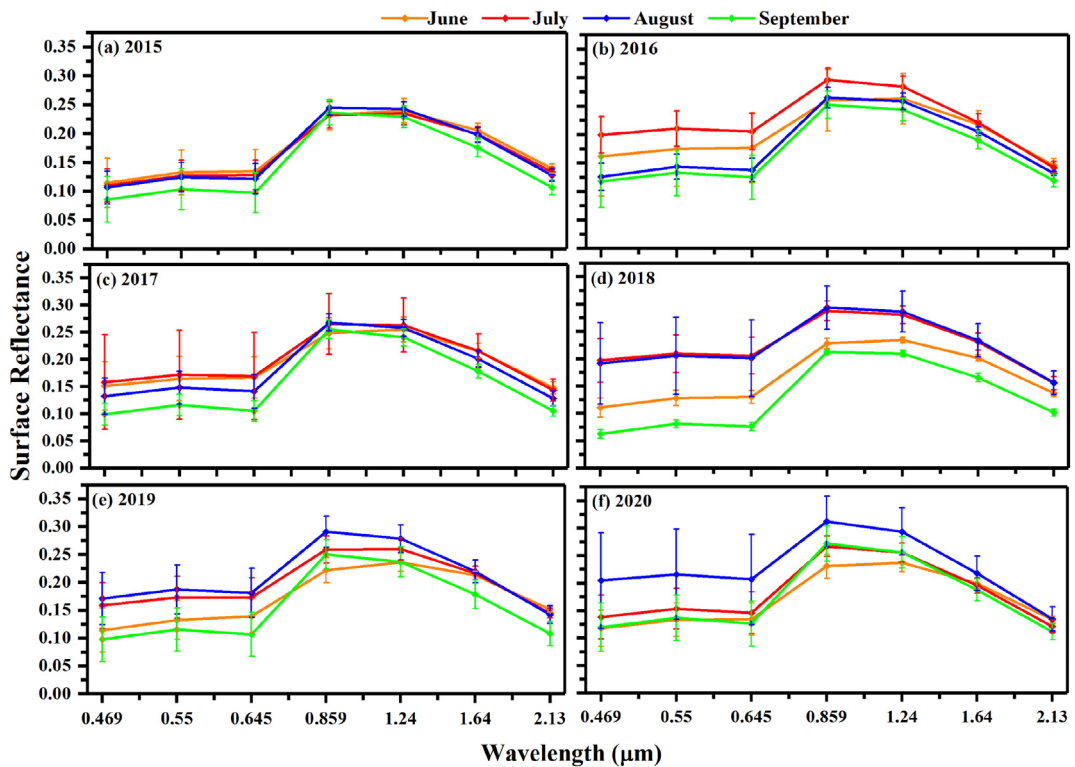


Fig. 4. Monthly variations of the spectral surface albedo over Anantapur during the southwest monsoon months from 2015 to 2020. The vertical bars represent the standard deviation from the monthly mean.

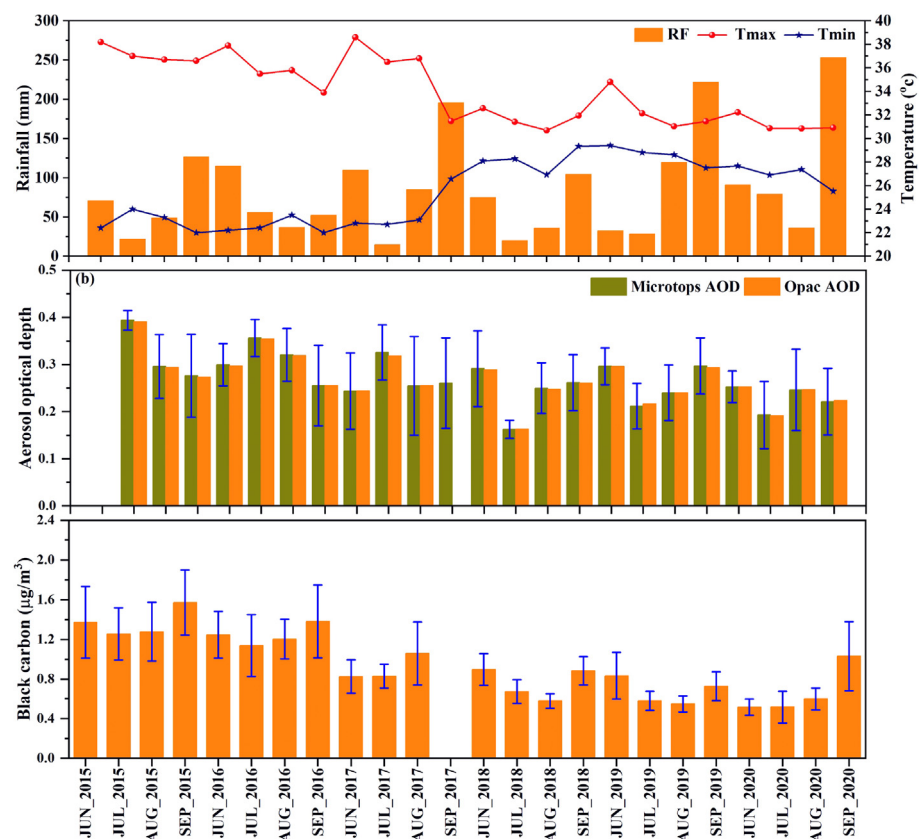


Fig. 5. Temporal variation of (a) rain fall, temperature (b) monthly mean MICROTOPS AOD₅₀₀ in comparison with OPAC derived AOD₅₀₀ (c) black carbon mass concentration over Anantapur during the southwest monsoon months from 2015 to 2020. The vertical bars represent the standard deviation from the monthly mean. The gap in the data series is attributed to lack of data.

drought monsoon years. The BC mass concentration ranges from 1.37 ± 0.33 to $0.76 \pm 0.12 \mu\text{g}/\text{m}^3$ (0.91 ± 0.26 to $0.66 \pm 0.24 \mu\text{g}/\text{m}^3$) during the drought monsoon years (normal monsoon years), with a mean value of $1.12 \pm 0.32 \mu\text{g}/\text{m}^3$ ($0.74 \pm 0.13 \mu\text{g}/\text{m}^3$) (Fig. 5c). During the drought monsoon years (normal monsoon years), the monthly mean BC for June, July, August, and September was 1.17 ± 0.25 (0.72 ± 0.18), 1.02 ± 0.31 (0.64 ± 0.17), 1.02 ± 0.38 (0.74 ± 0.28), and $1.28 \pm 0.35 \mu\text{g}/\text{m}^3$ ($0.88 \pm 0.21 \mu\text{g}/\text{m}^3$), respectively. Cooking (with fire wood), vehicle driving, brick kilns and waste burning are the potential sources of BC emissions that contribute to the high BC mass concentration over the measurement location. The high value of BC in September is mostly due to a change in air masses from southwesterly to northeasterly (Gopal et al., 2014; Kalluri et al., 2017). The presence of high BC during drought monsoon years suggested significant amounts of absorbing aerosols, which can affect the atmospheric temperature structure by generating additional heat in the environment over the observational location. The high BC mass concentration seen during the drought monsoon years is consistent with the high AOD and temperature measured during the same period.

4.3. Temporal variation of BC, boundary layer height, and ventilation coefficient

The BC mass concentrations have been influenced by the factors like natural or anthropogenic emissions, mesoscale atmospheric processes, local meteorology, and long-range transport in different regions (Dumka et al., 2010). Local meteorology is the main factor that influences BC mass concentration. Mixed layer height (MLH) represents the vertical diffusion capability of air pollutants, while wind speed (WS 10 m) indicates the horizontal diffusion capability. Combination of these two meteorological variables, yields the ventilation coefficient (VC), which is commonly used as an index to measure the vertical and horizontal capabilities of air diffusion. In this connection, the effect of boundary layer height and ventilation coefficient on BC mass concentration during drought and normal monsoon years is examined in Fig. 6. The VC values varied significantly during the months, emphasizing the importance of boundary layer processes and, aerosol dispersion. In addition, the assimilative capacity is relatively low in terms of the ventilation coefficient indicating a high pollution potential in the corresponding month.

During the drought monsoon years, the monthly mean BC (VC) for June, July, August, and September was 1.17 ± 0.24 (4761 ± 616), 1.02 ± 0.31 (6074 ± 653), 1.02 ± 0.38 (5415 ± 1142), and $1.28 \pm 0.35 \mu\text{g}/\text{m}^3$ ($3066 \pm 839 \text{ m}^2\text{sec}^{-1}$), respectively (Fig. 6). On the other hand, during normal monsoon years, the monthly mean BC (VC) for the

same period was 0.72 ± 0.18 (4826 ± 279), 0.64 ± 0.16 (5088 ± 1964), 0.73 ± 0.28 (4817 ± 821), and $0.87 \pm 0.21 \mu\text{g}/\text{m}^3$ ($3106 \pm 513 \text{ m}^2\text{sec}^{-1}$), respectively. However, in July and August, high levels of VC and low values of BC were recorded. But, in September, low VC and high BC values in the lower atmosphere were observed, indicating a high pollution potential. The daily mean values of MLH and VC were correlated with BC mass concentration to determine the impact of the MLH and VC on BC mass concentration, and the Pearson coefficient was estimated in both drought and normal monsoon years, as shown in Fig. 7. BC was shown to be negatively correlated with boundary layer height during the two measurement periods, which was more significant during drought the monsoon years ($r = -0.39$) than the normal monsoon years (-0.07) (Fig. 7a and c). The relationship between BC mass concentration and ventilation coefficient was negative, with a more significant correlation (-0.42) during the drought monsoon years than during the normal monsoon years (-0.16) (Fig. 7b and d). During normal monsoon years, low BC mass concentration is likely due to cloud scavenging, washout processes, and high VC. During the COVID lockdown period (25th March- 30th June 2020) and before COVID lockdown (1st - 24th March 2020), BC mass concentrations were about $1.74 \mu\text{g m}^{-3}$ and $1.12 \mu\text{g m}^{-3}$, respectively. The decrease of 43% of BC mass concentration during the lockdown period as compared to before lockdown is mainly attributable to the reduction of local human activities (Palle et al., 2021). As a result, atmospheric dynamics can explain a portion of the fluctuation in BC mass concentration across time. The findings are consistent with the investigation of Srivastava et al. (2012) over Delhi.

4.4. Spectral variations of single scattering albedo

One of the most important parameters for determining aerosol direct radiative forcing is the single scattering albedo. SSA values are primarily determined by aerosols' chemical composition and size (Dubovik et al., 2002; Takemura et al., 2002). Fig. 8 depicts the monthly mean spectral variation of SSA during the drought and normal monsoon years. During the drought monsoon years (normal monsoon years), the monthly mean value of SSA at $0.5 \mu\text{m}$ was 0.87 ± 0.01 (0.89 ± 0.01), 0.87 ± 0.02 (0.89 ± 0.02), 0.87 ± 0.02 (0.88 ± 0.02), and 0.85 ± 0.02 (0.87 ± 0.02), for June, July, August and September, respectively. The SSA magnitude was significantly higher in June, July, and August owing to the prevalence of coarse mode scattering particles (mineral dust). However, due to a mixing of aerosols from numerous sources, it has a considerable reduction with increasing wavelengths throughout September, especially during the drought

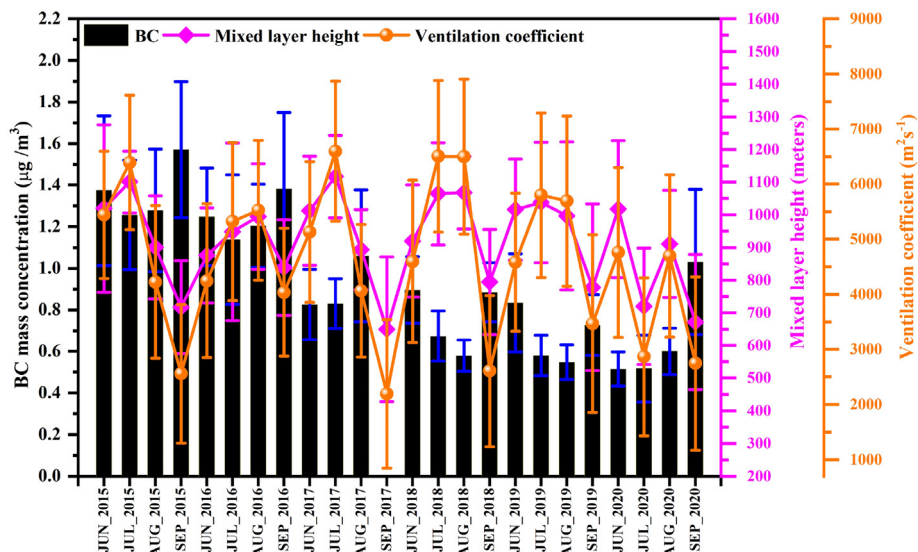


Fig. 6. Monthly mean variations of BC along with mixed layer height and ventilation coefficient over Anantapur during the southwest monsoon months from 2015 to 2020. The vertical bars represent the standard deviation from the monthly mean. The gap in the data series is attributed to lack of data.

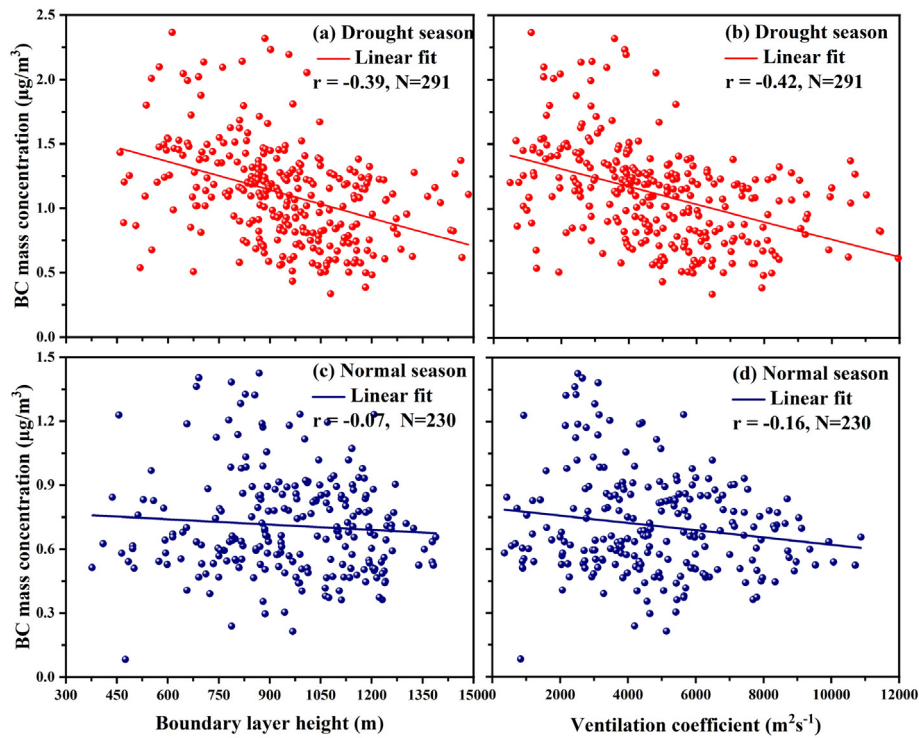


Fig. 7. Scatter plot of BC with boundary layer height and ventilation coefficient during the monsoon months from 2015 to 2020. Solid lines represent the linear least squares fit to the points. Regression slopes and correlation coefficients are written in each panel.

monsoon month September. This clearly shows a domination of absorbing aerosols over scattering particles and which is fairly in agreement with observed high BC aerosols. Previous studies (Vachaspati et al., 2018; Singh et al., 2004) clearly showed that as wavelength increased, SSA decreased due to the dominance of absorbing aerosols rather than the scattering particles.

4.5. Temporal variations of shortwave composite forcing, BC radiative forcing, forcing efficiency, and heating rate

The composite and BC aerosol radiative forcing at three different altitude levels (SUF, ATM, and TOA) throughout the southwest monsoon season from 2015 to 2020 is depicted in Fig. 9. The composite ATM shows a

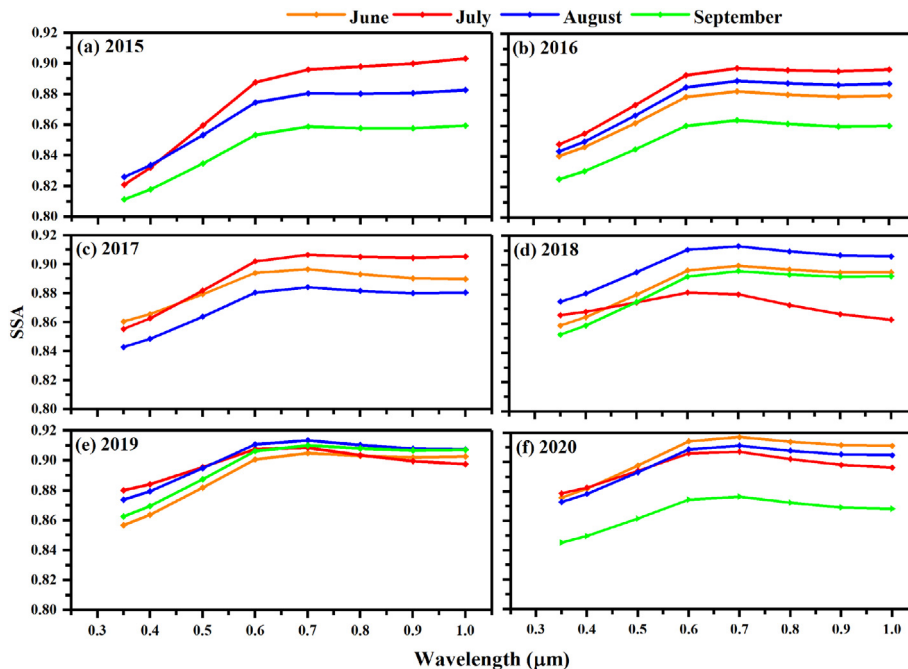


Fig. 8. Monthly mean spectral variation of single scattering albedo over Anantapur during the southwest monsoon months from 2015 to 2020. The gap in the data series is attributed to lack of data.

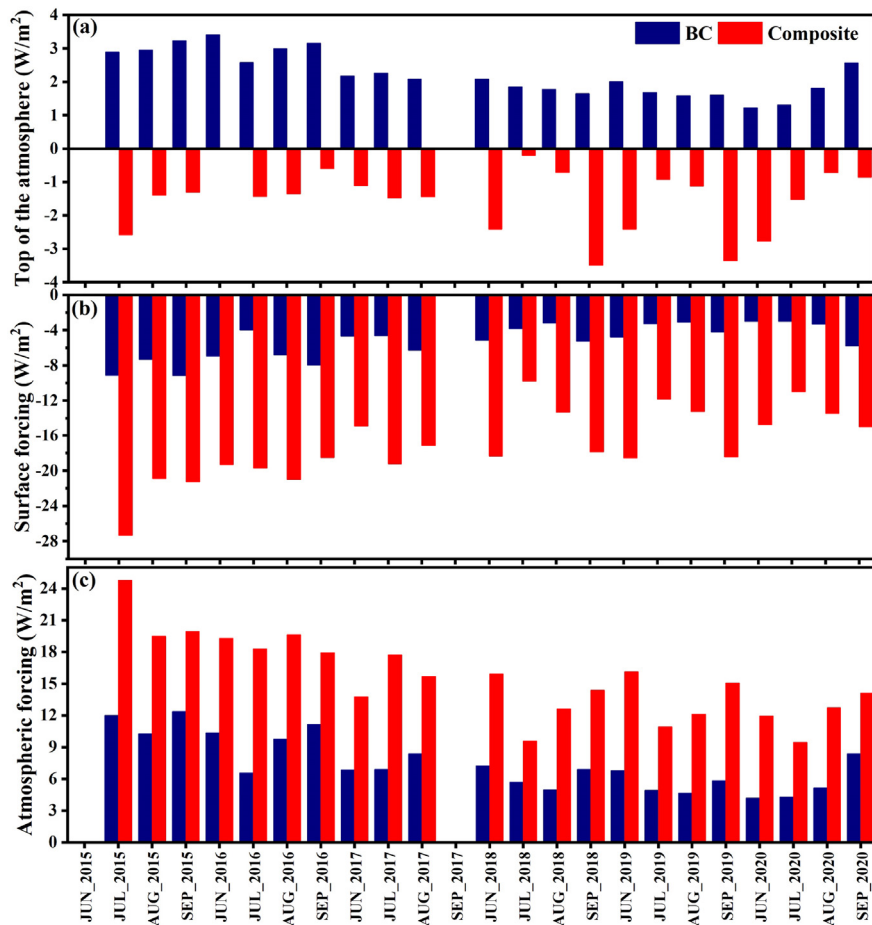


Fig. 9. Monthly variations of the direct shortwave composite aerosol forcing and BC aerosol forcing during the southwest monsoon months (a) top of the atmosphere (b) surface forcing and (c) atmospheric forcing. The gap in the data series is attributed to lack of data.

distinct annual variation during the two distinguishable periods, with the highest during the drought monsoon years ($17.4 \pm 4.1 \text{ Wm}^{-2}$) and lowest in the normal monsoon years ($13.6 \pm 2.4 \text{ Wm}^{-2}$). Similarly, aerosol induced SUF radiative forcing was stronger during the drought monsoon years ($18.8 \pm 4.4 \text{ Wm}^{-2}$) than that of normal monsoon years ($15.2 \pm 2.8 \text{ Wm}^{-2}$).

Further, there was a highest annual mean BC radiative forcing within the atmosphere in September ($8.9 \pm 2.7 \text{ Wm}^{-2}$), followed by August ($7.2 \pm 2.5 \text{ Wm}^{-2}$), June ($7.0 \pm 2.2 \text{ Wm}^{-2}$), and July ($6.7 \pm 2.7 \text{ Wm}^{-2}$). The maximum atmospheric forcing was observed in September, associated with a high surface BC mass concentration. In the current study, TOA forcing (BC) has remained positive regardless of the month demonstrating the warming character of the BC, resulting in a net cooling effect (negative forcing) at the surface. The highest and lowest ATM was recorded in September 2015 (12.4 Wm^{-2}) and June 2020 (4.2 Wm^{-2}), respectively, corresponding to the highest and lowest BC mass concentrations in the respective years. Moreover, there is a clear temporal variation in BC radiative forcing for the normal and drought monsoon years. During the drought monsoon years (normal monsoon years), the monthly mean BC forcing in ATM for June, July, August, and September was 8.8 ± 2.2 (5.9 ± 1.5), 8.0 ± 3.4 (5.3 ± 1.3), 8.3 ± 2.9 (6.0 ± 2.0), and $10.1 \pm 2.8 \text{ Wm}^{-2}$ ($7.1 \pm 1.8 \text{ Wm}^{-2}$), respectively. In the atmosphere, a higher BC aerosol loading leads to higher ATM (warming effect) and SUF forcing (cooling effect), but its effects on forcing are more favorable in the upper atmosphere (positive TOA forcing). During the drought monsoon years, the high BC mass concentration in the atmosphere causes significant atmospheric heating, which has the potential to alter regional atmospheric dynamics.

The magnitude of composite aerosol radiative forcing is determined not only by the chemical composition of particles but also by column abundance. As a result, it is essential to quantify radiative forcing efficiency, commonly defined as the rate of radiative forcing per unit of observed aerosol optical depth at 500_{nm} (Babu et al., 2007). During the drought monsoon years, the annual mean composite aerosol forcing efficiency at the surface, at the top, and within the atmosphere was $-65.4 \pm 7.1 \text{ Wm}^{-2}\tau^{-1}$, $-4.7 \pm 3.6 \text{ Wm}^{-2}\tau^{-1}$, and $60.6 \pm 7.3 \text{ Wm}^{-2}\tau^{-1}$, respectively (Table 1). Similarly, the forcing efficiency at the surface, top, and within the atmosphere during the normal monsoon years is -6.3 ± 2.8 , 60.0 ± 4.5 , and $53.8 \pm 5.1 \text{ Wm}^{-2}\tau^{-1}$, respectively. In drought monsoon years (normal monsoon years), the monthly composite aerosol forcing efficiency is higher (lower) due to the chemical composition in aerosols and aerosol loading. During the drought monsoon years (normal monsoon years), the monthly mean atmospheric heating for June, July, August, and September was 0.49 ± 0.06 (0.39 ± 0.05), 0.49 ± 0.2 (0.35 ± 0.06), 0.48 ± 0.11 (0.38 ± 0.05), and $0.49 \pm 0.07 \text{ Kday}^{-1}$ ($0.40 \pm 0.01 \text{ Kday}^{-1}$), respectively. Compared to the normal monsoon years ($0.38 \pm 0.06 \text{ Kday}^{-1}$), the monsoon atmospheric heating rate in the lower atmosphere was as high as $0.49 \pm 0.11 \text{ Kday}^{-1}$ during the drought monsoon years. It demonstrates the significant role of atmospheric aerosols, particularly absorbing aerosols like BC, in regulation to the thermal structure of the atmosphere by adding heat to the surroundings.

5. Conclusions

The current work presents a first assessment of the in-situ observed aerosol optical depth and BC mass concentration and their associated

Table 1

Forcing efficiency ($\text{W m}^{-2}\tau^{-1}$) from the top of the atmosphere (TOA), surface (SUR) and atmosphere (ATM) and heating rate (HR). NA indicates data not available.

Year	Month	TOA	SUFA	ATM	HR (K/day)
2015	JUN	NA	NA	NA	NA
	JUL	-6.558	-69.444	62.886	0.695
	AUG	-4.721	-70.646	65.925	0.547
	SEP	-4.755	-77.005	72.250	0.560
2016	JUN	-0.104	-64.483	64.379	0.541
	JUL	-4.012	-55.323	51.311	0.513
	AUG	-4.224	-65.504	61.280	0.551
	SEP	-2.354	-72.579	70.226	0.503
2017	JUN	-4.543	-61.089	56.546	0.386
	JUL	-4.543	-59.038	54.495	0.498
	AUG	-5.666	-67.308	61.641	0.440
	SEP	NA	NA	NA	NA
2018	JUN	-8.297	-62.976	54.678	0.447
	JUL	-1.264	-60.318	59.055	0.269
	AUG	-2.861	-53.365	50.504	0.354
	SEP	-13.353	-68.359	55.006	0.404
2019	JUN	-8.148	-62.649	54.501	0.453
	JUL	-4.357	-55.953	51.595	0.306
	AUG	-4.689	-55.216	50.527	0.340
	SEP	-11.305	-62.113	50.808	0.423
2020	JUN	-10.972	-58.292	47.319	0.336
	JUL	-7.903	-56.923	49.020	0.265
	AUG	-2.945	-54.661	51.716	0.357
	SEP	-3.902	-67.720	63.818	0.396

aerosol radiative characteristics over a semi-arid station in Anantapur during the southwest monsoon from 2015 to 2020. The important findings of the study are shown below;

- The observed annual mean AOD was 0.30 ± 0.02 and 0.24 ± 0.01 during drought and normal monsoon years, respectively.
- The monthly mean BC during the drought monsoon years (normal monsoon years) was 1.17 ± 0.25 (0.72 ± 0.18), 1.02 ± 0.31 (0.64 ± 0.17), 1.02 ± 0.38 (0.74 ± 0.28), and $1.28 \pm 0.35 \mu\text{g/m}^3$ ($0.88 \pm 0.21 \mu\text{g/m}^3$) for June, July, August, and September 2015, 2016, and 2018 (2017, 2019, and 2020) respectively.
- BC was negatively correlated with boundary layer height and ventilation coefficient during the two measurement periods. It is more significant during the drought monsoon years than in the normal monsoon years.
- A significant increase in SSA was observed in June, July, and August from visible to near-IR spectra because of the prevalence of coarse mode scattering particles. However, due to aerosol mixing from numerous sources, it has a considerable reduction with increasing wavelengths during September showing a predominant absorption rather than scattering aerosols.
- During the drought monsoon years, the estimated atmospheric heating rate was significantly higher ($0.49 \pm 0.06 \text{ Kday}^{-1}$) than that of the normal monsoon years ($0.38 \pm 0.06 \text{ Kday}^{-1}$). It indicates that aerosols are significant contributors to the increase in heat in the lower atmosphere over the semi-arid station, Anantapur.

CRediT authorship contribution statement

Rama Gopal Kotalo: conceptualized the experiment and edited - Original draft. Lokeswara Reddy Thotli, Bhavyasree Akkiraju, and Chakradhar Rao Tandule:designed the study & data collection. Raja Obul Reddy Kalluri, Balakrishnaiah Gugamsetty, carried out the scientific analysis of the data and writing the original draft. Kajjer Virupakshappa Usha and Siva Sankara Reddy Lingala: Formal analysis.

Declaration of competing interest

The authors declare that they have no known competing financial interests or personal relationships that could have appeared to influence the work reported in this paper.

Acknowledgement

The authors wish to thank the Indian Space Research Organization, Bangalore, for the financial support provided by ISRO-GBP under the ARFI and NOBLE Project. The authors would also like to thank two anonymous reviewers for their fruitful comments that have improved the manuscript.

References

- Albergel, C., Dutra, E., Munier, S., Calvet, J.C., Munoz-Sabater, J., de Rosnay, P., Balsamo, G., 2018. ERA-5 and ERA-interim driven ISBA land surface model simulations: which one performs better? *Hydroclim. Earth Syst. Sci.* 22, 3515–3532.
- Arnott, W.P., Hamasha, K., Moosmuller, H., Sheridan, P.J., Ogren, J.A., 2005. Towards aerosol light-absorption measurements with a 7-wavelength aethalometer: evaluation with a photoacoustic instrument and 3-wavelength nephelometer. *Aerosol Sci. Technol.* 39, 17–29.
- Ashraf, M., Routray, J.K., 2015. Spatio-temporal characteristics of precipitation and drought in Balochistan Province, Pakistan. *Nat. Hazards* 77, 229–254.
- Babu, S.S., Moorthy, K.K., Satheesh, S.K., 2007. Temporal heterogeneity in aerosol characteristics and the resulting radiative impacts at a tropical coastal station, part 2: direct short wave radiative forcing. *Ann. Geophys.* 25, 2309–2320.
- Babu, S.S., Manoj, M.R., Moorthy, K.K., Gogoi, M.M., Nair, V.S., Kompalli, S.K., Satheesh, S.K., Niranjan, K., Ramagopal, K., Bhuyan, P.K., Singh, D., 2013. Trends in aerosol optical depth over Indian region: potential causes and impact indicators. *J. Geophys. Res.* 118, 11794–11806.
- Bollasina, M., Niigam, S., Lau, K.M., 2008. Absorbing aerosols and summer monsoon evolution over South Asia: an observational portrayal. *J. Clim.* 21, 3221–3239.
- Cape, J.N., Coyle, M., Dumitrescu, P., 2012. The atmospheric lifetime of black carbon. *Atmos. Environ.* 59, 256–263.
- Dabani, I., Mishra, A.K., Sen, Z., 2017. Long-term spatio-temporal drought variability in Turkey. *J. Hydrol.* 552, 779–792.
- Dubovik, O., Holben, B.N., Eck, T.F., Smirnov, A., Kaufman, Y.J., King, M.D., Tanre, D., Slutsker, I., 2002. Variability of absorption and optical properties of key aerosol types observed in worldwide locations. *J. Atmos. Sci.* 59, 590–608.
- Dumka, U.C., Krishnamoorthy, K., Kumar, Rajesh, Hegde, P., Sagar, Ram, Pant, P., Narendra Singh Babu, S.S., 2010. Characteristics of aerosol black carbon mass concentration over a high altitude location in the Central Himalayas from multi-year measurements. *Atmos. Res.* 96 (4), 510–521.
- Dumka, U.C., Kaskaoutis, D.G., Tiwari, S., Safai, P.D., Attri, S.D., Soni, V.K., Singh, N., Mihalopoulos, N., 2018. Assessment of biomass burning and fossil fuel contribution to black carbon concentrations in Delhi during winter. *Atmos. Environ.* 194, 93–109.
- Ganguly, D., Jayaraman, A., Rajesh, T.A., Gadhavi, H., 2006. Winter time aerosol properties during foggy and nonfoggy days over urban center Delhi and their implications for short-wave radiative forcing. *J. Geophys. Res.* 111, D15217.
- Gocic, M., Trajkovic, S., 2014. Spatiotemporal characteristics of drought in Serbia. *J. Hydrol.* 510, 110–123.
- Gogoi, M.M., Moorthy, K.K., Babu, S.S., Bhuyan, P.K., 2009. Climatology of columnar aerosol properties and the influence of synoptic conditions: first-time results from the northeast region of India. *J. Geophys. Res.* 114, D08202.
- Gopal, K.R., Arafath, S.M.D., Lingaswamy, A.P., Balakrishnaiah, G., PavanKumari, S., Uma Devi, K., Siva Kumar Reddy, N., Raja Obul Reddy, K., Penchal Reddy, M., Reddy, R.R., Suresh Babu, S., 2014. In-situ measurements of atmospheric aerosols by using Integrating Nephelometer over a semi-arid station, southern India. *Atmos. Environ.* 86, 228–240.
- Gopal, K.R., Arafath, S., Balakrishnaiah, G., Raja Obul Reddy, K., Siva Kumar Reddy, N., Lingaswamy, A.P., PavanKumari, S., Uma Devi, K., Reddy, R.R., Babu, S.S., 2015. Columnar-integrated aerosol optical properties and classification of different aerosol types over the semi-arid region Anantapur. *Sci. Total Environ.* 527–528, 507–519.
- Gopal, R.K., Balakrishnaiah, G., Arafath, S.M., Raja Obul Reddy, K., Siva Kumar Reddy, N., Pavan Kumari, S., Mallikarjuna Reddy, P., 2017. Measurements of scattering and absorption properties of surface aerosols at a semi-arid site, Anantapur. *Atmos. Res.* 183, 84–93.
- Haroon, M.A., Zhang, J., Yao, F., 2016. Drought monitoring and performance evaluation of MODIS-based drought severity index (DSI) over Pakistan. *Nat. Hazards* 84, 1349–1366.
- Hersbach, H., Dee, D., 2016. ERA5 reanalysis is in production. *ECMWF Newslett.* 147.
- Hess, M., Koepke, P., Schultz, I., 1998. Optical properties of aerosols and clouds: the software package OPAC. *Bull. Am. Meteorol. Soc.* 79, 831–844.
- Hoesly, R.M., Smith, S.J., Feng, L., Klimont, Z., Janssens-Maenhout, G., Pitkanen, T., Seibert, J.J., Vu, L., Andres, R.J., Bolt, R.M., Bond, T.C., Dawidowski, L., Khodol, N., Kurokawa, J.I., Li, M., Liu, L., Liu, Z., Moura, M.C.P., O'Rourke, P.R., Zhang, Q., 2018. Historical (1750–2014) anthropogenic emissions of reactive gases and aerosols from the community emissions data system (CEDS). *Geosci. Model Dev.* 11, 369–408.
- Hussain, N.S., Chakradhar Rao, T., Balakrishnaiah, G., Rama Gopal, K., Raja Obul Reddy, K., Siva Kumar Reddy, N., Ramakrishna Reddy, R., 2018. Investigation of black carbon aerosols and their characteristics over tropical urban and semi-arid rural environments in peninsular India. *J. Atmos. Sol.-Terr. Phys.* 167, 48–57.
- Ichoku, C., Levy, R., Kaufman, Y.J., 2002. Analysis of the performance characteristics of the five-channel microtops II sun photometer for measuring aerosol optical thickness and perceptible water vapor. *J. Geophys. Res.* 107 (D13), 4179.
- IPCC, 2021. In: Masson-Delmotte, V., Zhai, P., Pirani, A., Connors, S.L., Péan, C., Berger, S., Caud, N., Chen, Y., Goldfarb, L., Gomis, M.I., Huang, M., Leitzell, K., Lonnoy, E., Matthews, J.B.R., Maycock, T.K., Waterfield, T., Yelekçi, O., Yu, R., Zhou, B. (Eds.), *Climate Change 2021: The Physical Science Basis. Contribution of Working Group I to the Sixth Assessment Report of the Intergovernmental Panel on Climate Change*. Cambridge University Press In Press.

- Kalluri, R.O.R., Gugamsetty, B., Kotalo, R.G., Nagireddy, S.K.R., Tandule, C.R., Thotli, L.R., Ramakrishna, R.R., Surendranair, S.B., 2016. Direct radiative forcing properties of atmospheric aerosols over semi-arid region, Anantapur in India. *Sci. Total Environ.* 566, 1002–1013.
- Kalluri, R.O.R., Balakrishnaiah, G., Rama Gopal, K., Reddy, V.S.N., ChakradharRao, T., Lokeshwara Reddy, T., NazeerHussain, S., Reddy, V.M., Reddy, R.R., Babu, S.S., 2017. Seasonal variation of near surface black carbon and satellite derived vertical distribution of aerosols over a semi-arid station in India. *Atmos. Res.* 184, 77–87.
- Kalluri, R.O.R., Xiaoyu, Z., Lei, B., 2019. Seasonal aerosol variations over a coastal city, Zhou-shan, China from CALIPSO observations. *Atmos. Res.* 218, 117–128.
- Kalluri, R.O.R., Gugamsetty, B., Kotalo, R.G., Thotli, L.R., Tandule, C.R., Bhavyasree, A., 2020a. Long-term (2008–2017) analysis of atmospheric composite aerosol and black carbon radiative forcing over a semi-arid region in southern India: model results and ground measurement. *Atmos. Environ.* 240, 117840.
- Kalluri, R.O.R., Zhang, X., Bi, L., Zhao, J., Yu, L., Kotalo, R.G., 2020b. Carbonaceous aerosol emission reduction over Shandong province and the impact of air pollution control as observed from synthetic satellite data. *Atmos. Environ.* 222, 117150.
- Kalluri, R.O.R., Gugamsetty, B., Tandule, C.R., Kotalo, R.G., Thotli, L.R., Rajuru, R.R., Palle, S.N.R., 2021. Impact of aerosols on surface ozone during COVID-19 pandemic in southern India: a multi-instrumental approach from ground and satellite observations, and model simulations. *J. Atmos. Sol. Terr. Phys.* 212, 105491.
- Kumar, M., Raju, M.P., Singh, R.S., Banerjee, T., 2017. Impact of drought and normal monsoon scenarios on aerosols induced radiative forcing and atmospheric heating in Varanasi over middle indo-gangetic plain. *J. Aerosol Sci.* 113, 95–107.
- Lau, K.M., Kim, K.M., 2006. Observational relationships between aerosol and asian monsoon rainfall, and circulation. *Geophys. Res. Lett.* 33, L21810.
- Lau, W.K.M., Kim, K.M., Shi, J.J., Matsui, T., Chin, M., Tan, Q., Peters-Lidard, C., Tao, W.K., 2017. Impacts of aerosol–monsoon interaction on rainfall and circulation over northern India and the himalaya foothills. *Clim. Dyn.* 49, 1945–1960.
- Levy, H., Horowitz, L.W., Schwarzkopf, M.D., Ming, Y., Golaz, J.C., Naik, V., Ramaswamy, V., 2013. The roles of aerosol direct and indirect effects in past and future climate change. *J. Geophys. Res. Atmos.* 118, 4521–4532.
- Li, Z., Zhao, X., Kahn, R., Mishchenko, M., Remer, L., Lee, K.H., Wang, M., Laszlo, I., Nakajima, T., Maring, H., 2009. Uncertainties in satellite remote sensing of aerosols and impact on monitoring its long-term trend: a review and perspective. *Ann. Geophys.* 27, 2755–2770.
- Liou, K.N., 2002. *An Introduction to Atmospheric Radiation*. Elsevier, New York, p. 583.
- Liu, D., Flynn, M., Gysel, M., Targino, A., Crawford, I., Bower, K., Choularton, T., Jurányi, Z., Steinbacher, M., Hüglin, C., Curtius, J., Kampus, M., Petzold, A., Weingartner, E., Baltensperger, U., Coe, H., 2010. Single particle characterization of black carbon aerosols at a tropospheric alpine site in Switzerland. *Atmos. Chem. Phys.* 10, 7389–7407.
- Liu, C., Yang, C., Yang, Q., Wang, J., 2021. Spatiotemporal drought analysis by the standardized precipitation index (SPI) and standardized precipitation evapotranspiration index (SPEI) in Sichuan Province, China. *Sci. Rep.* 11, 1280.
- Manoj, M.G., Devara, P.C.S., Safai, P.D., Goswami, B.N., 2010. Absorbing aerosols facilitate transition of indian monsoon breaks to active spells. *Clim. Dyn.* 37, 2181–2198.
- Manoj, M.R., Satheesh, S.K., Moorthy, K.K., Gogoi, M.M., Babu, S.S., 2019. Decreasing trend in blackcarbon aerosols over the indian region. *Geophys. Res. Lett.* 46, 2903–2910.
- McKee, T.B., Doesken, N.J., Kleist, J., 1993. The relationship of drought frequency and duration to time scales. Proceedings of the 8th Conference on Applied Climatology, Anaheim, CA, USA, 17, pp. 179–183.
- McMeeking, G.R., Good, N., Petters, M.D., McFiggans, G., Coe, H., 2011. Influences on the fraction of hydrophobic and hydrophilic black carbon in the atmosphere. *Atmos. Chem. Phys.* 11, 5099–5112.
- Mehr, A.D., Vaheddoost, B., 2019. Identification of the trends associated with the SPI and SPEI indices across Ankara, Turkey. *Theor. Appl. Clim.* 139, 1531–1542.
- Mishra, A.K., Singh, V.P., 2010. A review of drought concepts. *J. Hydrol.* 391, 202–216.
- Moteki, N., Kondo, Y., 2007. Effects of mixing state on black carbon measurements by laser-induced incandescence. *Aerosol Sci. Technol.* 41, 398–417.
- Osshima, N., Koike, M., Zhang, Y., Kondo, Y., Moteki, N., Takegawa, N., Miyazaki, Y., 2009. Aging of black carbon in outflow from anthropogenic sources using a mixing state resolved model: model development and evaluation. *J. Geophys. Res. Atmos.* 114, D06210.
- Palle, S.N.R., Tandule, C.R., Kalluri, R.O.R., Gugamsetty, B., Kotalo, R.G., Thotli, L.R., Akkiraju, B., Lingala, S.S.R., 2021. The impact of lockdown on eBC mass concentration over a semi-arid region in southern India: ground observation and model simulations. *Aerosol Air Qual. Res.* 21 (11), 210101.
- Ramanathan, V., Crutzen, P.J., Kiehl, J.T., Rosenfeld, D., 2001. Aerosols, climate, and the hydrological cycle. *Science* 294, 2119–2124.
- Ramanathan, V., Chung, C., Kim, D., Bettge, T., Buja, L., Kiehl, J.T., Washington, W.M., Fu, Q., Sikka, D.R., Wild, M., 2005. Atmospheric brown clouds: impacts on south asian climate and hydrological cycle. *Proc. Natl. Acad. Sci. U. S. A.* 102 (15), 5326–5333.
- Ricchiazzi, P., Yang, S.R., Gautier, C., Sowle, D., 1998. SBDART: a research and teaching software tool for plane-parallel radiative transfer in the Earth's atmosphere. *Bull. Am. Meteorol. Soc.* 79, 2101–2114.
- Sanap, S.D., Pandithurai, G., 2015. The effect of absorbing aerosols on indian monsoon circulation and rainfall: a review. *Atmos. Res.* 164–165, 318–327.
- Satheesh, S.K., Vinoj, V., Moorthy, K.K., 2010. Radiative effects of aerosols at an urban location in southern India: observations versus model. *Atmos. Environ.* 44, 5295–5304.
- Schwarz, J.P., Gao, R.S., Fahey, D.W., Thomson, D.S., Watts, L.A., Wilson, J.C., Reeves, J.M., Darbeheshti, M., Baumgardner, D.G., Kok, G.L., Chung, S.H., Schulz, M., Hendricks, J., Lauer, A., Kärcher, B., Slowik, J.G., Rosenlof, K.H., Thompson, T.L., Langford, A.O., Loewenstein, M., Aikin, K.C., 2006. Single-particle measurements of midlatitude black carbon and light-scattering aerosols from the boundary layer to the lower stratosphere. *J. Geophys. Res.* 111, D16207.
- Shalini, V., Narasimhulu, K., Raja Obul Reddy, K., Balakrishnaiah, G., Rama Gopal, K., Lokeshwara Reddy, T., Chakradhar Rao, T., Elijahethamma, B., Manjunatha, C., Ramakrishna Reddy, R., 2020. Chemical characterization and source identification of particulate matter at Ballari (15.15°N, 76.93°E), Karnataka over Southern Indian region. *J. Atmos. Sol. Terr. Phys.* 200, 105192.
- Shiraiwa, M., Kondo, Y., Moteki, N., Takegawa, N., Miyazaki, Y., Blake, D.R., 2007. Evolution of mixing state of black carbon in polluted air from Tokyo. *Geophys. Res. Lett.* 34, L16803.
- Shoaib, J., Falak, N.C., Ghulam, H.D., Kamran, A., Nir, Y.K., 2020. Exploring the evolution of drought characteristics in Balochistan, Pakistan. *Appl. Sci.* 10, 913.
- Singh, R.P., Dey, S., Tripathi, S.N., Tare, V., Holben, B.N., 2004. Variability of aerosol parameters over Kanpur, northern India. *J. Geophys. Res.* 109, D23206.
- Srivastava, A.K., Singh, S., Tiwari, S., Bish, D.S., 2012. Contribution of anthropogenic aerosols in direct radiative forcing and atmospheric heating rate over Delhi in the indo-Gangetic Basin. *Environ. Sci. Pollut. Res.* 19, 1144–1158.
- Takemura, T., Nakajima, T., Dubovik, O., Holben, B.N., Kinne, S., 2002. Single-scattering albedo and radiative forcing of various aerosol species with a global three-dimensional model. *J. Clim.* 15, 333–352.
- Tandule, C.R., Kalluri, R.O.R., Gugamsetty, B., Kotalo, R.G., Thotli, L.R., Rajuru, R.R., Vaddin, S., 2020. Decadal climatology of the spatial and vertical distributions of tropospheric aerosols over the Arabian Sea based on satellite observations. *Int. J. Climatol.* 40, 4676–4689.
- Tirivarombo, S., Osupile, D., Eliasson, P., 2018. Drought monitoring and analysis: standardised precipitation evapotranspiration index (SPEI) and standardised precipitation index (SPI). *Phys. Chem. Earth Parts A/B/C* 106, 1–10.
- Tran, T.V., Tran, D.X., Myint, S.W., Latorre-Carmona, P., Ho, D.D., Tran, P.H., Dao, H.N., 2019. Assessing spatiotemporal drought dynamics and its related environmental issues in the mekong river delta. *Remote Sens.* 11, 2742.
- Vachaspati, C.V., ReshmaBegam, G., NazeerAhmed, Y., Raghavendra Kumar, K., Reddy, R.R., 2018. Characterization of aerosol optical properties and model computed radiative forcing over a semi-arid region, Kadapa in India. *Atmos. Res.* 209, 36–49.
- Veefkind, J.P., de Haan, J.F., Brinksma, E.J., Kroon, M., Levelt, P.F., 2006. Total ozone from the ozone monitoring instrument (OMI) using the DOAS technique. *IEEE Trans. Geosci. Remote Sens.* 44 (5), 1239–1244.
- Virkkula, A., Mäkelä, T., Hillamo, R., Yli-Tuomi, T., Hirsikko, A., Hämeri, K., Koponen, I.K., 2007. A simple procedure for correcting loading effects of aethalometer data. *J. Air Waste Manag. Assoc.* 57, 1214–1222.
- Wang, C., Kim, D., Ekman, A.M.L., Barth, M.C., Rasch, P.J., 2009. Impact of anthropogenic aerosols on indian summer monsoon. *Geophys. Res. Lett.* 36, L21704.
- Wang, X., Zhuo, L., Li, C., Engel, B.A., Sun, S., Wang, Y., 2019b. Temporal and spatial evolution trends of drought in northern Shaanxi of China: 1960–2100. *Theor. Appl. Clim.* 139, 965–979.
- Wang, Y., Liu, G., Guo, E., 2019a. Spatial distribution and temporal variation of drought in Inner Mongolia during 1901–2014 using standardized precipitation evapotranspiration index. *Sci. Total Environ.* 654, 850–862.
- Weingartner, E., Saathoff, H., Schnaiter, M., Streit, N., Bitnar, B., Baltensperger, U., 2003. Absorption of light by soot particles: determination of the absorption coefficient by means of aethalometers. *J. Aerosol Sci.* 34 (10), 1445–1463.
- Willis, M.D., Healy, R.M., Riemer, N., West, M., Wang, J.M., Jeong, C.H., Wenger, J.C., Evans, G.J., Abbatt, J.P.D., Lee, A.K.Y., 2016. Quantification of black carbon mixing state from traffic: implications for aerosol optical properties. *Atmos. Chem. Phys.* 16, 4693–4706.
- Zhang, G., Han, B., Bi, X., Dai, S., Huang, W., Chen, D., Wang, X., Sheng, G., Fu, J., Zhou, Z., 2015. Characteristics of individual particles in the atmosphere of Guangzhou by single particle mass spectrometry. *Atmos. Res.* 153, 286–295.
- Zhang, Y., Zhang, Q., Cheng, Y., Su, H., Kecorius, S., Wang, Z., Wu, Z., Hu, M., Zhu, T., Wiedensohler, A., He, K., 2016. Measuring the morphology and density of internally mixed black carbon with SP2 and VTDMA: new insight into the absorption enhancement of black carbon in the atmosphere. *Atmos. Meas. Tech.* 9, 1833–1843.
- Zhifang, P., Shibo, F., Lei, W., Wunian, Y., 2020. Comparative Analysis of Drought Indicated by the SPI and SPEI at Various Timescales in Inner Mongolia, China. *Water* 12 (7), 1925.

Endorsement Certificate from the Mentor & Host Institute

This is to certify that:

- I. The applicant, Mr. Thotli Lokeshwara Reddy, will assume full responsibility for implementing the project.
- II. The fellowship will start from the date on which the fellow joins University/Institute where he/she implements the fellowship. The mentor will send the joining report to the SERB. SERB will release the funds on receipt of the joining report.
- III. The applicant, if selected as SERB-NPDF, will be governed by the rules and regulations of the University/ Institute and will be under administrative control of the University/Institute for the duration of the Fellowship.
- IV. The grant-in-aid by the Science & Engineering Research Board (SERB) will be used to meet the expenditure on the project and for the period for which the project has been sanctioned as indicated in the sanction letter/order.
- V. No administrative or other liability will be attached to the Science & Engineering Research Board (SERB) at the end of the Fellowship.
- VI. The University/Institute will provide basic infrastructure and other required facilities to the fellow for undertaking the research objectives.
- VII. The University/Institute will take into its books all assets received under this sanction and its disposal would be at the discretion of Science & Engineering Research Board (SERB).
- VIII. University/Institute assume to undertake the financial and other management responsibilities of the project.
- IX. The University/Institute shall settle the financial accounts to the SERB as per the prescribed guidelines within three months from the date of termination of the Fellowship.

Dated: 08-08-2023

Signature of the Mentor:



Dr. K. KRISHNA REDDY
Professor
Department of Physics
YOGI VEMANA UNIVERSITY
Vemanapuram, Kadapa - 516 003
Andhra Pradesh

Dated: 08.08.2023

Signature of the Registrar of University/Head of

REGISTRAR

Institute Seal of the Institution **YOGI VEMANA UNIVERSITY**
KADAPA-516 005.



Undertaking by the Principal Investigator

To

The Secretary
SERB, New Delhi

Sir

I Prof. K. Krishna Reddy hereby certify that the research proposal Prediction of large-scale spatial and temporal variability of droughts over Indian region submitted for possible funding by SERB, New Delhi is my original idea and has not been copied/taken verbatim from anyone or from any other sources. I further certify that this proposal has been checked for plagiarism through a plagiarism detection tool i.e., Turnitin approved by the Institute and the contents are original and not copied/taken from any one or many other sources. I am aware of the UGCs Regulations on prevention of Plagiarism i.e., University Grant Commission (Promotion of Academic Integrity and Prevention of Plagiarism in Higher Educational Institutions) Regulation, 2018. I also declare that there are no plagiarism charges established or pending against me in the last five years. If the funding agency notices any plagiarism or any other discrepancies in the above proposal of mine, I would abide by whatsoever action taken against me by SERB, as deemed necessary.



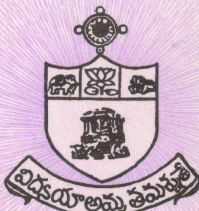
Signature of PI with date

Dr. K. KRISHNA REDDY
Name/designation
Professor
Department of Physics
YOGI VEMANA UNIVERSITY
Vemanapuram, Kadapa - 516 003
Andhra Pradesh.

Sl. No.

01889

Sri Krishnadevaraya University



Faculty of Science

Reg. No. 18A504004

Sri Krishnadevaraya University hereby confers the Degree of

Master of Philosophy

on Thotli Lokeswarareddy

Son / Daughter of Thotli Kotireddy

in recognition for his/ her research work on

"CHARACTERISTICS OF THE MORNING RISE OF INVERSION AND SHEAR GENERATED LAYERS USING DOPPLER SODAR"

in the Department of Physics

he / she having been found duly qualified for the same in First

with effect from

16/03/2020

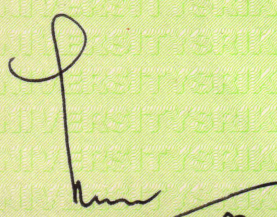


Given under the seal of the University



S.V. PURAM
ANANTAPUR - 515003,
ANDHRA PRADESH, INDIA

Dated : 1.0 AUG 2020


Vice-Chancellor



అంధ్రప్రదేశ్ ప్రభుత్వం

రామ-వార్డు సచివాలయ శాఖ



APGSWS 02919835

GOVERNMENT OF ANDHRA PRADESH
INCOME & ASSET CERTIFICATE FOR ECONOMICALLY WEAKER SECTIONS

Application No



EWS230318072276

Date : 29/03/2023

VALID FOR THE YEAR 2022-2023

This is to certify that Shri/Smt./Kumar **THOTLI LOKESWARA REDDY** son/daughter/wife of **THOTLY KOTI REDDY** permanent resident of **13-35** village/Street **THUMMALA** Post office **THUMMALA** District **SRI SATHYA SAI** in the State/ Union Territory **ANDHRA PRADESH** Pin Code **515556** Whose photograph is attested below belongs to Economically Weaker Sections, Since the gross annual income* of his/her family** is below Rs.8 Lakh (Rupees Eight Lakh Only) for the financial year **2021-2022** His/her family does not own or possess any of the following assets***:

- I. 5 acres of agricultural land and above;
- II. Residential flat of 1000sq.ft. and above;
- III. Residential plot of 100sq.yards and above in notified municipalities;
- IV. Residential plot of 200sq.yards and above in areas other than the notified municipalities.

Shri/Smt./Kumari **THOTLI LOKESWARA REDDY** belongs to the **OC (REDDY)** caste which is not recognized as a Scheduled Caste, Scheduled Tribe and Other Backward Classes (Central List).

Signature with seal of Office

Name : V Reddy Sekhar
Designation : Tahsildar
Mandal : Amadagur

Recent Passport size photo
attached photograph of
the applicant



* Note : Income covered all the sources i.e salary, agriculture, business, profession,etc.

** Note : The term "Family" for the purpose include the person, who seeks benefits of reservation, his/her parents and siblings below the age of 18 years also his/her spouse and children below the age of 18 years.

*** Note : The property held by a "Family" in different locations or different place/cities have been clubbed by applying the land or property holding test to determine EWS status.

Digitally Signed.
Name: VELAGA REDDY
SEKHAR
Date: 29-Mar-2023 14:37:28

Page 1 of 1

Note : This is a Digitally Signed Certificate, does not require physical signature and this certificate can be verified at www.gramawardsachivalayam.ap.gov.in by furnishing the application number mentioned in the Certificate.

ANDHRA PRADESH

GOVERNMENT OF ANDHRA PRADESH



SHORT CV OF MENTOR

Web site: <https://yvu.edu.in/home/kkrishnareddy>

Career In Research:

- Chief Scientist, Japan Agency for Marine Science & Technology (JAMSTEC), Japan
- Adviser and faculty, International School on Atmospheric Radar (ISAR), Taiwan
- Post-Doctoral Fellow, Japan, The Netherlands, and Taiwan
- Coordinator, Sem-arid-zonal Atmospheric Research Centre (SARC), ISRO
- Principal Investigator, Severe Thunderstorm Observational and Regional Modelling (STROM) over the North-East region of India, Ministry of Earth Sciences (MoES)
- Principle Investigator, Village Information Systems (APCOST)
- Coordinator, DST-FIST Program @YVU

Academics and Administration:

@ Yogi Vemana University, Kadapa	@ Krishna University, Machilipatnam
Director, Centre for Distance & Online Education	Registrar
Dean, Faculty of Science	Finance Officer
Head, Department of Physics	Principal (i/C)
Principal & Chief Warden	Dean, College Development Council
Member, Executive Council	Convener & Member, Academic Senate
Vice-Principal & Additional Chief Warden	Chairman, Central Purchase Committee
Dean, Students Welfare	
Dean, Examinations	
Dean, School of Physical Sciences	
Director, YVU-UGC	
Head & Chairman, BoS	
VC nominee & Member, Central Purchase Committee	

Awards:

- A.P. Scientist (APSA) Award, Andhra Pradesh Council of Science & Technology (APCOST)
- Young Scientist, International Union on Radio Science (URSI)
- Secretary, Indian Association of Physics Teachers (IAPT)
- A.P. State Best University Teacher Award, Govt. of A.P.
- Dr. Palle Rama Rao Award for Physical Sciences, Science City of Andhra Pradesh

Honors and Recognitions

- Fellow, Institute of Electronics & Telecommunications (IETE), New Delhi
- Founder Fellow, Andhra Pradesh Academy of Sciences (APAS), Amaravati
- Fellow, Telangana Academy of Sciences (TAS), Hyderabad
- Member & Researcher, Tenth Indian Scientific Expedition to Antarctica
- Member and Faculty, International School on Atmospheric Radar (ISAR)
- Member, Severe Thunderstorm Observational and Regional Modelling (STROM) over the North-East region of India
- Member, High-level Committee of experts for the establishment of Doppler Weather Radar over India, India Meteorological Department, New Delhi
- Member, Technical Committee, Govt. of Karnataka, Cloud Seeding, Bengaluru
- Member, Network of Doppler Weather Radar, Karnataka Natural Disaster Management Corporation (KNMDC), Bengaluru

1. Personal Details and General Information	
Name (In Capital Letters)	KRISHNAREDDIGARI KRISHNA REDDY
Date of Birth (Day/Month/Year)	25-10-1962
Father's Name	Late. Shri. K. Sreeramulu Reddy
Mother's Name	Late. Smt. K. Krishnamma
Spouse and Children	Dr. B. Mythili and Ms. K. Saaketha
Permanent Address	3/167-4, S S M Residency
Correspondence Address	ARP Colony, Prakash Nagar Kadapa - 516004
Mobile Phone No.	9966220933
Email ID	krishna.kkreddy@gmail.com krishna.kkreddy@yvu.edu.in

2. Present Position

i.	Designation	Professor
ii.	Organization	Yogi Vemana University, Kadapa
iii.	Pay Scale	Rs.37400/- to Rs.67,000/-
iv.	Date of Appointment	22 nd January 2013
v.	Total Experience (in years and months)	<p>37-yrs 07-m in Academics & Research</p> <p>a) 10-Yrs 05-m as Professor b) 15-Yrs 07-m as a faculty c) 13-Yrs 10-m exclusively Aboard as a Research Scientist/PDF after PhD d) 07-Yrs 09-m during PhD</p>

3. Education Qualifications (In chronological order from latest to Graduation level)

Sl. No	Qualification	University	Year	Subject(s)/Topic(s)	% Achieved
i.	Doctor of Philosophy (Ph.D.)	Sri Venkateswara University Tirupati	1993	<i>Remote Sensing of the Troposphere using Acoustic Sounder (SODAR) and studies on Microwave Propagation over Southern India</i>	----
ii.	Master of Philosophy (M.Phil.)		1988	<i>Microwave propagation studies: Effect of Fresnel zone clearance on LOS communication links</i>	65.6
iii.	Master of Science (M.Sc.)		1986	<i>Solid State Physics and Applied Spectroscopy</i>	55.6
iv.	Bachelor of Science (B.Sc.)	S.V. Arts College, Tirupati	1983	<i>Mathematics, Physics, and Chemistry</i>	60.5

4. Academic/Research Experience & Responsibilities (In chronological order from latest to oldest)

Sl. No	Position and Institute/University	Duration		Experience		
		From	To	Years	Month	Days

Professional Experience: 22 years 09 months 14 days

1	Professor (by Selection) , Department of Physics, Yogi Vemana University, Kadapa	22-01- 2013	Till date	10	05	00
2	Associate Professor (by Selection) Yogi Vemana University, Kadapa	11-11- 2008	21-01-2013	04	03	10
3	Assistant Professor (by Selection) Yogi Vemana University, Kadapa	27-06-2007*	10-11-2008	01	04	14
4	Chief Research& Development Scientist & Research Scientist Japan Agency for Marine and Earth Technology Center (JAMSTEC), Yokosuka, Japan	01-04-2001	21-12-2007	06	08	21

5. Research Scientist/ Post-Doctoral Research Experience: 07 years 02 months						
5	Researcher , Telecommunications Advancement Organization (TAO), Communication Research Laboratory, Tokyo, Japan	15-10-2000	31-03-2001	00	05	16
6	Visiting Research Fellow Nagoya University, Nagoya, Japan	15-10-1999	14-10-2000	01	00	00
7	Post-Doctoral Fellow , Science & Technology Agency Communication Research Laboratory (CRL), Tokyo, Japan	15-11-1997	14-10-1999	01	11	00
8	Post-Doctoral Fellow Delft University of Technology The Netherlands	01-04-1996	14-11-1997	01	07	00
9	Post-Doctoral Fellow National Central University, Taiwan					
10	Research Associate (CSIR) Sri Venkateswara University, Tirupati	03-01-1994	31-03-1996	02	02	28
6. Doctoral Research Experience: 07 years 09 months						
11	Senior Research Fellow Sri Venkateswara University, Tirupati	Oct. 1990	Dec.1993	03	02	00
12	Researcher , X Scientific Expedition to Antarctica Dept. of Ocean Development (DOD)	Nov.1990	Mar.1991	00	05	00
13	Junior Research Fellow Sri Venkateswara University, Tirupati.	Sep.1986	Oct.1990	04	02	00
Total Academic/Research Experience				37	03	19
* Extra-Ordinary Leave from 01-08-2007 to 22-12-2007						
7. Research Specializations(s)						
Sl. No.	Research Interest					
i.	Atmospheric Physics & Remote Sensing: Clouds, Aerosols, Boundary-Layer Physics					
ii.	Atmospheric Dynamics, Radiation Budget, Climate, Radiation Transfer Models					
iii.	Satellite and Doppler Radar & Lidar Remote Sensing of Aerosols and Clouds and Assessment of their impact					
iv.	Radar and Monsoon meteorology					
v.	Prediction of cyclones, thunderstorms, heavy rainfall, monsoon, mesoscale convective precipitating systems, and Global Climate Change					
vi.	Rain drop-size Distribution using ground-based and Satellite sensors					
8. Training Courses/Workshops Attended:						
Sl. No.	Conference/Workshop		Venue & Dates			
1.	Workshop on Physics of Mesosphere Stratosphere-Troposphere interactions with special emphasis on MST radar techniques		The Abdus Salam International Centre for Theoretical Physics (ICTP), Trieste, Italy, 13-24 Nov.2000			
2.	2 nd ICTP-URSI-ITU/BDT School on the Use of Radio for Digital Communications in Developing Countries		The Abdus Salam International Centre for Theoretical Physics (ICTP), Trieste, Italy, 01-19 Feb.1999			
3.	Atmospheric Interactions: Downward and Upward coupling to the middle and Upper atmosphere		The Abdus Salam International Centre for Theoretical Physics (ICTP), Trieste, Italy, 05-16 Feb.1996			
4.	Scientific Aspects of the Rural Communications in Developing Countries		The Abdus Salam International Centre for Theoretical Physics (ICTP), Trieste, Italy, 01-05 Mar.1993			
5.	3 rd ICTP-URSI College on Theoretical and Experimental Radio-propagation Physic		The Abdus Salam International Centre for Theoretical Physics (ICTP), Trieste, Italy, 01-28 Feb.1993			

9. Present Research Scholars Guiding						
S. No.	Author(s)	Title	Name of Journal	Volume	Page	Year
1	B. Rohini, K. Bharghavi, P. Rajesh, P. Lakshmi Bharathi, H. Sushmitha, C.V. Krishna Reddy, and K. Krishna Reddy	South-West and North-East Monsoon Precipitations Bright Band Characteristics over Kadapa, Semi-arid Regions of India	International Journal for Research in Applied Science & Engineering Technology (IJRASET)	11(V)	4502-4506	2023
2	Seela, B.K. Janapati, J. Lin, P.-L. Lan, C.-H.; Shirooka, R., Hashiguchi, H., and K. Krishna Reddy	Raindrop Size Distribution Characteristics of the Western Pacific Tropical Cyclones Measured in the Palau Islands	Remote Sensing	14(3)	470	2022
3	Vinay Kumar, S. B. Surendra Prasad, K. Krishna Reddy, S. K. Dhaka, R. K. Choudhary, M. Venkatarami Reddy, and Shu-Peng Ho	Temperature perturbations in the troposphere and lower stratosphere over a semi-arid region during the 2010 solar eclipse	Pure and Applied Geophysics	179	2487–2499	2022
4	Seela, B.K., Janapati, J., Kalath Unnikrishnan, C., Lin, P.-L., Le Loh, J., Chang, W.-Y., Kumar, U., K. Krishna Reddy, Lee, D.-I., VenkatramiReddy, M.	Raindrop Size Distributions of North Indian Ocean Tropical Cyclones Observed at the Coastal and Inland Stations in South India	Remote Sensing	13(16)	3178	2021
5	Jayalakshmi Janapati, Balaji Kumar Seela, Pay-Liam Lin, Pao. K. Wang, Chie-Huei Tseng, K. Krishna Reddy, Hiroyuki Hashiguchi, Lei Feng, Subrata Kumar Das, and C. K. Unnikrishnan	Raindrop size distribution characteristics of Indian and Pacific Oceans tropical cyclones	Journal of the Meteorological Society of Japan	98(2)	299–317	2020
6	Jayalakshmi Janapati, Balaji Kumar Seela, Pay-Liam Lin, Pao. K. Wang, Chie-Huei Tseng, K. Krishna Reddy, Hiroyuki Hashiguchi, Lei Feng, Subrata Kumar Das, and C. K.	Raindrop size distribution characteristics of Indian and Pacific Oceans tropical cyclones	Journal of the Meteorological Society of Japan	98 (2)	299-317	2020

	Unnikrishnan					
7	Rajesh Macherla, R. Madhuri, Y.Md. Riyazuddin, P. Vamsi Krishna Reddy, and K. Krishna Reddy	Discerning precipitating Clouds for Bright band characterization over Kadapa, Semi-arid regions of India	International Journal of Research and Analytical Reviews (IJRAR)	6(1)	103-113	2019
8	Rajesh Macherla, P. Vamsi Krishna Reddy and K. Krishna Reddy	Long-term observations on Virga clouds over Kadapa, Semi-arid regions of India	Journal of Emerging Technologies and Innovative Research (JETIR)	6(1)	749-755	2019
9	B. Surendra Prasad, Vinay Kumar, K. Krishna Reddy, S.K. Dhaka, Malik Shristy, M. Venkatarami Reddy, and U. Muralikrishna	Perturbations in the Earth's atmosphere over the Indian region during the total solar eclipse on 22 July 2009	Journal of Meteorological Research	33(4)	1-14	2019
10	T. Rajitha Madhu Priya, K. Krishna Reddy, M. Venkata Ramanaiah, and Ashok Kumar Sharma	Some aspects of the convective boundary layer structure over complex terrain in tropical semiarid regions of Rayalaseema	International Journal of Current Advanced Research	07(5)	13082-13087	2018
11	Suneetha, R., S. Balaji Kumar, Mohammed Waaiz, G. Mahboob Basha, and K. Krishna Reddy	Deployment of Lightning Sensors for an understanding of Lightning Thunderstorm precipitating systems over the North-East Region of India	Journal of Emerging Technologies and Innovative Research (JETIR)	5(4)	614-622	2018
12	Suneetha, R., S. Balaji Kumar, Mohammed Waaiz, G. Mahboob Basha, and K. Krishna Reddy	Study of Microphysical and Thermodynamic indices in forecasting pre-monsoon thunderstorms over Guwahati during STORM-2009 and 2010	International Journal of Creative Research Thoughts (IJCRT)	6(2)	670-684	2018
13	T. Amaranatha Reddy, S. Vijaya Lakshmi, and K. Krishna Reddy	Direct Aerosol Radiative Forcing Uncertainties due to different Factors in Different Environments	International Journal of Research in Advent Technology (IJART)	6(1)	46-56	2018
14	Hari Krishna, A, Mohammed Waaiz, G Mahboob Basha, and K. KrishnaReddy	Village Information Systems - Prediction of weather for the benefit of farmers	International Journal for Research in Applied Science & Engineering Technology (IJRASET)	6(1)	580-590	2018
15	Hari Krishna, A, K. Krishna Reddy, Mohammed Waaiz, G Mahboob Basha	Deployment of Automatic Weather Station for Village Information Systems over Kadapa and Nellore	Journal of Emerging Technologies and Innovative Research (JETIR)	5(1)	76-83	2018